



Norwegian University  
of Life Sciences

**Master's Thesis 2023 60 ECTS**

Faculty of Environmental Sciences and Natural Resource Management

# **Stabilization of PFAS contaminated soil with waste-based biochar sorbents**

**Clara Benedikte Mader Lade**

Environment and Natural Resources, soil and environment specialisation

[This page has been left blank intentionally]

## Abstract

The widespread use of per- and polyfluoroalkyl substances (PFAS) for decades has caused worldwide soil- and groundwater contamination, due to their mobility and persistency. Few existing technologies are suitable for PFAS remediation, hence a great need has arisen for new remediation technologies for PFAS impacted sites. Biochar is a carbonaceous material produced by heating biomass in absence of oxygen and has in recent years increasingly been investigated for PFAS adsorption in both water and soil. In addition to stabilization of contaminants, biochar also contributes to climate change mitigation by locking up carbon from rapidly decomposing biomass, thereby reducing potential emissions of CO<sub>2</sub> to the atmosphere. The use of waste as the biomass for biochar production can further contribute to the transition into a more circular economy.

In this study, the effects of different waste-based biochars on sorption of PFAS in soil, was investigated through up-flow column percolation tests. A sandy soil with  $0.57 \pm 0.04\%$  TOC, originating from a former firefighting training facility in the Oslo region was used. The soil was contaminated with aqueous film forming foam (AFFF), containing mainly perfluorooctanesulfonic acid (PFOS), and was packed in columns with 1% (w/w) biochar. The experiment tested 6 different types of biochar, produced from the following 5 feedstocks: clean wood chip pellets (CWC), digested sewage sludge from two different WWTPs (DSS-1 and DSS-2), dewatered raw sewage sludge (DWSS) and waste timber (WT, activated and non-activated). As sludge often is contaminated with e.g., PFAS, handling and disposal can therefore be problematic. Using sludge in the production of biochar, instead of landfilling or incineration, can thus provide a more sustainable solution, as PFAS concentrations have been shown to be significantly reduced after pyrolysis. PFAS analyses were carried out for soil from the columns, for the original soil, and for leachate samples from each column collected at different liquid to solid ratios (L/S).

PFOS leaching was reduced in all columns amended with biochar, compared to the control column. The activated WT biochar and the three sewage sludge-based biochars (DSS-1, DSS-2, DWSS) proved to be better sorbents for PFAS originating from the AFFF contaminated soil, than the two non-activated wood-based sorbents (CWC and WT). The leaching of PFOS by biochar amendment was reduced in the following order: aWT (99.9%) > DWSS ( $98.9 \pm 0.24\%$ ) > DSS-2 (97.8%) > DSS-1 (91.6%) >> CWC ( $42.4 \pm 5.1\%$ ) > WT (33.7%). Distribution coefficients for PFAS sorption to biochar ( $\log K_d$ , L/kg) showed similar trends and were highest for sorption to the aWT (e.g.,  $\log K_d$  PFOS = 5.09 L/kg). In addition, the four best sorbents also

showed reductions of dissolved organic carbon (DOC) concentrations in the leachate. Evaluation of possible DOC-facilitated transport of PFAS in the aqueous phase led to the conclusion of DOC concentrations having a significant effect on PFAS concentrations in the leachate, for PFAS with CF-chains shorter than 8. Stronger PFAS sorption was seen with longer CF-chain lengths. The higher sorption strength of the aWT and the sludge-based biochars, were explained by larger pore diameters ( $> 0.7$  nm) which were able to accommodate the detected PFAS with maximum molecular diameters of 1.02 - 2.2 nm, whereas the majority of the pores in CWC and WT were too small to accommodate PFAS.

This is the first ex-situ column study to show that waste/sludge-based biochars can be an effective alternative to e.g. fossil based activated carbon for remediation of PFAS contaminated soil. Furthermore, the application of waste-based sorbents for cleaning of contaminated soil, contributes to circular economy, by utilizing waste fractions as a resource, reducing the content of contaminants in the biochar after pyrolysis, and stabilizing contaminants in soil, in addition to sequestering carbon. A special case of this was the very effective treatment of PFAS contaminated soil by amendment with the DWSS biochar, which was made from sewage sludge contaminated with PFAS originating from the same firefighting training facility as the soil.

## Sammendrag

Utbredt bruk av per- og polyfluorerte alkylforbinner (PFAS) i flere tiår har medført verdensomspennende jord- og grunnvannsforurensing, grunnet egenskaper som gir høy mobilitet og gjør dem vanskelig å bryte ned. Det finnes få eksisterende behandlingsmetoder som er egnet til å fjerne PFAS fra jord og vann, og det er derfor nødvendig med utvikling av nye alternativer. Biokull er et karbonholdig materiale som produseres når biomasse varmes opp uten tilgang på oksygen, og har i senere år i økende grad blitt undersøkt for bruk til PFAS adsorpsjon i både vann og jord. I tillegg til stabilisering av miljøgifter, er biokullbruk også et tiltak mot klimaendringer, ettersom pyrolyseprosessen binder karbon fra rask nedbrytbar biomasse, og dermed reduserer potensielle utslipp av CO<sub>2</sub> til atmosfæren. Bruken av avfall som biomasse til biokull produksjon kan ytterligere bidra til overgangen mot en mer sirkulær økonomi.

I denne masteroppgaven er effekten av avfallsbaserte biokull til sorpsjon av PFAS i jord blitt undersøkt vha. kolonneforsøk. En sandig jord fra et tidligere brannøvingsfelt i Oslo området, med et TOC innhold på  $0.57 \pm 0.04\%$ , ble brukt i forsøket. Jorden var forurensset med PFAS holdig brannskum, som hovedsakelig inneholdt perfluorooctansulfonsyre (PFOS), og ble pakket i kolonner med 1% (w/w) biokull. Eksperimentet testet 6 ulike typer av biokull, som var produsert av fem forskjellige avfallsmaterialer: pellets av treflis (CWC), utrånnet avløpsslam fra to forskjellige renselanlegg (DSS-1 og DSS-2), avvannet avløpsslam (DWSS) og resttrevirke (WT, aktivert og ikke-aktivert). Avløpsslam er ofte forurensset med f.eks. PFAS, og derfor kan håndtering og deponering av slam være problematisk. Bruk av slam til produksjon av biokull i stedet for deponering eller forbrenning, kan derfor være en mer bærekraftig løsning, da PFAS konsentrasjoner i biokull har vist seg å bli signifikant redusert etter pyrolyse. PFAS analyser ble utført på jorden fra kolonnene, på den originale jorden, og på eluatprøver fra hver kolonne, tatt ved ulike væske-faststoff-forhold (L/S).

PFOS utlekking ble redusert i alle kolonner hvor biokull var tilsatt, sammenlignet med kontrollkolonnen. Det aktiverte WT biokullet og de tre slambaserte biokullprøvene (DSS-1, DSS-2 og DWSS) viste seg å være bedre sorbenter for PFAS enn de to ikke-aktiverte tre-baserte biokullprøvene (CWC og WT). Tilførsel av biokull reduserte utlekkingen av PFOS i følgende rekkefølge: aWT (99.9%) > DWSS ( $98.9 \pm 0.24\%$ ) > DSS-2 (97.8%) > DSS-1 (91.6%) >> CWC ( $42.4 \pm 5.1\%$ ) > WT (33.7%). Fordelingskoeffisienter for PFAS sorpsjon til biokull ( $\log K_d$ , L/kg) viste liknende tendenser og var høyest for sorpsjon til aWT (f.eks.  $\log K_d$  PFOS = 5.09 L/kg). I tillegg viste de fire beste sorbentene reduserte konsentrasjoner av løst organisk

karbon (DOC) i utlekkingsvannet. Muligheten for transport av PFAS via DOC-PFAS-komplekser i vannfasen ble vurdert vha. linear regresjon, og det ble konkludert at DOC konsentrasjonen hadde en signifikant effekt på PFAS konsentrasjonen i vannfasen, gjeldene for PFAS med CF-kjedelengde mindre enn 8. For PFAS med lengre CF-kjeder ble det observert sterkere sorpsjon. Den høyere sorpsjonsstyrken for aWT biokullet og de slambaserte biokullprøvene kan forklares med at de hadde et større porevolum for porer med diameter  $> 0.7$  nm, noe som gjorde det mulig å romme de aktuelle PFAS med maksimale molekyllære dimensjoner på 1.02 - 2.2 nm. I motsetning til dette var flertallet av porene i CWC og WT biokullene for små til å romme PFAS molekylene.

Dette er det første studiet med ex-situ kolonnetester som viser at avfall/slambaserte biokull kan være et effektivt alternativ til f.eks. fossilbaserte aktiverte biokull til stabilisering av PFAS forurenset jord. I tillegg bidrar stabilisering av forurenset jord med avfallsbaserte biokull også til en sirkulær økonomi. Dette gjøres ved å utnytte avfallsfraksjoner som ressurs, redusere mengden av miljøgifter i biokullet etter pyrolyse, og stabilisere forurensing i jord, i tillegg til å binde karbon. Et spesielt godt eksempel på dette var den effektive stabiliseringen av PFAS forurenset jord ved tilførsel av DWSS biokull, som var produsert av PFAS forurenset slam med opprinnelse fra et avløpsrensaneanlegg som er påvirket av forurensing fra samme brannøvingsfelt som jorden.

[This page has been left blank intentionally]

## Preface

This thesis concludes my master's degree in Environment and Natural Resources (Miljø og Naturressurser) at the Norwegian University of Life Sciences, faculty of Environmental Sciences and Natural Resource Management (MINA). The thesis is estimated to 60 ECTS points, and the work presented was carried out from mid-August 2022 to mid-May 2023. The work was done in collaboration with the Norwegian Geotechnical Institute (NGI) in Oslo, as part of the research project Valorization of Organic Waste into Sustainable Products for Clean-up of Contaminated Water, Soil, and Air (VOW), which partly is funded by the Research Council of Norway.

The main supervisor of this project was Gerard Cornelissen, while Erlend Sørmo was co-supervisor. Gerard is the project leader of the VOW project, while Erlend is taking his PhD within the project. This thesis builds on the work done by Erlend and Katinka Krahn for her master thesis (NMBU, 2022), which also was part of the VOW project.

The VOW project is a joint industry project in sustainable development (BIA-Bærekraft) led by NGI in collaboration with Lindum AS, Scanship AS, VEAS, Mivanor AS, SINTEF Energy Research AS and VESAR, while University of Florida (USA), Agroscope (Switzerland), Huan University (China) and the Technical University of Denmark, DTU, are academic partners of the project. The project is planned to end in 2023.

During the 9 months of working on this thesis, my interest in research of environmental science and organic chemistry has grown, and I am very pleased with the work I am presenting here. Furthermore, I feel very lucky that I got the opportunity to carry out the PFAS analysis of my samples with the help of Junjie Zhang, at the Norwegian University of Science and Technology (NTNU) in Trondheim, with financial support from NGI. The two weeks I spend in the lab, at the Department for Chemistry, was both challenging with a very steep learning curve and rewarding, as this was one of my first times being introduced to advanced analytical chemistry. I am also very proud to tell that my work was accepted for an oral presentation at the Biochar Summit 2023, which I will attend the 13<sup>th</sup> and 14<sup>th</sup> of June. Furthermore, together with my supervisors and the VOW project, I hope to publish my results as a research paper in a peer-reviewed journal later this year.

Norwegian University of Life Sciences, 15.05.2023

*Clara Benedikte Mader Lade*



## Acknowledgments

First and foremost, I would like to thank my supervisors, Gerard Cornelissen and Erlend Sørmo, for great supervision and knowledge sharing. They have believed in me and pushed me to write an even better thesis, with their high expectations and good ideas. Their knowledge and passion for environmental science have truly inspired me.

I am also very grateful for all the help I got from Junjie Zhang, both for helping me process more than 100 samples at NTNU, but also for answering my countless questions on e-mail about peak integration and calculation of PFAS concentrations.

I also owe a big thank you to Geir Wold Åsli, who assisted me in setting up the 9 columns, and for helping whenever there was a problem that I could not solve on my own.

Andreas Botnen Smebye also deserves a thank you, for the idea and help on how to compute  $K_d$  values from my data via a model. Even though this was a much more difficult method, it was all worth it for the better results.

Furthermore, I am very grateful for the discussions and good ideas from Michel Hubert. His positive attitude and encouraging words have truly helped me through some of the tougher periods.

A special thanks to Nicolas Estoppey, Viona Demmer and Caroline Berge Hansen, who made the long days in the lab a bit more fun. Furthermore, their help in the lab also meant a great deal to me. The help from Karen Ane Skjennum for picking up the soil at Orendalen also deserves a thank you. Help and assistance from Katinka Muri Krahn for both writing a great master thesis and research paper that I could build my results on, and her help with many other things, was deeply appreciated.

I am also very grateful for being allowed to use the lab at NGI, and work from their office. In addition, all the nice employees at NGI deserves a thanks, both for asking me how I was doing, the help with small and big things, and for including me in different activities.

Lastly, I would like to thank my family and friends for the help and support during the last 9 months. Especially I want to thank my boyfriend for being so supportive and understanding during particularly the last stages of writing. He also joined me on my two weeks trip to NTNU, which was much appreciated.

[This page has been left blank intentionally]

## Abbreviations

<b>AC</b> Activated carbon	<b>GenX</b> 2,3,3,3-tetrafluoro-2-(1,1,2,2,3,3,3-heptafluoropropoxy)-propanoate
<b>AFFF</b> Aqueous film forming foam	<b>GW</b> Groundwater
<b>BC</b> Biochar	<b>IS</b> Internal standard
<b>CWC</b> Clean wood chips	<b>LCA</b> Life cycle assessment
<b>diSAMPAP</b> bis[2-(N-ethylperfluorooctane-1-sulfonamido)ethyl] phosphate	<b>LC-MS/MS</b> Liquid chromatography coupled with tandem mass spectrometry
<b>DOC</b> Dissolved organic carbon	<b>LOD</b> Limit of detection
<b>DSS-1</b> Digested sewage sludge 1	<b>LOQ</b> Limit of quantification
<b>DSS-2</b> Digested sewage sludge 2	<b>LSE</b> Liquid-solid extraction
<b>DWD</b> Drinking Water Directive	<b>L/S</b> Liquid to solid ratio
<b>DWSS</b> Dewatered sewage sludge	<b>MeOH</b> Methanol
<b>ECHA</b> European Chemicals Agency	<b>MQ</b> Milli-Q water
<b>EEA</b> European Economic Area	<b>NGI</b> Norwegian Geotechnical Institute
<b>EFSA</b> European food safety authority	<b>PAC</b> powdered activated carbon
<b>ESI</b> Electrospray ionization	<b>PES</b> Polyether sulfone
<b>FOSA</b> Perfluorooctanesulfonamides	<b>PFAA</b> Perfluoroalkyl acids
<b>FOSAA</b> Perfluorooctanesulfonamidoacetic acids	<b>PFAS</b> per- and polyfluoroalkyl substances
<b>FTS</b> Fluorotelomer sulfonates	<b>PFBS</b> Perfluorobutanesulfonic acid
<b>6:2 FTS</b> 1H,2H-Perfluorooctane sulfonate (6:2)	<b>PFCA</b> Perfluoroalkyl carboxylic acids
<b>8:2 FTS</b> 1H,2H-Perfluorodecan sulfonate (8:2)	<b>PFHpA</b> Perfluoroheptanoic acid
<b>GAC</b> Granular activated carbon	<b>PFHxA</b> Perfluorohexanoic acid
	<b>PFHxS</b> Perfluorohexanesulfonic acid
	<b>PFOA</b> Perfluorooctanoic acid

<b>PFOS</b> Perfluorooctanesulfonic acid	<b>REACH</b> Registration, Evaluation, Authorisation and Restriction of Chemicals
<b>PFOSA</b> Perfluorooctane sulfonamide	
<b>PFPA</b> Perfluoroalkyl phosphonic acids	<b>SA</b> Surface area
<b>PFPIA</b> Perfluoroalkyl phosphinic acids	<b>SaMPAP</b> Perfluorooctane sulfonamidoethanol-based phosphate
<b>PFSA</b> Perfluoroalkane sulfonic acids	<b>SPE</b> Solid phase extraction
<b>PMT</b> Persistent, Mobile and Toxic substances	<b>SVHC</b> Substances of Very High Concern
<b>vPvM</b> very Persistent and very Mobile substances	<b>TA</b> Target analyte
<b>POM</b> Polyoxymethylene	<b>TIC</b> Total inorganic carbon
<b>POPs</b> Persistent Organic Pollutants	<b>TOC</b> Total organic carbon
<b>PP</b> Polypropylene	<b>TWI</b> Tolerable weekly intake
<b>PV</b> Pore volume	<b>VOW</b> Valorization of Organic Waste
<b>PZC</b> Point of zero charge	<b>WWTP</b> Wastewater treatment plant
	<b>ZeroPM</b> Zero pollution of persistent, mobile substances

## Symbols

<b>AF</b> Attenuation factor	<b>k<sub>rap</sub></b> Rate constant for rapid PFAS desorption from soil
<b>AR</b> Absolute recovery	<b>k<sub>slow</sub></b> Rate constant for slow PFAS desorption from soil
<b>C<sub>leachable</sub></b> Cumulative concentration of PFAS leached from the soil	<b>k<sub>w</sub></b> Flow rate of water through the column
<b>C<sub>s</sub></b> Concentration of PFAS in solid phase	<b>M(t)<sub>measured</sub></b> Mass of PFAS in soil over time, measured
<b>C<sub>soil</sub></b> Concentration of PFAS in soil	<b>M(t)<sub>modelled</sub></b> Mass of PFAS in soil over time, modelled
<b>C<sub>w</sub></b> Concentration of PFAS in aqueous phase	<b>M<sub>desorbed,total</sub></b> Cumulative desorbed mass of PFAS after L/S 5
<b>D<sub>eff</sub></b> Effective cross-sectional diameter of PFAS molecule	<b>ME</b> Matrix effect
<b>D<sub>max</sub></b> Maximum diameter of PFAS molecule	<b>M<sub>soil,dw</sub></b> Mass of soil in the column in dry weight
<b>F<sub>rap</sub></b> Fraction of rapid PFAS desorption from soil	<b>M<sub>tot</sub></b> Total mass of PFAS
<b>F<sub>slow</sub></b> Fraction of slow PFAS desorption from soil	<b>n<sub>F</sub></b> Freundlich coefficient of non-linearity
<b>K<sub>d</sub></b> Solid-liquid distribution coefficient	<b>pK<sub>a</sub></b> Acid dissociation constant
<b>K<sub>d,BC</sub></b> Biochar-water distribution coefficient	<b>R</b> Retardation factor
<b>K<sub>d,soil</sub></b> Soil-water distribution coefficient	<b>RR</b> Relative recovery
<b>K<sub>d,tot</sub></b> Soil+biochar-water distribution coefficient	<b>V<sub>w</sub></b> Volume of eluate sample
<b>K<sub>F</sub></b> Freundlich distribution coefficient	<b>θ</b> Porosity of soil
<b>k<sub>PFAS</sub></b> Rate constant for PFAS desorption from soil	<b>ρ<sub>b</sub></b> Bulk density of soil

# Table of Contents

<b>ABSTRACT</b> .....	<b>III</b>
<b>SAMMENDRAG</b> .....	<b>V</b>
<b>PREFACE</b> .....	<b>VIII</b>
<b>ACKNOWLEDGMENTS</b> .....	<b>IX</b>
<b>ABBREVIATIONS</b> .....	<b>XI</b>
<b>SYMBOLS</b> .....	<b>XIII</b>
<b>1 GENERAL INTRODUCTION</b> .....	<b>1</b>
<b>2 CHARACTERISTICS OF PFAS, SOIL REMEDIATION AND BIOCHAR</b> .....	<b>3</b>
2.1 PFAS .....	3
2.1.1 AFFF.....	3
2.1.2 Classification and properties .....	4
2.1.3 PFAS in the environment .....	5
2.1.4 Regulation of PFAS .....	6
2.2 SOIL REMEDIATION.....	8
2.2.1 Soil excavation.....	8
2.2.2 Soil washing.....	8
2.2.3 Destruction technologies.....	9
2.2.4 Biological remediation .....	10
2.2.5 Immobilisation.....	10
2.3 BIOCHAR.....	12
2.3.1 Application of biochar .....	14
2.3.2 Surface chemistry influencing adsorption .....	14
2.4 MECHANISMS INFLUENCING PFAS SORPTION.....	15
2.4.1 Hydrophobic interactions .....	15
2.4.2 Electrostatic interactions.....	15
2.4.3 Hydrogen bonding.....	16
2.4.4 Acid dissociation constants ( $pK_a$ ).....	16
2.4.5 Sorption attenuation .....	17
2.5 OBJECTIVES .....	18
2.6 HYPOTHESES.....	18
<b>3 MATERIALS AND METHODS</b> .....	<b>20</b>
3.1 BIOCHAR SORBENTS .....	20
3.1.1 Pyrolysis.....	21

3.2	SOIL .....	22
3.2.1	<i>Grain size distribution analysis</i> .....	23
3.3	COLUMN EXPERIMENT .....	23
3.3.1	<i>Triplicates</i> .....	24
3.3.2	<i>Mixing of soil and biochar</i> .....	24
3.3.3	<i>Column setup and packing</i> .....	24
3.3.4	<i>Start-up of the leaching test</i> .....	26
3.4	SAMPLE PREPARATION FOR ANALYSIS .....	27
3.4.1	<i>Splitting of samples</i> .....	27
3.4.2	<i>pH and electrical conductivity</i> .....	28
3.4.3	<i>DOC and TOC analysis</i> .....	28
3.5	INSTRUMENTAL ANALYSIS OF PFAS .....	29
3.5.1	<i>Solid-phase extraction (SPE) of leachate samples</i> .....	29
3.5.2	<i>Liquid-solid extraction (LSE) of soil samples</i> .....	30
3.5.3	<i>LC-MS/MS</i> .....	31
3.5.4	<i>Quality assurance and quality control</i> .....	32
3.6	DATA ANALYSIS .....	35
3.6.1	<i>PFAS leaching</i> .....	35
3.6.2	<i>Distribution coefficients (<math>K_d</math>)</i> .....	36
3.6.3	<i>Groundwater infiltration based on L/S ratios</i> .....	40
3.7	DATA HANDLING.....	40
3.8	UNCERTAINTY .....	40
3.8.1	<i>Relative standard deviation</i> .....	41
<b>4</b>	<b>RESULTS AND DISCUSSION .....</b>	<b>43</b>
4.1	BIOCHAR PROPERTIES .....	43
4.1.1	<i>Pore volume and surface area</i> .....	44
4.1.2	<i>Point of zero charge</i> .....	48
4.2	PFAS IMMOBILISATION BY BIOCHAR AMENDMENT .....	49
4.2.1	<i>Reduction of PFAS in leachate</i> .....	53
4.3	DOC-FACILITATED PFAS TRANSPORT AND TOC INFLUENCE .....	56
4.3.1	<i>PFAS and DOC correlation</i> .....	58
4.4	DISTRIBUTION COEFFICIENTS ( $K_d$ ).....	61
4.4.1	<i>Link between <math>K_d</math> and PFAS properties</i> .....	66
4.4.2	<i>Attenuation factor</i> .....	68
4.5	ESTIMATION OF GROUNDWATER CONTAMINATION WITH PFAS.....	71
<b>5</b>	<b>CONCLUSION, IMPLICATIONS AND FURTHER WORK .....</b>	<b>74</b>
5.1	WIDER IMPLICATIONS .....	76

5.1.1	Remediation of the AFFF-affected site .....	76
5.2	RECOMMENDATIONS FOR FURTHER WORK .....	79
<b>8</b>	<b>BIBLIOGRAPHY .....</b>	<b>80</b>
<b>APPENDIX A</b>	<b>PH AND ELECTRICAL CONDUCTIVITY .....</b>	<b>90</b>
<b>APPENDIX B</b>	<b>GRAIN SIZE DISTRIBUTION ANALYSIS .....</b>	<b>91</b>
<b>APPENDIX C</b>	<b>DOC AND TOC ANALYSIS .....</b>	<b>92</b>
<b>APPENDIX D</b>	<b>LC-MS/MS.....</b>	<b>94</b>
D.1	QA/QC AND INSTRUMENT PARAMETERS .....	94
D.2	LIST OF ANALYSED PFAS.....	96
<b>APPENDIX E</b>	<b>PFAS CONCENTRATIONS IN LEACHATE AND SOIL .....</b>	<b>101</b>
E.1	PFAS LEACHATE CONCENTRATIONS .....	101
E.2	PFAS SOIL CONCENTRATIONS.....	107
E.3	PFAS MASS BALANCES.....	110
<b>APPENDIX F</b>	<b>RECOVERY TEST .....</b>	<b>112</b>
<b>APPENDIX G</b>	<b>REFERENCE SOIL.....</b>	<b>117</b>



# 1 General Introduction

The increasing soil- and groundwater contamination with organic substances, is a widespread problem around the globe. In many cases, the uncontrolled spread of chemicals compromises the quality of our drinking water, or in worst case scenarios expose people to hazardous chemicals with acute or chronic effects.

In the last couple of years, a group of "forever chemicals" called PFAS (per- and polyfluoroalkyl substances) has been getting increasing attention in the media, due to their use in many consumer products (Egge, 2021; Salvidge, 2022; Tvede & Bech, 2023). These chemicals have many beneficial properties as being both water- and oil repellent as well as heat resistant, but also have a downside of being mobile, bioaccumulative, and persist in the environment for longer than any other synthetical substances (Buck et al., 2011; ECHA, 2023b; OECD, 2013). As a result of the widespread use, these compounds seem to appear in the environment in increasing amounts, contaminating soil, air, surface- and groundwater (ECHA, 2023b; Prevedouros et al., 2006). Some PFAS also pose risk to human health, harming the development of foetuses, lowering fertility and acting as endocrine disruptors, in addition to potentially being carcinogenic (ECHA, 2023b).

Only a few PFAS are restricted and regulated today, mostly perfluorooctanesulfonic acid (PFOS) and perfluorooctanoic acid (PFOA) (Lovdata, 2004; Stockholm Convention, 2019), causing a continuous release to the environment. Another problem is the ongoing development of new PFAS compounds with similar properties for industrial purposes, to evade restrictions and regulations of existing PFAS, such as perfluorobutanesulfonic acid (PFBS) and 2,3,3,3-tetrafluoro-2-(1,1,2,2,3,3,3-heptafluoropropoxy)-propanoate (GenX) substituting respectively for PFOS and PFOA (ECHA, 2023b; Norden, 2013). Though, stricter and wider regulations are being proposed and evaluated by the European Chemicals Agency (ECHA), such as an European restriction on all types of PFAS, proposed by five European countries including Norway (ECHA, 2023b).

It is thus important to regulate the production and use of PFAS. However, it is also of great importance to remediate and limit the spread of already existing PFAS contamination. Today there exists a wide selection of options for remediation of soil contamination, such as biological degradation, chemical oxidation, stabilization and thermal treatment processes (Ross et al., 2018; Travar et al., 2020). However, many of these treatments only have limited effect on PFAS, due to their unique properties and behaviour in the environment, which changes with

structure and chain length. Shorter chained PFAS have been shown to create higher difficulty for conventional treatment technologies and remediation methods, due to their high mobility, compared to PFAS with longer chains which are more hydrophobic (Hale et al., 2016; Mahinroosta & Senevirathna, 2020; Ross et al., 2018). Furthermore, many of the current treatment methods that might work on PFAS are not very sustainable, due to being energy intensive, destroys the soil and soil organisms, disturbance of biodiversity, high carbon emissions and generally entail high environmental impacts (Mahinroosta & Senevirathna, 2020; Ross et al., 2018; Sparrevik et al., 2011; Travar et al., 2020). Hence, there is a great need for new technologies, both in- and ex-situ, for clean-up and remediation of PFAS affected sites. The use of waste-based biochars for stabilization of PFAS contaminated soil show promising results as a technology that are both sustainable and highly effective on PFAS (Krahn et al., 2023). This thesis will thus present and assess this novel technology for PFAS stabilization in soil.

## 2 Characteristics of PFAS, soil remediation and biochar

### 2.1 PFAS

Per- and polyfluoroalkyl substances (PFAS) is a large group of synthetic fluorinated aliphatic organic chemicals which have substituted all H atoms for F atoms on at least one moiety, and have the general formula  $C_nF_{2n+1}$  – (Buck et al., 2011; ECHA, 2023b; OECD, 2013). The definition of PFAS has since been revised by OECD (2021), to define all fluorinated substances containing "*at least one fully fluorinated methyl or methylene carbon atom (without any H/Cl/Br/I to attached to it).*", though with a few exceptions. This means that any substance with a perfluorinated methyl or methylene group ( $-CF_3, -CF_2-$ ) can be denoted PFAS. The C-F bond is very strong and stable, making these compounds persistent in the environment as there is no evidence of biodegradation of PFAS, and the group is thus called "forever-chemicals" (Buck et al., 2011; Kissa, 2001b; Krafft & Riess, 2015). The growing list include more than 12,000 substances registered as PFAS (EPA, 2021). The structure of PFAS can also generally be described as a fluorinated hydrophobic "tail" and a hydrophilic "head", which gives these compounds the unique surfactant properties of being both water and oil repellent while having a hydrophilic head, resulting in lower surface tension of a liquid or interfacial tension of liquid and solid (Buck et al., 2011; Ross et al., 2018). The longer the hydrophobic and oleophobic "tail" is, the less water soluble the compound is. This property makes them convenient for many everyday products, such as non-stick coatings for e.g., pans, waterproof textiles, paper and packaging but are also seen in e.g., cosmetics and for medical uses (Buck et al., 2011; Mahinroosta & Senevirathna, 2020; OECD, 2013). Another property of PFAS is heat resistance, making them ideal for use in firefighting foams (e.g., aqueous film forming foam, AFFF) and other firefighting equipment as protective clothing (Buck et al., 2011; OECD, 2013). PFAS have been used widely for these industrial and commercial purposes since the 1950s, and consequently this group of chemicals have been detected in the environment and organisms (Buck et al., 2011).

#### 2.1.1 AFFF

Aqueous film forming foam (AFFF) is one of the most commonly used foams in firefighting and has been extensively applied by fire-fighters to extinguish petroleum- or other flammable liquid fires, due to its surfactant properties (Norden, 2013). The inclusion of typically PFOS, PFOA and fluorotelomer compounds makes the foam thermally stable and decreases surface tension. It furthermore gives the foam abilities to form a thin film, which spreads and seals out oxygen by coating the burning liquid, thereby extinguishing the fire and preventing reignition

(Dauchy et al., 2017; Schaefer et al., 2008). The use of AFFF is often associated with firefighting training facilities at military- and civil airports, but is also used at municipal fire departments and oil refineries, among other places (Dauchy et al., 2017; Norden, 2013; Paul et al., 2009). Investigations of firefighting training facilities in Norway has shown contamination with PFAS from AFFF at several airports including Oslo airport at Gardermoen (Avinor, 2012; Høisæter et al., 2019; Høisæter & Breedveld, 2022). The use of PFOS in AFFF at the firefighting training facilities owned by Avinor (state-owned company operating most civil airports in Norway) was phased out in 2001, while foam containing PFAS was phased out in 2012 (Avinor, 2012). The use of PFOS in AFFF was banned in Norway in 2007 (Avinor, 2012), while organofluorine AFFF was banned in 2011 (Hale et al., 2016).

### 2.1.2 Classification and properties

PFAS can be divided into different groups depending on their properties and chemical structure. A general classification given by OECD (2013), divides PFAS into non-polymers and polymers. In this thesis the main focus will be on non-polymers, more specifically perfluoroalkyl acids, as this group includes the compounds typically found in AFFF and are the most well-studied group of PFAS.

Perfluoroalkyl acids (PFAA) covers four different sub-groups: perfluoroalkyl carboxylic acids (PFCA), perfluoroalkane sulfonic acids (PFSA), perfluoroalkyl phosphonic acids (PFPA) and perfluoroalkyl phosphinic acids (PFPiA) (OECD, 2013), of which the two first are of interest for this thesis. PFCA covers compounds with a fluorinated carbon chain differing in length and a carboxylic acid functional group. PFSA have a fluorinated carbon chain similar to PFCA, but their functional group is a sulfonic acid instead. Other non-polymers of interest in this thesis are fluorotelomer sulfonates (FTS), perfluorooctanesulfonamides (FOSA), perfluorooctanesulfonamidoacetic acids (FOSAA), and perfluorooctane sulfonamidoethanol-based phosphate (SaMPAP). FTS are very similar to PFSA, as they share the same functional group, but differs in the chain construction, having two CH<sub>2</sub> moieties located between the CF-chain and the sulfonic acid functional group. This makes it possible for them to degrade to PFSA and can therefore be referred to as precursors. The groups of FOSA and FOSAA covers similar molecules with CF-chain lengths of 8. FOSA have a sulfonamide functional group that may have a methyl or ethyl group attached to it. FOSAA have similar constructions but have in addition a carboxylic acid attached to the sulfonamide group. SaMPAP consists of a group of N-ethylfluorooctanesulfonamidoethanol-based polyfluoroalkyl phosphate esters, which might occur as diesters, and are also considered possible PFOS precursors (Benskin et al., 2012).

The chain length of PFAS will determine different properties of the compound such as ability to bioaccumulate, solubility and sorption efficiency, where long chained PFAS are considered more bioaccumulative, less water soluble and have higher sorption efficiency than short-chain PFAS (Buck et al., 2011; Higgins & Luthy, 2006). PFCA with 7 and more perfluoroalkyl carbons, PFSA with 6 and more perfluoroalkyl carbons, and other PFAS with a carbon chain length of 7 or more, are referred to as long-chain PFAS (Buck et al., 2011; OECD, 2013; Ross et al., 2018).

Many PFAS, such as the PFAA, are acids. These are either present as protonated or anionic form, depending on their acid dissociation constant ( $pK_a$ ) and pH of the environment they occur in (Buck et al., 2011). Properties of the acid functional group are further described in section 2.4.

### 2.1.3 PFAS in the environment

The emission of PFAS to the environment can originate from many different sources, both direct and indirect. Sources of direct emission may be from the manufacture of PFAS containing products via wastewater, gases, or solid waste, or the use and disposal of the products (OECD, 2013; Prevedouros et al., 2006). The use of firefighting foam also leads to direct spread of PFAS to soil and water from point sources (Prevedouros et al., 2006). Indirect sources include chemical reaction impurities or degradation of precursors, either biotically or abiotically, which then form other PFAS (Buck et al., 2011; Prevedouros et al., 2006).

When first emitted to the environment, PFAS are transported via different routes depending on their physicochemical properties and persist due to their strong chemical bonds, possibly exposing humans via food, drinking water, dust, and air, among other things (Fromme et al., 2009). The transportation of PFAS in soil may both happen in the saturated and unsaturated zone due to the hydrophilic functional group, but adsorption to soil might also occur, depending on different soil parameters as soil mineralogy, pH, clay and organic carbon content (Mahinroosta & Senevirathna, 2020).

Large amounts of PFAS also ends up at wastewater treatment plants, potentially accumulating longer chained PFAS in the sewage sludge (Bolan et al., 2021). This produces a lot of problems, as conventional treatment of wastewater is not able to efficiently remove PFAS from the water or sludge (Bolan et al., 2021).

#### 2.1.4 Regulation of PFAS

Hardly any PFAS out of the thousands registered, are today regulated or restricted in Norway and the European Union. The current Norwegian normative value for soil is 0.1 mg/kg d.w. and does only apply to PFOS, where concentrations above this threshold are categorised and must be handled as contaminated soil (Lovdata, 2004). In 2019 a new normative value of 0.003 mg/kg d.w. for both PFOS and PFOA was suggested by the Norwegian Geotechnical Institute (NGI) at the request of the Norwegian Environment Agency (NGI, 2020), though the proposed value has not been implemented. A safety threshold for PFAS in food was established in 2018 by the European food safety authority (EFSA), for the tolerable weekly intake (TWI) for PFOS and PFOA of 13 ng and 6 ng per body weight, respectively (EFSA Panel on Contaminants in the Food Chain, 2018). However, in 2020 a new TWI was set by EFSA of 4.4 ng per kg of body weight for the sum of PFOA, PFNA (perfluorononanoic acid), PFHxS (perfluorohexanesulfonic acid) and PFOS (EFSA Panel on Contaminants in the Food Chain, 2020). For drinking water, no official limit for PFAS have been established in Norway. In 2020 EU's Drinking Water Directive (DWD) from 1998 was revised and modified to include limit values for PFAS in drinking water (ECHA, 2023d). The DWD now includes limit values for the total concentration of PFAS in drinking water of 0.50 µg/L, and the sum of 20 selected PFAS of 0.10 µg/L, which are considered a concern for human consumption, where either one or both of the limits can be used (European Union, 2020). The DWD are not enacted in the European Economic Area (EEA) yet, but are under assessment (Regjeringen.no, 2023). The new limit values will first come into force by 12<sup>th</sup> January 2026, where member states must ensure to meet the values for water intended for human consumption (European Union, 2020).

Only two PFAS are targeted as Persistent Organic Pollutants (POPs) and regulated as this class of chemicals. POPs are a class of chemicals which persist in the environment and accumulate in tissues of living organisms, thus pose a risk for their health and the environment, and are regulated through the Stockholm Convention and Aarhus Protocol (ECHA, 2023c). ECHA (2023c) states that this class includes pesticides, industrial chemicals and unintentional by-products formed during industrial processes, degradation, or combustion. These pollutants have many transportation paths, including air, water and migratory species, resulting in spread to remote areas where they never have been produced or used (ECHA, 2023c). Only PFOS and PFOA are regulated through this protocol, while PFHxS is expected to be included from the end of 2023 (ECHA, 2023b). PFOA is listed under compounds that must be eliminated from production and use, while PFOS should be restricted in production and use (Stockholm

Convention, 2019). PFHxS will be included in the same group as PFOA, requiring production and usage elimination. Proposed PFAS for listing and regulation as POPs under the convention as POPs, includes long-chain PFCA and related compounds. This covers PFCA with carbon chain lengths of 9 to 21 and their precursors (Stockholm Convention, 2019).

A few PFAS are listed as Substances of Very High Concern (SVHC) under the European Union regulation of chemicals REACH (Registration, Evaluation, Authorisation and Restriction of Chemicals), which lists substances that presumably can cause serious and irreversible effects on the environment and human health. Substances that are on the authorisation list include perfluoroheptanoic acid (PFHpA), PFBS and the PFOA-substitute GenX. Furthermore, some PFAS are on the candidate list, including PFOA, PFHxS and PFCA of carbon chain length 9-14 (ECHA, 2023b). Two similar groups of substances, also listed under REACH, are the Persistent, Mobile and Toxic substances (PMT) and very Persistent and very Mobile substances (vPvM) (Hale et al., 2020). These groups cover substances that pose a risk to drinking water resources, due to properties that allow them to persist and travel long distances in the aquatic environment. Substances recognized under these two groups can then be assessed by the European Member States and ECHA, whether they fulfil the criteria or not, to be included and identified as SVHC, and furthermore restricted.

In 2021 a new project called "ZeroPM: Zero pollution of persistent, mobile substances", were launched under the Chemicals Strategy for Sustainability Towards a Toxic-Free Environment by the EU (Hale et al., 2022). This project has the three main goals of prevent, prioritize, and remove persistent and mobile substances, that are a threat for the environment and human health, including a number of PFAS. The project strives to increase knowledge and guidance towards minimization of use, emission and pollution of entire substance groups that are persistent and mobile (Hale et al., 2022).

A new proposal for restriction of PFAS under REACH by five European countries (Germany, Denmark, the Netherlands, Sweden, and Norway) are now under evaluation by ECHA. The proposed ban will cover a wide range of production, placing and market uses of the whole substance class of PFAS, above a set concentration limit of 25 ppb for any PFAS measured with target PFAS analysis, 250 ppb for the sum of PFAS in a targeted analysis and 50 ppm for PFAS measured as total fluorine (ECHA, 2023a; ECHA, 2023b). Furthermore, an additional proposal for PFAS restriction, not included in the wider restriction, of all PFAS in firefighting foam are being evaluated by ECHA (ECHA, 2023b).

## 2.2 Soil remediation

Around 10,000 sites are today registered as suspected or identified to be contaminated in Norway, where about a thousand of these are heavily polluted and need to be remediated (Miljøstatus, 2023). If no actions are taken on these sites, the contaminants could harm the environment and humans living near the sites, in addition to being spread to surface- or groundwater. It is therefore important to know the source, the mobility, the toxicity, and the risk of the contamination. Despite the wide range of remediation options available today for contaminated sites, not all can be applied to PFAS contamination, due to the unique properties of this substance group. A few techniques, and their impact on PFAS, will be outlined here.

### 2.2.1 Soil excavation

A widely used remediation method is excavation and transportation of the soil to a landfill, "dig and dump". However, this strategy is getting less popular, since it roughly moves the problem from one site to another, and the landfilling is very costly (Hale et al., 2017; Ross et al., 2018; Travar et al., 2020). In addition, landfills are a burden to the area, and can ultimately damage the biodiversity and natural resources. Another reason for not preferring this method any longer, is the need for treatment and monitoring at landfills, which is not always fulfilled (Hale et al., 2017; Ross et al., 2018). Landfilled soils may be contained by barriers, but it is very difficult to ensure complete containment, allowing no infiltration, leaching or other disturbances. Particularly concerning PFAS contaminated soils, the substances with shorter chains may be especially prone to be released in the leachate, due to higher mobility, which can lead to contamination of drinking water (Knutsen et al., 2019; Mahinroosta & Senevirathna, 2020; Travar et al., 2020). Even if landfills have treatment of the leachate, many facilities are inadequate in removing PFAS, because of the treatment method not being suitable for PFAS removal (Busch et al., 2010; Travar et al., 2020).

### 2.2.2 Soil washing

Soil washing is a method that leaches PFAS from the soil particles and can be performed both in- and ex-situ (Bolan et al., 2021; Hale et al., 2017; Ross et al., 2018; Travar et al., 2020). The use of both water and other extraction agents as methanol/ammonium hydroxide, methanol/sodium hydroxide or acetonitrile can be used, depending on the method (Travar et al., 2020). Although water was found to extract more PFOS than methanol or acetonitrile from soil samples in the study by Hale et al. (2017), indicating that water was a better extraction agent. Hubert et al. (2023) found that separation of the coarse-grained and fine-grained fractions optimized the soil washing, and that PFAS with shorter chains were washed out using less water



than longer chained PFAS. Soil washing also creates less hazardous waste that needs handling or disposal at landfills. It is however important to treat the contaminated leachate after washing, to avoid any additional spread to the environment. Furthermore, the treatment is very energy-intensive and expensive on field scale, in addition to destroying all life in the soil (Mahinroosta & Senevirathna, 2020).

### 2.2.3 Destruction technologies

Contaminated soil can also be treated with destruction technologies, where the contaminants are directly destroyed in the soil by e.g., thermal treatment, ball milling or chemical oxidation (Mahinroosta & Senevirathna, 2020; Ross et al., 2018; Travar et al., 2020). However these methods are not the best options for remediation of PFAS, due to the strong C-F bonding and high melting points, as well as destruction of the soil not being very sustainable (Mahinroosta & Senevirathna, 2020).

#### Thermal treatment

Thermal treatment works by exposing the soil to high temperatures above the melting point of the compound, usually between 850 and 1200 °C (Mahinroosta & Senevirathna, 2020; Travar et al., 2020). The PFAS are then vaporized and thereby separated from the soil, while they subsequently are destroyed by the high temperatures (Mahinroosta & Senevirathna, 2020). Nevertheless, this method needs a high initial investment and have high operational costs, as high temperatures are required for vaporization and destruction of PFAS (Mahinroosta & Senevirathna, 2020).

#### Ball milling

Ball milling is a method where stainless steel balls, of 5 to 10 mm in diameter, and contaminated soil are rotated in a ball mill. This causes the soil particles to reduce in size and a reaction occurs at the chemical surfaces of the particles, destroying the contaminant (Mahinroosta & Senevirathna, 2020; Ross et al., 2018). The occurring reaction is referred to as mechanochemical destruction, which is caused by the mechanical force, resulting in potential generation of transient temperature rise, among other things (Bolan et al., 2021; Ross et al., 2018; Zhang, K. et al., 2013). Addition of co-milling agents, such as potassium hydroxide (KOH), may result in higher destruction percentage of PFAS (Mahinroosta & Senevirathna, 2020; Zhang, K. et al., 2013). However, this method also has some implications, as the structure of the soil itself is destroyed, and the possibility of soil organisms surviving this treatment is very low.

## Chemical oxidation

The use of highly reactive chemicals for oxidation of organic contaminants have shown to be effective at breakdown of PFAS to some extent (Ross et al., 2018). This method converts the contaminants to carbon dioxide or other substances with high capacity for degradation (Mahinroosta & Senevirathna, 2020). The conversion of precursors to PFAA and breakdown have been shown to be effective for PFCA, while degrading PFSA demonstrated more difficulty (Ross et al., 2018). The degradation efficiency when using chemical oxidation also depend on pH, temperature and the concentration of the oxidation agent (Travar et al., 2020). In addition, combination with other methods may be necessary to remove PFAS completely (Mahinroosta & Senevirathna, 2020). However, concerns of in-situ application include the significant generation of short-chain PFAS with higher mobility, in addition to disturbance of nearby drinking water sources by the discharge of highly reactive chemicals, if not extracted properly (Mahinroosta & Senevirathna, 2020; Ross et al., 2018).

### 2.2.4 Biological remediation

Biological remediation is advantageous to many other remediation methods, as it requires lower cost and less disruption to soil- and water environments (Mahinroosta & Senevirathna, 2020). The method can be used to clean up sites contaminated by different organic pollutants, either by microbial degradation of the pollutant through oxidation in aerobic conditions, or reduction in anaerobic conditions. However, application of bioremediation on PFAS is limited, as this group of substances do not readily biodegrade due to the strong C-F bonds (Mahinroosta & Senevirathna, 2020; Ross et al., 2018). Biotransformation of several PFAA to shorter chain PFAA (Ross et al., 2018), or fluorotelomer-based compounds into more stable compounds as PFOS and PFOA, may happen with microbial presence (Mahinroosta & Senevirathna, 2020; Travar et al., 2020).

### 2.2.5 Immobilisation

The immobilisation or stabilization of compounds in soil, can be carried out by amendment added to the soil which adsorbs or stabilizes the compounds. This results in reduced leaching and lower bioavailability of the contaminant (Smernik, 2009). There exist several different amendments for stabilization or adsorption of PFAS, including minerals, compost, biomaterials, resins, molecularly imprinted polymers, activated nanotubes, activated carbon (AC, either as powdered, PAC or granular, GAC) and biochar (Du et al., 2014; ITRC, 2018; Travar et al., 2020). The effectiveness of the amendments on PFAS depends both on soil

characteristics, PFAS chain length and functional groups, in addition to material specific properties (ITRC, 2018).

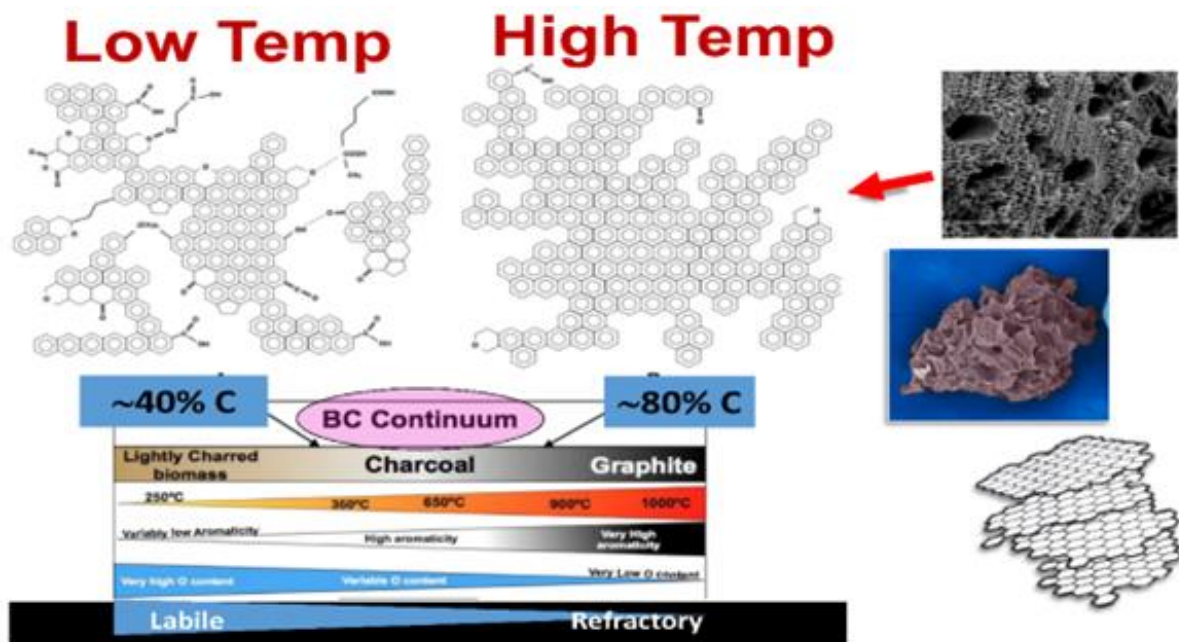
Carbonaceous materials have shown great potential for PFAS sorption and stabilization in soil, compared to other adsorbents (Bolan et al., 2021; Du et al., 2014; Söregård et al., 2019; Söregård et al., 2020). These carbonaceous sorbents include both biochar, which can be activated to AC, and AC derived from either fossil materials or biomass. In a study by Hale et al. (2017), sorption of AC, compost, and montmorillonite on AFFF contaminated soil were compared. The batch leaching tests showed that AC amendment resulted in almost complete removal of PFOS in the leachate, while compost and montmorillonite demonstrated much lower reduction percentages. Du et al. (2014) also reported that AC is widely used and is a very popular adsorbent, due to the low cost and broad applicability.

Some studies have shown that AC is a better sorbent than biochar for PFAS, though biochar also performs well on sorption of especially long-chained PFAS (Fabregat-Palau et al., 2022; Kupryianchyk et al., 2016; Söregård et al., 2020; Zhang & Liang, 2022). However, Sparrevik et al. (2011) found that fossil anthracite-based AC, made from coal originating from China, had a higher environmental impact than biomass derived AC made from coconut waste, using a Life Cycle Assessment (LCA) to evaluate the impact. This result was including the primary effect of using AC as amendment for remediating contaminated sediments and the materials' impact on the surrounding marine ecosystem. Additionally, the LCA revealed that using biomass derived AC had the same environmental impact as natural recovery, due to the positive effect of carbon sequestration. The conclusion that AC based on biomass instead of coal is more sustainable, suggests that non-activated biochar will have an even lower environmental impact than biomass-based AC, due to less energy and resource use when activation is excluded from the production. Even though activation of biomass- or coal-based AC have demonstrated higher sorption strength than biochar, recent studies have shown that when optimally engineered, biochar may be just as effective as AC or activated biochar for PFAS sorption and PFAS removal from wastewater (Krahn et al., 2023; Sørmo et al., 2021). Additionally, a co-benefit of biochar amendment is the contribution to carbon sequestration and thereby mitigation of climate change, which makes biochar even further attractive (Lehmann, 2007). Moreover, the use of waste fractions, such as crop residues, waste timber or sewage sludge, to produce biochar also contributes to the recycling of resources and are therefore a promising technology in a circular low carbon economy.

## 2.3 Biochar

Biochar is a carbonaceous material made from various types of biomasses, which has been heated in an oxygen-limited environment. This process is called pyrolysis. The biomass used for biochar production, also called feedstock, can consist of possibly any type of biomass, e.g., wood, crop residues or even manure, though the type of feedstock and pyrolysis temperature influences the properties of the biochar (Ahmad et al., 2014; Lehmann & Joseph, 2009). Organic material is thermally decomposed during pyrolysis, where increasing temperatures creates a product higher in carbon content, and mainly composed of a network of aromatic ring structures with fewer O's and H's attached, as illustrated on figure 1 (Zimmerman & Mitra, 2017). Most materials will leave their original structure imprinted in the biochar, thereby influencing physical and structural characteristics of the product. This will contribute to the majority of the microporosity in the biochar (Lehmann & Joseph, 2009). However, it is expected that the most influential structural parameter is the pyrolysis temperature, since many of the fundamental physical changes are temperature dependent (Ahmad et al., 2014; Lehmann & Joseph, 2009). Generally, it is seen that higher pyrolysis temperature leads to higher surface area, higher aromaticity and lower polarity, which result in more effective adsorption of hydrophobic organic contaminants to the biochar surface (Ahmad et al., 2014). Furthermore, increasing pyrolysis temperature also leads to a more refractory material (Zimmerman & Mitra, 2017). The product itself may resemble charcoal but differs in the aspects of production and intended use. While charcoal is produced for fuel and energy purposes, biochar has the intention of being used for environmental management (Ahmad et al., 2014).

Activation of biochar increases the porosity and surface area further, by opening new and widening already existing pores in the biochar, leading to increased sorption capacity (Downie et al., 2009; Hagemann et al., 2018). This treatment can be done as either chemical- or physical activation. Chemical activation is done by mixing the feedstock with an activation agent, where  $ZnCl_2$ , KOH or  $H_3PO_4$  are mostly used. The chosen activation agent, the dose of the agent, intensity of the mixing, the temperature and duration will define the degree of activation (Hagemann et al., 2018).



**Figure 1:** The dependency of pyrolysis temperature on biochar properties, such as structure, carbon content and stability, among other things (Zimmerman & Mitra, 2017).

Physical or thermal activation is the most frequently used activation method and are usually done with either CO<sub>2</sub> or steam (H<sub>2</sub>O). Physical activation is often a complementary step after pyrolysis, where the carbonaceous material is subjected to oxidizing gas at high temperatures, usually > 750 °C (Downie et al., 2009; Hagemann et al., 2018). This results in creation of new micropores (< 2 nm), which leads to higher sorption capacity, caused by easier accessibility of smaller pores for adsorbing substances (Downie et al., 2009; Hagemann et al., 2018). Modification of the biochar surface by steam, leading to higher pore volume and surface area, is caused by the release of volatile gasses, removal of trapped particles, corrosion of the surface and emission of syngases. Alternatively, modification by CO<sub>2</sub> creates carbon monoxide, resulting in formation of a microporous structure from the reaction between CO<sub>2</sub> and the carbon in the biochar (Panwar & Pawar, 2022). Activation with CO<sub>2</sub> leads mostly to creation of new pores, while steam activation will widen existing pores (Hagemann et al., 2018). The activation process therefore results in C loss and lower yields of the product. The degree of physical activation (characterized by burn-off during activation) and activation time will affect the porosity, where longer retention time and higher activation degree will lead to higher porosity, due to increasing mass loss (Downie et al., 2009; Hagemann et al., 2018; Sørmo et al., 2021). However, net destruction of porosity may happen with too high activation degree (Hagemann et al., 2018). Activation also creates new oxidized functional groups, including phenolic, ketonic and carboxylic groups (Hagemann et al., 2018), and a surface that is more aromatic (Sajjadi et al., 2019), all of which result in improved adsorption affinity. However, with higher

degree of activation, oxidation of the surface leads to loss of functional groups, and the surface becomes mostly aromatic (Krull et al., 2009).

### 2.3.1 Application of biochar

Biochar can be used for many different purposes, such as soil improvement, waste management, remediation of various contaminants, or for carbon sequestration (International Biochar Initiative, 2015; Lehmann & Joseph, 2009). When biochar is applied to soil, it can improve the properties of the soil, leading to higher water retention capacity, decrease in nutrient leaching, improved soil structure and liming effect on acidic soils, which can result in higher crop yields (Ahmad et al., 2014). Biochar amendment can also help stabilize contaminants in soil, where contaminants are immobilized through sorption, making them less bioavailable (Smernik, 2009), as described in section 2.2.5.

When applying biochar to soil with the intention of limiting the spread of contaminants, the aim is to increase the distribution coefficient,  $K_d$ , which describes the distribution of a substance between the solid and aqueous phase at equilibrium. With an increase in the  $K_d$  value, the ratio of the concentration in the solid phase to the aqueous phase is increased, due to adsorption onto the solid phase.

### 2.3.2 Surface chemistry influencing adsorption

Adsorption of organic molecules to biochar depends on mechanisms as electrostatic interactions, hydrophobic interactions, electron donor-acceptor interaction, pore filling and partitioning. The degree of adsorption depends on sorbate- and biochar properties, which are determined by the feedstock and pyrolysis temperature, among other things (Ambaye et al., 2021).

The surface of biochar is mostly negatively charged, making electrostatic interaction with contaminants possible (Ahmad et al., 2014). This will lead to adsorption of cationic organic compounds to the negatively charged surface of the biochar and repulsion of anionic compounds (Du et al., 2014). However, it is possible for the biochar surface to be positively charged, depending on the point of zero charge (PZC) of the biochar. This means that the biochar surface charge is pH-dependent, where an increase in pH will result in stronger negative charge. In contrast, biochar can be positively charged at low pH, which makes adsorption of anionic species possible (Ambaye et al., 2021; Amonette & Joseph, 2009). The surface charge can also be influenced by the ionic strength of the surrounding solution, which can neutralize the negative surface charge of the biochar, reducing the electrostatic repulsion of negatively

charged compounds. The degree to which this affects sorption, depends on the PZC of the biochar and the pH of the solution (Ahmad et al., 2014). Adsorption of polar compounds take place through hydrogen bonding between oxygen containing moieties on the biochar surface and the compound, whereas non-polar compounds are adsorbed to hydrophobic sites on the biochar (Ahmad et al., 2014). The adsorption of aromatic compounds to graphene-like structures on the biochar, is mostly occurring by electron donor-acceptor interaction, where the  $\pi$ -electrons on the biochar either work as electron donor and acceptor, depending on the surface functional groups (Ambaye et al., 2021). Sorption to biochar is also influenced by partitioning, where the adsorbate diffuses into the non-carbonized sites on the biochar, which is especially effective at high compound concentrations. In contrast, pore filling is more important at lower concentrations, where organic compounds are adsorbed into the meso- and micropores of the biochar (Ambaye et al., 2021).

## 2.4 Mechanisms influencing PFAS sorption

Various mechanisms play a part in sorption of PFAS to different sorbents. The fluorinated carbon chain and the functional head group can perform different interactions, based on composition of the molecule.

### 2.4.1 Hydrophobic interactions

The strength of the hydrophobic effect of the fluorinated PFAS chain increases with each additional  $\text{CF}_2$  moiety (Higgins & Luthy, 2006), caused by increase in cavity formation energy, making the molecule less soluble in water (Sigmund et al., 2022). The sum of forces, that limit the dissolution of the molecule, is caused by less water-water hydrogen bonds in the hydration layer of the non-polar CF-chain compared to the bulk water phase, that holds a greater organization of water molecules. This leads to a disruption of the cohesive energy of water (Kissa, 2001a; Sigmund et al., 2022). The hydrophobic CF-chain will likely be attracted to hydrophobic regions of adsorbents, despite PFAS being oleophilic as well (Du et al., 2014). Nevertheless, the hydrophobic interaction between the fluorinated chain and adsorbents as biochar are believed to be one of the most important sorption mechanisms of long-chain PFAS (Fabregat-Palau et al., 2022; Higgins & Luthy, 2006; Krahn et al., 2023; Sørmo et al., 2021).

### 2.4.2 Electrostatic interactions

Electrostatic interaction may also be recognized as significant for adsorption of anionic PFAS to positively charged sorbents. Mostly the ionizable functional group behaves as the negative charge, but the fluorinated tail may also engage in the electrostatic interaction (Du et al., 2014).

Electrostatic repulsion of the anionic functional group may also lead to repulsion between PFAS and negatively charged biochar (Sigmund et al., 2022). Although, this may be overwhelmed by the hydrophobicity of the tail, as the CF-chain length increases. Divalent cation bridging may also enhance sorption of anionic PFAS to the negatively charged biochar surface. This is induced by inorganic cations, which form a bridge between the two negative charges (Du et al., 2014; Sigmund et al., 2022; Tang et al., 2017). Due to the high electronegativity of the fluorine atoms, the fluorinated chain exerts a negative charge around the tail (Kissa, 2001b). The CF-chain may therefore establish weak interactions with positively charged surfaces, although the hydrophobic effect of the tail primarily overcomes the effect of the negative charge (Du et al., 2014). Even so, the hydrophobic tail can be adsorbed to anionic surfaces as biochar through hydrophobic interactions, despite the electrostatic repulsion (Du et al., 2014).

### 2.4.3 Hydrogen bonding

Hydrogen bonds are not very likely to be formed, due to the hydrophobic CF-chain which repels water. Furthermore, the small size and high electronegativity of fluorine result in low polarizability, which decreases the ability to undergo weak intermolecular interaction as hydrogen bonding or van der Waals interactions (Du et al., 2014; Kissa, 2001b). These properties are also what makes PFAS both hydrophobic and oleophilic. However, the functional groups of PFAS that contain oxygen atoms (e.g. carboxylic- or sulfonic acids) are able to carry out hydrogen bonding with adsorbents containing -NH, -OH or -COOH functional groups, when the PFAS functional group acts as the acceptor (Du et al., 2014). This interaction is believed to entail PFAS sorption. Furthermore, charge assisted hydrogen bonding between the carboxylic functional group and oxygen-containing surface groups on the sorbent has been proven, and might even be stronger than normal hydrogen bonding, if the acidic sites on the sorbent have similar  $pK_a$  as the adsorbate (Du et al., 2014; Sigmund et al., 2022).

### 2.4.4 Acid dissociation constants ( $pK_a$ )

PFAS are generally readily dissociated in water at environmental pHs, as they are present in anionic form rather a protonated form, in addition to their acid dissociation constants ( $pK_a$ ) being much smaller than that of water (Mahinroosta & Senevirathna, 2020). Specific  $pK_a$  values for individual PFAS are subject to a lot of discussion in the literature because they are difficult to obtain, due to their surfactant properties and the seemingly increase in  $pK_a$  at higher concentrations. Even so, the acid dissociation constants are central for understanding the transportation and fate in the environment (Vierke et al., 2013).  $pK_a$  values presented by Vierke et al. (2013) for 12 PFAS, including PFOA, perfluorohexanoic acid (PFHxA), PFOS, PFHxS and



PFBS, were all smaller than 1.6. In addition, Du et al. (2014) listed values of no higher than 0.4, for 6 PFAS also including the 5 previously listed. These low  $pK_a$  values imply almost complete deprotonation at neutral pH. However, studies show that the  $pK_a$  increases with longer chain lengths (Rayne & Forest, 2009). Furthermore, as PFSA are believed to be strong acids, they will completely dissociate under all environmental conditions (Ding & Peijnenburg, 2013). Whereas a higher difficulty is involved with determining  $pK_a$  values for PFCA as they are considered to be weak acids (Ding & Peijnenburg, 2013; Rayne & Forest, 2009).

#### 2.4.5 Sorption attenuation

The listed sorption mechanisms of PFAS may all be influenced by sorption attenuation. Attenuation is the reduced sorption strength of a sorbent, which is caused by the presence of soil and/or other contaminants, which can lead to competitive sorption. Attenuation by soil is caused by organic matter which can initiate pore clogging of the sorbent, while smaller dissolved organic molecules increase the competition for sorption sites (Du et al., 2014). Presence of other contaminants similar in size, structure and functionally to PFAS, can also compete for sorption sites (Cornelissen & Gustafsson, 2006; Du et al., 2014).

## 2.5 Objectives

The main aim of this thesis was to study effects of different waste-based biochars on sorption and transport of PFAS in soil. The means to achieve the aim was to test PFAS sorption to biochar through up-flow column percolation tests and compare the transport of PFAS in the saturated zone, in scenarios of biochar- and no biochar amendments. The soil used was a PFAS contaminated soil from a former firefighting training facility located at a Norwegian civil airport in the Oslo region.

The research questions used to achieve the main aim of the thesis were the following:

- I. Which influence do amendment with the various types of waste-based biochars to PFAS contaminated soil have on sorption and transport of PFAS, compared to soil with no biochar amendment?
- II. What effect will the different biochar types have on dissolved organic carbon (DOC) transport and its potential transport of PFAS?
- III. How is the effect of the biochars reduced in presence of soil with legacy contamination?
- IV. How will PFAS structure and/or chain length influence the remediation effect of the biochar?

To achieve this, stabilization of PFAS contaminated soil with biochar produced from 5 different feedstocks, was tested in this study. The 5 feedstocks included: clean wood chip pellets, raw sewage sludge, digested sewage sludge from two different wastewater treatment plants and waste timber (activated and non-activated). To study the sorption effects of the different types of biochar on contaminated soil, leachate- and soil samples from the different columns were subsequently analysed for PFAS and compared.

## 2.6 Hypotheses

The research questions were explored through testing the following hypotheses, corresponding to the four research questions:

- I.a Waste-based biochar produced from sewage sludge will reduce PFAS leaching more effectively than (non-activated) wood-based biochar. Effective PFAS treatment in water with sludge-based sorbents was seen by Krahn et al. (2023), and is expected to be similar for soil.
- II.a Biochar amendment will lead to lower DOC content in leachate, due to adsorption of DOC onto the biochar.

- II.b Following hypothesis II.a, reduced DOC content will result in less PFAS desorption from soil, thereby limiting complexation between PFAS and DOC, leading to less transport of PFAS in the water phase.
- I.b + II.c Activation of (waste-based) biochar will lead to higher sorption of PFAS and DOC than non-activated biochar, due to higher specific surface area and the creation of more and larger pore structures.
- III.a Attenuation of single PFAS sorption to biochar will occur in the presence of soil and a mixture of PFAS, as these will induce competition for sorption sites.
- IV.a Biochar amendment will have a smaller effect on sorption of PFAS with shorter chains, as water purification have been shown be to very challenging for short-chain PFAS (Appleman et al., 2014).

### 3 Materials and methods

The column experiment conducted in this study, consisted of a setup with 9 columns, and had the aim to test the effects of different waste-based biochars on the leaching of PFAS. Soil from a former firefighting training facility was used in the columns, which was heavily contaminated with different perfluorinated compounds, but primarily PFOS. The experiment was conducted in the environmental chemistry laboratory at the Norwegian Geotechnical Institute (NGI) in Oslo. The preparation and analysis of the column leachate samples and soil from the columns, with and without biochar amendment, were conducted at the Department of Chemistry at Norwegian University of Science and Technology (NTNU) in Trondheim. The column tests, sampling, sample preparation for analysis and data analysis were conducted by the author of this thesis.

#### 3.1 Biochar sorbents

In this study, 6 types of biochar (BC) made from 5 different feedstocks were selected for testing in the column experiment:

- **CWC – BC – 700:** Clean Wood Chips, produced from logging and forestry residues. Biochar produced at a pyrolysis temperature of 700 °C.
- **DSS-1 – BC – 700:** Digested sewage sludge 1, a waste product after anaerobic digestion of sewage sludge and food waste for biogas production. Biochar produced at a pyrolysis temperature of 700 °C.
- **DSS-2 – BC – 800:** Digested sewage sludge 2, a waste product after anaerobic digestion of sewage sludge for biogas production. Biochar produced at a pyrolysis temperature of 800 °C.
- **DWSS – BC – 700:** De-watered raw sewage sludge, hydrolysed at 170 °C. Biochar produced at a pyrolysis temperature of 700 °C.
- **WT – BC – 785:** Waste timber, including various wood products discarded by citizens and businesses (no impregnated wood). Biochar produced at a pyrolysis temperature of 785 °C.
- **aWT – BC – 900 – 1.00-CO<sub>2</sub>:** Waste timber, (same feedstock as for WT-BC-785). Biochar produced at a pyrolysis temperature of 900 °C and activated 100% with CO<sub>2</sub>.

The abbreviations for the feedstocks were partly adopted from Sørmo et al. (2023). The three sewage sludges originate from three different wastewater treatment plants (WWTP). The de-watered raw sewage sludge, used as feedstock for the DWSS biochar, originated from a WWTP

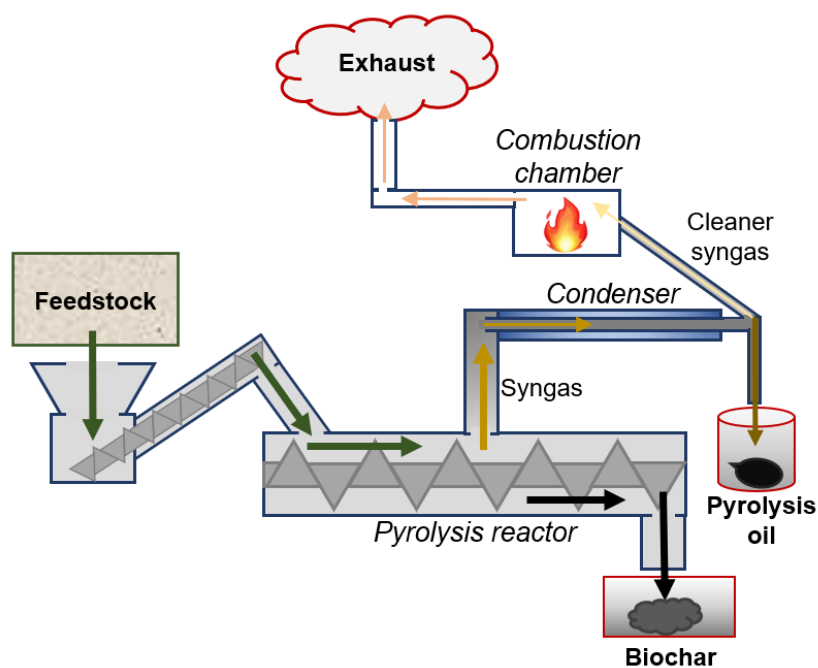
located near the same firefighting training facility that provided the soil for this experiment. The WWTP therefore treats water from this area, leading to the sewage sludge being contaminated with PFAS from the firefighting foam previously used at this site. The DWSS feedstock, in addition to the four other feedstocks used to produce the biochar studied in this thesis, was analysed by Sørmo et al. (2023) and found to all contain PFAS prior to pyrolysis.

All the 6 different biochar types were produced prior to this thesis for the VOW project (Valorization of Organic Waste) and have been used in other publications including: Krahn et al. (2023); Sørmo et al. (2020); Sørmo et al. (2021) and Sørmo et al. (2023).

The biochars were milled using a ball mill (Retsch ISO 9001) at 80 rpm for 10 min, to a fine powder < 1 mm in diameter. The biochar was then transferred into plastic bags and stored at room temperature until the start of the experiment.

### 3.1.1 Pyrolysis

The pyrolysis of the 5 different feedstocks were carried out using Biogreen<sup>®</sup> technology at a medium scale pyrolysis unit located at Lindum AS (Drammen, Norway), made by ETIA Ecotechnologies (now part of VOW ASA). The various feedstocks were dried and pelletised prior to the pyrolysis. The unit operates by feeding the pellets into the pyrolysis chamber where a rotating screw (Spirajoule<sup>®</sup>) moves the feedstock through the chamber while converting it to biochar (Sørmo et al., 2023). The rotational frequency of the screw controls the retention time in the reactor, while the electrically heated screw controls the heat (maximum 900 °C) (Sørmo et al., 2023). The pyrolysis gas is quickly separated from the biochar and condensed into pyrolysis oil, while remaining gas is combusted with propane, ensuring a clean combustion (Krahn et al., 2023). Figure 2 shows the pyrolysis system used for producing the biochar. The feeding rates were between 5 and 10 kg/h, while the retention time was 20 min for all feedstocks, except for the DWSS biochar where it was 40 min. Pyrolysis temperature is considered the main treatment parameter and varied among the 6 biochars, between 700 and 900 °C (see section 3.1 for specific temperatures). Before starting the pyrolysis, the chamber and connecting pipes were flushed with N<sub>2</sub> for 10 minutes (Sørmo et al., 2023). The aWT biochar was produced at an experimental pyrolysis unit PYREKA (Pyreg, Dörth, Germany). The unit has a 1 m long heated auger reactor that is continuously fed with the feedstock. For CO<sub>2</sub> activation of the biochar, CO<sub>2</sub> was injected into a stream of N<sub>2</sub> for direct exposure of the feedstock, leading to a one-step pyrolysis and activation process (Hagemann et al., 2020; Sørmo et al., 2021).



**Figure 2:** Illustration of the pyrolysis unit used at Lindum AS, which produced most of the biochar used in this thesis (Sørmo et al., 2023).

### 3.2 Soil

The soil investigated in the present work originated from a former firefighting training facility located at a Norwegian civil airport in the Oslo region. Use of AFFF on this location has led to contamination of the soil. The soil was picked up from the Lindum Oredalen AS landfill and was stored in three big  $\sim 1 \text{ m}^3$  containers at the landfill and mixed prior to depositing. Sampling of 5 large buckets of soil ( $\sim 10 \text{ L}$  each) was carried out using randomized multiple grab sampling from all three containers. The containers were open at the top, exposing the soil to the air, and the upper few centimeters of the soil were therefore moved to the side with a shovel. Then the soil in each container was divided into four squares of equal size. A small shovel was used to transfer the soil into the buckets, by taking two shovels of soil from each of the four squares in each of the three containers. This procedure was repeated two times in total for each of the 5 buckets. The 5 buckets of soil were then transported to the laboratory at NGI in Oslo, where they were stored in the dark at  $4 \text{ }^\circ\text{C}$ .

About  $10 \text{ L}$  of the soil was dried at  $60 \text{ }^\circ\text{C}$  for about 48 hours. After drying, the soil was sieved with a  $4 \text{ mm}$  sieve by hand. The sieve was washed with water and soap, followed by a wash with MeOH:deionised water (50:50, % v/v) before use. Organic material (roots, straws, branches) larger than  $4 \text{ mm}$ , that made it through the sieve, were removed manually with a pair of tweezers. The weight of the sieved soil was  $12.591 \text{ kg}$ .

### 3.2.1 Grain size distribution analysis

To obtain a grain size distribution analysis for soil classification, soil samples from each of the 9 columns were collected after the leaching experiment. The soil samples were dried at 110 °C and sieved according to an internal standard at NGI (LLP007: Bestemmelse av kornfordeling ved sikting). The dried soil was manually mixed, and to get a representative sample for sieving, the soil was collected using randomized multiple grab sampling. The sample consisted of minimum 100 g. dried soil, which was first weighed, and then transferred into the tower of sieves. The following sieves were used in the setup [mm]: 8.0, 4.0, 2.0, 1.0, 0.5, 0.250, 0.125 and 0.063. The soil was sieved for 15 min, whereafter each fraction was weighed. All sieves were washed and then dried for at least 30 min in a 110 °C oven, in between each sieving, to make sure the sieves were completely dry. The fractions for each sample were plotted in a graph showing the cumulative particle size.

The soil was classified as a medium sand and had a TOC content of  $0.57 \pm 0.04\%$ . Cumulative particle size analysis curves for all the soil samples were very similar, and the result is therefore only showed for the unamended soil in Appendix B.

### 3.3 Column experiment

The up-flow column percolation tests consisted of 9 columns, all packed with AFFF impacted soil mixed with different types of biochar. By pumping water from the bottom to the top of the column, 6 Liquid to solid (L/S) ratios of eluate were collected from each column: L/S 0.1, 0.2, 0.5, 1, 2 and 5.

The 9 columns consisted of:

- **1: Control:** AFFF-soil
- **2: CWC:** AFFF-soil and CWC-BC-700
- **3: DSS-1:** AFFF-soil and DSS-1-BC-700
- **4: DWSS 1:** AFFF-soil and DWSS-BC-700
- **5: DWSS 2:** AFFF-soil and DWSS-BC-700
- **6: DWSS 3:** AFFF-soil and DWSS-BC-700
- **7: WT:** AFFF-soil and WT-BC-785
- **8: DSS-2:** AFFF-soil and DSS-2-BC-800
- **9: aWT:** AFFF-soil and aWT-900-1.00-CO<sub>2</sub>

### 3.3.1 Triplicates

Analytical and experimental triplicates were used in this experiment, to get an estimate of variations in experimental data resulting from uncertainties in the experimental and analytical method. The experiment included three columns with the same biochar (DWSS), to get an estimate of variability within the columns e.g. inhomogeneous packing and water flow through the columns. Leachate samples from one column were split in three before the different analyses, to get an estimation of analytical uncertainty. Column 2 (CWC) was randomly chosen for this. Soil from each column was also analysed in triplicate, except for the three DWSS columns, for estimation of analytical uncertainty.

### 3.3.2 Mixing of soil and biochar

After the preparation of both soil and biochar, the two were mixed before packing the columns. In a fume hood, mixing of sieved soil and biochar in a plastic bag took place. 1000 g of soil plus 1% (w/w) of biochar ( $10.00 \text{ g} \pm 0.03 \text{ g}$ ) was weighed on a scale. The bag was closed and shaken to mix the soil and biochar together. The same procedure was carried out for the different biochar types, so that each column would contain a soil-BC mixture prepared with the same procedure. A plastic bag only containing sieved soil was also prepared for the control column. All 9 plastic bags of soil were stored in the dark at 4 °C until packing of the columns.

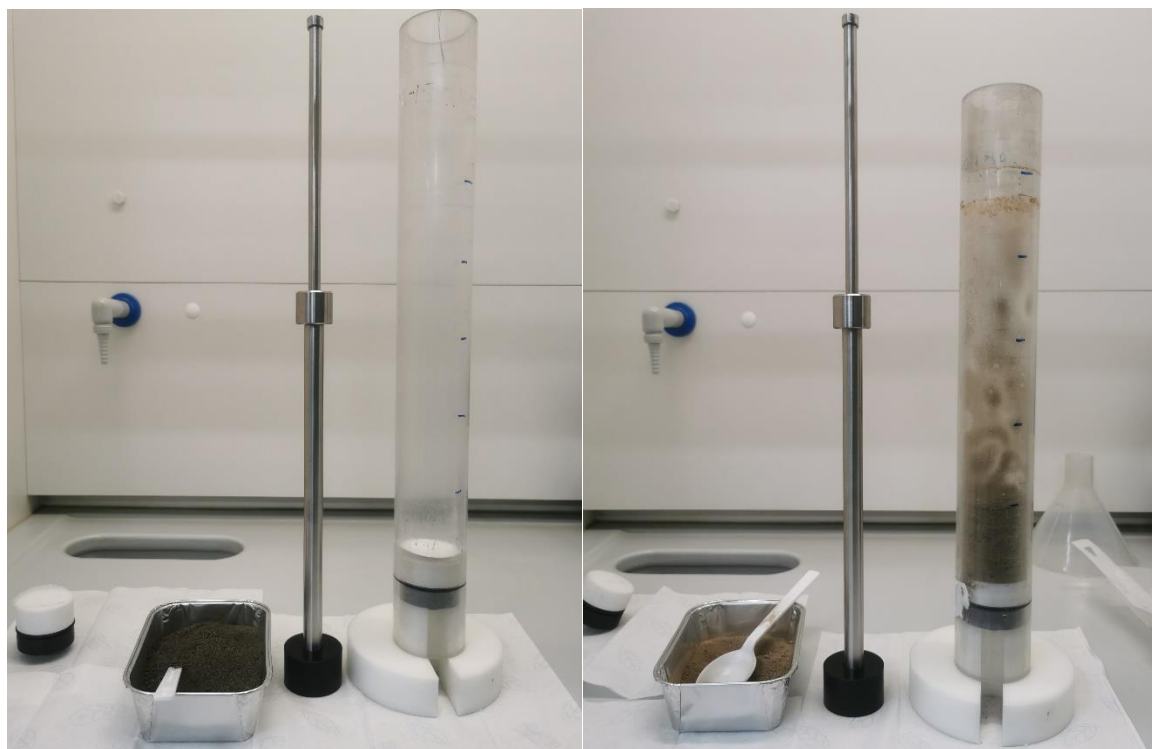
### 3.3.3 Column setup and packing

The column experiment followed a setup described by NGI, which is based on the European standard setup for waste characterization: CEN/TS 14405 (NGI, 2016).

The experiment consisted of a setup of 9 columns made of transparent Plexiglas, with an inner diameter of 5 cm and 43-50 cm in height. Each column was closed and sealed by identical top- and bottom lids made from polyoxymethylene (POM), with a polypropylene (PP) grid and a 0.45 µm polyether sulfone (PES) membrane filter in each end (PP-grid placed between lid and filter). The PP-grid in the inlet and outlet of the columns was included to ensure uniform flow through the column. The column, top- and bottom lid and two PP-grids were first weighed before packing the column. The column was then closed by the bottom lid, with the PP-grid and PES membrane filter placed on top of the lid. Soil-BC mixture was then filled into the column, up to 6 cm above the bottom lid. The soil-BC mixture was then compacted by a piston with a weight of 125 g being dropped three times from the highest position on the piston. 6 cm of soil-BC mixture was again filled into the column and was compacted with the piston in the same way as before. This procedure was repeated a total of 5 times, until the column was filled



with 30 cm of soil-BC mixture. A PES membrane filter was again placed on top of the soil-BC mixture, followed by a PP-grid, and closed by the top lid. The columns and piston can be seen on figure 3. The packed and sealed column was then weighed again. This procedure was followed for packing of all 9 columns. The weight of the soil-BC mixture packed into each column was  $854.75 \pm 11.25$  g.



**Figure 3:** Packing of the columns included the soil-BC mixture, the piston used for compacting the soil and the column closed with the bottom lid. On top of the bottom lid a PP-grid and a  $0.45 \mu\text{m}$  PES membrane filter was placed. Here the column is positioned on a stand, with the piston to its left.

All columns were put on a stand and placed on a laboratory bench at room temperature for ~1 day. Each column was then connected with Teflon and silicon tubes to a peristaltic pump and saturated with Milli-Q water, by pumping water through the bottom of the column until it came out of the top into the outlet tube, where the pump was stopped. A clamp was put on the tube between the pump and column to stop the water from draining out of the column. The columns were left to equilibrate for at least three days. The column setup can be seen on figure 4.

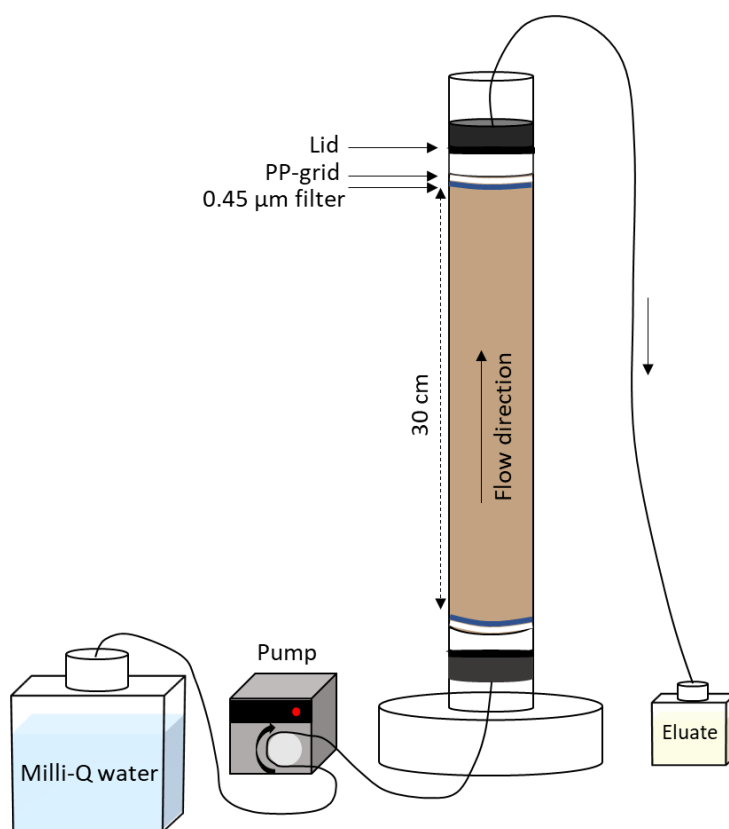
54 high-density polyethylene (HDPE) bottles of different sizes, for collecting the eluate were washed, weighed, and marked. The bottles were washed with MeOH:Milli-Q (50:50, % v/v) and weighed.

Generally, it was attempted to use equipment not containing PFAS to avoid cross contamination during the experiment. E.g., silicon tubes were used when possible, instead of Teflon tubes.

Although this was not possible for the whole column setup, it should not be of any major concern, since the concentrations of possibly added PFAS from equipment most likely would be very low, and therefore not be able to have any definitive effect on the high concentrations of the soil.

### 3.3.4 Start-up of the leaching test

After the equilibration period, which varied between 5 and 6 days among the columns, the pumps were started again on all 9 columns. During the collection of eluate for L/S 0.1, with a duration of about 5.5 hours, the flow rate was monitored and adjusted 4-5 times, by checking the weight of the collected eluate over time. The flow rate was during the whole leaching test attempted to be 12.25 mL/h on average, and between 10.6 and 13.9 mL/h. The average flowrate for the columns ended up being between 12.33-12.68 mL/h. For monitoring the flow rate, the weight of eluate, the time, and a reading from a digital frequency meter, measuring the frequency in the pump in Hz, were noted. From this information, together with a target flow rate, a new frequency in Hz were calculated, to meet the wished flow rate. The flow rate on the pump could then be adjusted if needed.

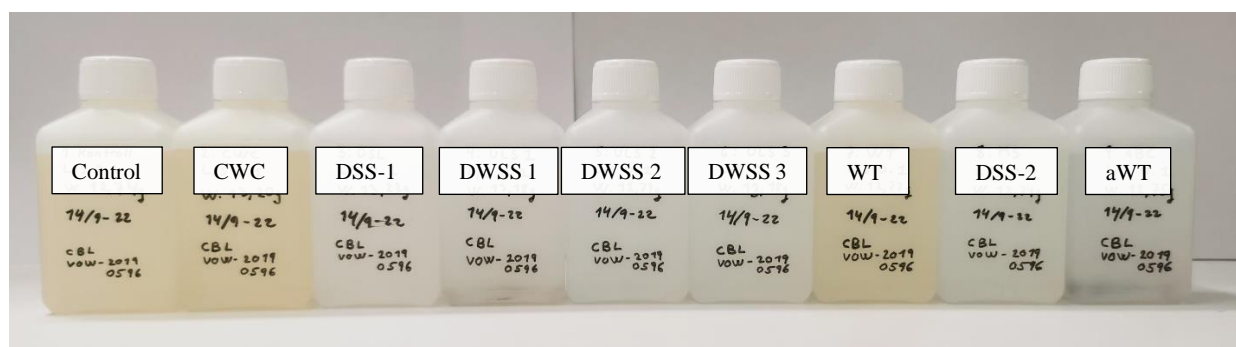


**Figure 4:** Schematic of the column set-up. Milli-Q water was pumped through the column and eluate was collected.

When the targeted L/S ratio was obtained, the bottles were replaced by new bottles collecting eluate for the next L/S ratio. The time of bottle replacement and weight of eluate fraction was noted and used to calculate the exact L/S ratio and overall flow rate of the column. During collection of eluate, the flow rate was checked and adjusted if necessary at least three times per L/S ratio, but up to 10 times for L/S 5. The leaching test took in total 15 days from start to end of collecting L/S 0.1 to L/S 5, excluding the equilibrium period. All samples of eluate were stored in the dark at 4 °C after collection and until analysis.

### 3.4 Sample preparation for analysis

After the leaching test was done, the pumps were stopped, and the columns were emptied for soil. Triplicates of the soil for PFAS analysis of between 50 and 100 g. were sampled in plastic bags from each column, except for the three DWSS columns, where only one sample per column was prepared. The rest of the soil were dried at 110 °C for the preparation of grain size distribution analysis, as described in section 3.2.1. A sample of the original soil (not used in a column) was also sampled in triplicate for PFAS analysis. The 24 soil samples were stored in the dark at 4 °C until analysis.



**Figure 5:** The 9 bottles of L/S 0.1 eluate, from column 1 to 9 showed from left to right.

The leaching test provided 6 L/S-ratios per column resulting in a total of 54 water samples of leachate from the 9 columns. Figure 5 shows the L/S 0.1 eluate from all 9 columns. Column 2 containing CWC biochar was decided to be analysed in triplicate, resulting in 66 samples for analysis. The parameters analysed for in the leachate samples included PFAS, dissolved organic carbon (DOC), pH, electrical conductivity and metals (results not included in this study). Parameters analysed for in the soil samples included PFAS and total organic carbon (TOC).

#### 3.4.1 Splitting of samples

Each leachate sample was split in four, for the different analyses. PFAS, metal and DOC analyses each required 50 mL of sample and were stored in 50 mL Falcon tubes (PP), while pH

and electrical conductivity was measured in the same 10 mL sample in a small glass tube. The falcon tubes for DOC analysis were rinsed with Milli-Q water before use.

All samples of L/S 0.1 and 0.2 were diluted to get a total volume of 155 mL per L/S ratio, since these samples only had a volume of between 76.34-86.58 mL. For samples from column 2 (CWC), which were analysed in triplicate, L/S 0.5 and 1 also needed to be diluted to get enough sample, since a total volume of 445 mL was needed per L/S ratio from this column. The dilution was carried out by weighing the sample and the added Milli-Q water, to get the most precise dilution. The dilution was carried out so the samples would be diluted as little as possible, and the dilution factor was therefore different for all the samples.

### 3.4.2 pH and electrical conductivity

pH and electrical conductivity of the leachate samples were measured in a 10 mL sample. The two parameters were not measured in triplicate for column 2 (CWC), to minimise the dilution of the samples for the other three analyses. pH was measured with an InoLab pH Level 2 pH meter from WTW, while electrical conductivity was measured on a LF 538 Conductivity Meter also from WTW. The pH meter was calibrated before use with solutions of pH 4, 7 and 11. Both sensors were rinsed thoroughly with Milli-Q water in between measurements. A list of pH and electrical conductivity for all samples can be found in Appendix A.

### 3.4.3 DOC and TOC analysis

66 leachate samples were analysed for dissolved organic carbon, while 24 soil samples were analysed for total organic carbon. Both analyses were carried out by ALS Laboratory Group Norway AS. TOC analysis was following the EN 13137:2001 standard method, where the TOC in the sample is determined by the difference between measurements of total carbon (TC) and total inorganic carbon (TIC). The TC is determined by measuring the released amount of CO<sub>2</sub> after combustion of the sample. TIC is also determined by the released CO<sub>2</sub>, but as a result of acid treatment. The standard method NS-EN 1484 was used for DOC analysis, which determines the amount of organic carbon-based compounds that can pass through a 0.45 µm filter. The principle of the analysis is to oxidize the organic carbon in the water sample to CO<sub>2</sub>, followed by measurement of the released CO<sub>2</sub>. Prior to this, any inorganic carbon that might be present in the sample are removed.

### 3.5 Instrumental analysis of PFAS

The 66 leachate samples and 24 soil samples were analysed for 39 different PFAS by LC-MS/MS, at the Department of Chemistry at Norwegian University of Science and Technology (NTNU) in Trondheim. A complete list of the target analytes and internal standards, with acronyms, CAS, formula and determination parameters in the LC-MS/MS instrument can be found in Appendix D. The following sections will provide a detailed description of the sample preparation, instrument analysis, quality assurance and quality control.

#### 3.5.1 Solid-phase extraction (SPE) of leachate samples

Solid-phase extraction (SPE) was used to prepare the leachate samples for analysis of PFAS. The extraction procedure was based on Arvaniti et al. (2014), with a few modifications. The method concentrates the aqueous sample (the mobile phase) into a solvent extract, by passing it through a stationary phase, which retains and separates the polar compounds. Using a solvent with higher affinity, the target analytes are then extracted from the stationary phase, followed by concentration and reconstitution to the desired volume. The extract can then be used for quantification of target analytes using LC-MS/MS. To compensate for differences in the extraction percentages and instrumental response in the mass spectrometer, a mixture of internal standards (ISs) is added to all samples.

For the extraction of PFAS target analytes in the filtered leachate samples, Strata™-X Polymeric cartridges (200 mg/ 6 mL) were used. The cartridges were bought from Phenomenex and have a surface modified styrene divinylbenzene as sorbent polymer, working as the stationary phase. The polymer has a particle diameter of 33 µm and surface area of 800 m<sup>2</sup>/g. All samples were spiked with three ISs which consisted of perfluorooctanesulfonate <sup>13</sup>C<sub>8</sub> sodium salt (PFOS-<sup>13</sup>C<sub>8</sub>), perfluorooctanoic acid <sup>13</sup>C<sub>8</sub> (PFOA-<sup>13</sup>C<sub>8</sub>) and <sup>1</sup>H,<sup>2</sup>H-perfluorooctane sulfonate (6:2) <sup>13</sup>C<sub>2</sub> (6:2 FTS-<sup>13</sup>C<sub>2</sub>), prepared in methanol at 1 mg/L.

For the sample preparation, 50 mL of each leachate sample was adjusted to pH ~4 with (6-8 drops of) 1 M acetic acid. The pH was tested with pH strips in at least every 6th sample. All the samples were then spiked with 10 µL IS, and vortexed prior to SPE.

The cartridges were placed in a Supleco® Visiprep™ SPE Vacuum Manifold with disposable liners also from Supleco®, positioned at the opening of the cartridges. The liners adjusted the flow rate of the sample through the cartridge, making it exit as individual droplets. First, the cartridges were conditioned with 6 mL of MeOH followed by equilibration with 10 mL of Milli-Q water adjusted to pH 3 using acetic acid. Conditioning resulted in wetting of the sorbent

polymer, creating a suitable environment for adsorption of the analytes. Equilibration removed residual sorbent from the conditioning and maximized the interaction between the analyte and sorbent. The samples were then loaded into the cartridges, by pouring directly from the 50 mL tube, and were allowed to flow through the sorbent polymer by gravity. Afterwards, the cartridges were washed with 2 mL MeOH:Milli-Q (40:60, % v/v), to remove any matrix interferences from the sorbent polymer. The cartridges with sorbent polymer were then dried for ~30 min under vacuum at ~50.8 mmHg (2 inHg), by attaching a pump to the Visiprep™ SPE Vacuum Manifold. The target analytes were extracted from the sorbent polymer by elution with 4 mL of MeOH, a solvent for which the analytes exhibit a higher affinity, and collected in a 15 mL PP centrifuge tube from VWR®. In a TurboVap® LV from Biotage, the eluents were concentrated at 45 °C and under a stream of nitrogen at 5-10 psi, to ~0.1 mL and reconstituted with MeOH:Milli-Q (50:50, % v/v) to a final volume of 0.5 mL. The extracts were then vortexed and transferred into 2 mL glass vials and stored at -19 °C until analysis.

### 3.5.2 Liquid-solid extraction (LSE) of soil samples

Liquid-solid extraction (LSE) was used to prepare soil samples for analysis of PFAS. The procedure was based on Asimakopoulos et al. (2014) with a few modifications, also described in Sørmo et al. (2023). The method is a sample-preparation used for the same purpose as SPE, but for extraction of analytes in solid samples, before quantification using LC-MS/MS.

Before the sample preparation, the soil samples were freeze dried at -30 °C for approximately two days in an Alpha 1-4 LD Plus freeze dryer, supplied by Martin Christ. The samples were weighed before and after freeze drying.

For the extraction, a sample of 0.20 – 0.25 g. was used and transferred into a 15 mL PP centrifuge tube from VWR®. Before LSE, 10 µL of the same IS used for SPE, was added to each sample, followed by 300 µL 1 M ammonium acetate and 3 mL ethyl acetate, used as the solute. The samples were vortexed prior to LSE, and were then loaded into a Branson 3510-DTH Ultrasonic Cleaner for 45 minutes of ultrasonication at 40 °C. The ultrasonication was used to extract the target analytes from the solid matrix into the added solvent. Afterwards, the samples were centrifuged for 5 minutes at 4000 rpm in an Eppendorf™ 5810 centrifuge. After centrifugation, the supernatant (ethyl acetate) was collected using glass pipettes and transferred into a new 15 mL PP centrifuge tube. 3 mL of ethyl acetate was again added to the soil sample, and the LSE was repeated 3 times in total, to a final volume of ~ 9 mL supernatant was collected. 2 mL of Milli-Q water was then added to the 9 mL supernatant and vortexed for 30 s, then

centrifuged once again at 4000 rpm for 5 minutes, followed by collection and transfer of the supernatant into a new PP centrifuge tube. The collected ethyl acetate was then concentrated to almost dryness under a stream of nitrogen at 5-10 psi and 35 °C in a TurboVap® LV from Biotage. The samples were reconstituted in MeOH:Milli-Q (50:50, % v/v) to a final volume of 0.5 mL. Finally, the extracts were vortexed and transferred into 2 mL glass vials and stored at -19 °C until analysis.

### 3.5.3 LC-MS/MS

For the quantification of PFAS in the water- and soil samples, liquid chromatography coupled with tandem mass spectrometry (LC-MS/MS) was used. The liquid chromatography was carried out on an ACQUITY UPLC System connected to a Xevo TQ-S tandem quadrupole mass spectrometer, both supplied by Waters™. The column used for separation of target analytes in the LC system, was a Kinetex C18 column (30 x 2.1 mm, 1.3 μm, 100Å Phenomenex) serially connected to a Phenomenex C18 guard column (2.1 mm). The mobile phases introduced into the column was water with 2 mM ammonium acetate as the water phase (A) and methanol as the organic phase (B), with a flow rate of 0.25 mL/min and a temperature of 30 °C. A volume of 4 μL of each sample was injected, with a run-time of 6 minutes. During the run-time, varying percentages of the mobile phases were introduced, with a gradient of 80:20% (A:B) at the initial and final time step. A wash solvent for pre- and post-injection wash of MeOH:Milli-Q (50:50, % v/v) + 0.1% formic acid was used, for 8 and 10 seconds respectively. Ionization of the analytes in the mass spectrometer was performed by electrospray ionization source (ESI) in negative mode. The LC-MS/MS analysed for 39 different PFAS. A complete list of information about the tune parameters for the ESI- and other instrument parameters can be found in Appendix D. After complete LC-MS/MS analysis of all samples, the data was processed automatically in the MassLynx v. 4.1 software, while integration of peaks were performed in TargetLynx. Each peak was manually examined and corrected for errors from the automatic integration, if necessary. All peaks were also reviewed for correct retention time (RT), being within ± 0.05 seconds of the standards for each analyte.

### Dilution

After LC-MS/MS analysis of a number of trial samples, it was discovered that the samples had higher concentrations of PFAS than expected. This led to high background noise, which resulted in complications of detecting the IS for the LC-MS/MS, since the added IS preferably should match the concentration of target analytes in the samples. Therefore, all samples (both leachate- and soil samples), were diluted until it was possible to detect the IS. The leachate

samples were diluted 25 times, by mixing 470  $\mu\text{L}$  MeOH:Milli-Q (50:50, % v/v) with 20  $\mu\text{L}$  of the sample and adding 10  $\mu\text{L}$  of IS. The soil samples were diluted 4 times by mixing 375  $\mu\text{L}$  MeOH:Milli-Q (50:50, % v/v) with 125  $\mu\text{L}$  of the sample, but no new addition of IS. Also, two new points of 50 and 100  $\mu\text{g/L}$  were added to the calibration curve, due to the high concentrations.

### 3.5.4 Quality assurance and quality control

To achieve reliable identification and quantification, the acquired data must be held to a certain quality. Different parameters for assurance of quality and reliability of LC-MS/MS analysis and quantification are hence introduced in this section.

#### Pre- and post-extraction spikes

Analysis of compounds in a complex matrix, can result in lower detected concentrations than initial analyte concentration. This is caused by loss during e.g., the extraction and clean up steps in the sample preparation. The percent recovered of the initial analyte concentration after the extraction, can be quantified by pre- and post-extraction spikes. This is carried out by spiking samples, preferably matching the matrix of the experiment samples, with a known concentration of the target analytes (TA-mix) and IS, before and after the extraction, whereupon the recovery of the analytes can be determined. Ion enhancement or suppression can also occur in samples with matrix effect, due to the sample matrix competing for ionization energy, thereby suppressing the target analytes. This can result in quantification of higher or lower concentrations of the target analytes than reality. The method of pre- and post-extraction spikes can be used to determine any matrix effects and is also used as validation of the analytical technique.

#### Recovery test

A recovery test was performed for both leachate- and soil samples, to evaluate the extraction of the target analytes. The test included 2 blank samples, 3 spiked samples (pre-extraction matrix spike), 2 matrix matched samples (post-extraction matrix spike) and 2 quality control samples (QC). The recovery test for the leachate samples consisted of 4 mL of the liquid sample matrix (mixture of all the leachate samples) and 46 mL of Milli-Q water, to match the matrix of the experiment samples. The recovery test for the soil samples consisted of 0.20 – 0.25 g of the solid sample matrix (a mixture of all the soil samples), to match the matrix of the soil. The samples were spiked with a mixture of the target analytes (TA-mix) of 20  $\mu\text{g/L}$  and IS of 1



mg/L. Blank samples were only spiked with IS, while the other samples were spiked with both TA-mix and IS, either before or after extraction.

After analysis of the recovery test samples, the results were used to compute the absolute recovery (AR), the relative recovery (RR) and the matrix effect (ME), using the following equations:

$$AR_N\% = \frac{A_{SP} - A_B}{A_{MM} - A_B} \times 100\%$$

$$AR_{IS}\% = \frac{A_{SP,IS}}{A_{MM,IS}} \times 100\%$$

$$RR\% = \frac{AR_N}{AR_{IS}} \times 100\%$$

$$ME\% = \left( \left( \frac{A_{MM} - A_B}{A_{std}} \right) - 1 \right) \times 100\%$$

Where:

*A* = Area of peak

*N* = Native standard

*IS* = Internal standard

*SP* = Spiked sample (pre-extraction matrix spike)

*MM* = Matrix matched sample (post-extraction matrix spike)

*B* = Blank sample

*std* = Calibration curve standard

Absolute- and relative recovery of 100% reflects recovery of all analytes. Additionally, relative recovery indicates how well the extraction of a specific target analyte is compared to the individual ISs, reflecting which IS best for calibration of this target analyte. This means, that the IS having a relative recovery closest to 100% is best for calibration of this specific target analyte. ME > 0% indicates ion enhancement, while ME < 0% indicates ion suppression. Values for AR, RR and ME can be seen in Appendix F.

### Blanks and reference material

Two blanks, consisting of Milli-Q water, were prepared during the sample splitting in the environmental lab at NGL. These went through SPE and LC-MS/MS analysis like the other leachate samples, to see if any contaminants were present in the lab during the experiment and

sample preparation. Most of the target analytes were below LOD in the blank samples, while a few had very low concentrations.

Similar to the blank water samples, two reference material samples were included in the soil analysis and went through the LSE and LC-MS/MS analysis like the other soil samples. The reference material was the Standard Reference Material<sup>®</sup> 2781 "Domestic Sludge" from the National Institute of Standards and Technology (NIST), USA. The reference material has certified values for perfluorinated compounds, which can be seen in Appendix G. Due to the high concentrations of PFOS in the soil, a high background noise led to low recovery of PFOS from the TA-mix in the recovery test samples. This resulted in negative AR and RR values of PFOS in the soil samples, and the reference material was instead used to verify the analytical method for PFOS in soil.

During LC-MS/MS solvent blanks of pure methanol were analysed to monitor for cross-contamination and carry over in the instrument. A calibration standard solution was also analysed to monitor potential signal drifting (the standard of 5 µg/L was used).

#### Internal Standard method and calibration curves

The internal standard method was used to quantify PFAS concentrations and to assure greater accuracy in the measurements. The method also compensates for losses during sample preparation and analytical errors as matrix effects and losses during the extraction. The internal standard is added to all samples in a known amount and concentration, where the ratio between signals of IS and target analytes can be used to quantify the concentrations in the samples, when related to a calibration curve of the IS. The amount of IS added to the samples should preferably be in the same concentration range as the target analytes in the samples. A compound used as IS should fulfil requirements as not being naturally present in the sample and must have similar physical-chemical properties to the target analyte. Three stable isotope labelled compounds (PFOS-<sup>13</sup>C<sub>8</sub>, PFOA-<sup>13</sup>C<sub>8</sub> and 6:2 FTS-<sup>13</sup>C<sub>2</sub>) were used in this case to meet the requirements and were used to cover the 39 target analytes.

A 13-point calibration curve ranging from 0.01 to 100 µg/L was prepared of the 1 mg/L IS and 20 µg/L TA-mix in MeOH and Milli-Q water. The curve was adjusted for each compound, with a minimum of 6 calibration points. The adjustment was done to get a more accurate fit for low or high concentrations, preferably having the concentrations in the middle of the curve. The obtained R<sup>2</sup> values for the detected analytes demonstrated a satisfactory linear response with values of R<sup>2</sup> > 0.98 for both leachate and soil samples, except for bis[2-(N-ethylperfluorooctane-

1-sulfonamido)ethyl] phosphate (diSAMPAP) ( $R^2 > 0.97$  for both leachate and soil), PFHxA ( $R^2 > 0.97$  for leachate), Perfluoropentane sulfonic acid (PFPeS) ( $R^2 > 0.97$  for soil), Perfluoroheptanoic acid (PFHpA) ( $R^2 > 0.96$  for soil) and Perfluorododecane sulfonic acid (PFDoDS) ( $R^2 > 0.93$  for soil).

The IS used in the calibration curve for quantification of each target analyte was determined by the IS having a mean RR% closest to 100%. For some target analytes the most structurally similar IS was chosen for quantification instead. This was only the case, if the most structurally similar IS had a RR% of almost the same, as the IS with RR% closest to 100%. The IS used for each target analyte can be seen in Appendix F.

### Correction of concentrations

All leachate sample concentrations were corrected with the  $AR_N\%$ , due to the high dilution factor and addition of new IS after the SPE in connection with the dilution. The target analytes PFPeA, 6:2 FTS and PFHxS were corrected using the  $AR_{IS}\%$  from 6:2 FTS- $^{13}C_2$ , due to very high  $AR_N\%$  ( $> 270\%$ ). Perfluorooctane sulfonamide (PFOSA) and diSAMPAP had low  $AR_N\%$  ( $< 15\%$ ) but were still corrected and included in the results.

### Limit of Detection and Quantification

The limit of detection (LOD) is the lowest amount of analyte detectable in a sample, meaning the lowest amount of analyte that can confidently be differentiated from background noise. But not all amounts detected are quantifiable. The limit of quantification (LOQ) is the amount of analyte that can be quantified as an exact value. The LOD and LOQ are determined individually for each analyte. In this study, the LOD were set to the lowest concentration on the calibration curve, while LOQ were determined as three times LOD. LOD and LOQ for each analyte can be seen in Appendix E together with the PFAS concentrations in leachate and soil.

## 3.6 Data analysis

The section includes equations used in the different analyses carried out on the data obtained from the column tests.

### 3.6.1 PFAS leaching

The content of PFAS leached from the soil ( $C_{leachable}$ ) was defined as the released amount of PFAS during the experiment per dry weight of soil in the column, given as:

$$C_{leachable}[\mu g \text{ kg}^{-1}] = \frac{C_w[\mu g \text{ L}^{-1}] \times V_w[L]}{M_{soil,dw}[kg]} \quad (1)$$

Where  $C_w$  is the concentration of PFAS in the eluate,  $V_w$  is the volume of the eluate and  $M_{soil,dw}$  is the mass of the soil in the column in dry weight.

The reduced leaching of PFAS in soil with biochar amendment relative to unamended soil is given as:

$$Reduction [\%] = \left( \frac{C_{leachable,unamended}[\mu g \text{ kg}^{-1}] - C_{leachable,biochar}[\mu g \text{ kg}^{-1}]}{C_{leachable,unamended}[\mu g \text{ kg}^{-1}]} \right) \times 100 \quad (2)$$

To create a mass balance ( $M_{tot}$ ) of PFAS in the amended soil, the total amount of PFAS would include PFAS content in the eluate ( $M_w$ ), the soil ( $M_{soil}$ ) and the sorbent ( $M_{biochar}$ ). Since the soil and biochar were analysed as one mixture, the mass of soil and sorbent are given as one parameter ( $M_{soil+biochar}$ ):

$$\begin{aligned} M_{tot,amened}[\mu g] &= M_w[\mu g] + M_{soil+biochar}[\mu g] \\ &= (C_{w,L/S_n}[\mu g \text{ L}^{-1}] \times V_{w,L/S_n}[L] + C_{w,L/S_{n+1}}[\mu g \text{ L}^{-1}] \times V_{w,L/S_{n+1}}[L] + \dots) + C_{soil,end}[\mu g \text{ kg}^{-1}] \times M_{soil,dw}[kg] \end{aligned} \quad (3)$$

Where  $C_{w,L/S_n}$  is the concentration of PFAS in the eluate of the n'th L/S ratio, and  $V_{w,L/S_n}$  is the volume of eluate of the same n'th L/S ratio. The  $M_{tot,amended}$  can then be compared to the total mass in unamended soil:

$$M_{tot,unamended}[\mu g] = C_{soil,i}[\mu g \text{ kg}^{-1}] \times M_{soil,dw}[kg] \quad (4)$$

Where  $C_{soil,i}$  is the initial concentration of PFAS in the unamended soil.

The two mass balances should ideally be the same:

$$M_{tot,amended} = M_{tot,unamended} \quad (5)$$

### 3.6.2 Distribution coefficients ( $K_d$ )

Distribution coefficients,  $K_d$ , for PFAS distributed between the solid and the aqueous phase, were determined using a model that predicted the mass of PFAS in the soil over time. The  $K_d$

values were determined at the actual aqueous concentration. A traditional linear sorption model, that determine the distribution at one concentration point was not used, as non-linearity in sorption of PFAS to biochar previously has been reported (Hale et al., 2016; Krahn et al., 2023). Non-linearity is caused by occupation of adsorption sites in the order of the gain in energy they enable, resulting in a decrease in  $K_d$  with higher concentrations (Sigmund et al., 2022). Furthermore, as different concentrations were measured at the different L/S ratios, a model that included all aqueous concentrations would describe the solid-water distribution better than just choosing to calculate the  $K_d$  from concentrations measured at one specific L/S ratio.

A rate constant for PFAS desorption from the soil ( $k_{PFAS}$ ) was estimated by the model, using the measured mass of PFAS in the soil at time zero of the experiment. A 1<sup>st</sup> order model was used based on a contaminant leaching model described by NGI (2021), given as:

$$M(t)_{modelled}[\mu g] = M(0)_{measured}[\mu g] \times e^{-k_{PFAS}[\min^{-1}] \times t[\min]} \quad (6)$$

Where  $M(0)_{measured}$  was deduced as:

$$M(0)_{measured}[\mu g] = M_{desorbed,total}[\mu g] + C_{soil,remaining}[\mu g \text{ kg}^{-1}] \times M_{soil,dw}[\text{kg}] \quad (7)$$

$M_{desorbed,total}$  is the cumulative desorbed mass after L/S 5, describing everything that was leached from the soil during the experiment, while  $C_{soil,remaining}$  is the remaining concentration after the leaching experiment, measured in the soil samples.  $M(t)_{measured}$  was directly calculated from the individual leached concentrations. Subsequently, equation ( 6 ) was solved by adjusting the desorption rate constant,  $k_{PFAS}$ , by minimizing the cumulative squared error between  $\ln(M(t)_{measured})$  and  $\ln(M(t)_{modelled})$  using the solver tool in MS Excel.

Using the rate constant ( $k_{PFAS}$ ) and the known flow rate of the water through the column ( $k_w$ ), the retardation factor (R) could be determined by isolation from the following equation:

$$k_{PFAS}[\min^{-1}] = \frac{k_w[\min^{-1}]}{R [-]} \quad (8)$$

The distribution coefficient,  $K_d$ , could finally be computed using the retardation factor, the bulk density ( $\rho_b$ ) and porosity ( $\theta$ ) of the soil:

$$R[-] = 1 + \left( \frac{K_d[L\ kg^{-1}] \times \rho_b[g\ mL^{-1}]}{\theta[-]} \right) \quad (9)$$

For some scenarios, a 1<sup>st</sup> order two-compartment model was used instead, to be able to describe both rapid and slow desorption of PFAS from the soil (Cornelissen et al., 1997; Cornelissen et al., 1998):

$$M(t)_{modelled}[\mu g] = M(0)_{measured}[\mu g] \times F_{rapid}[-] \times e^{-k_{rapid}[\min^{-1}] \times t[\min]} \\ + M(0)_{measured}[\mu g] \times F_{slow}[-] \times e^{-k_{slow}[\min^{-1}] \times t[\min]} \quad (10)$$

Where  $F_{rapid}$  and  $F_{slow}$  are the fractions of rapid and slow desorption, and  $k_{rapid}$  and  $k_{slow}$  are the rapid and slow desorption rate constants. The model was used assuming  $k_{slow} \ll k_{rapid}$  and solved in the same way as equation (6), solving for four variables instead of one.

The resulting  $K_d$  values from the 1<sup>st</sup> order one-compartment model described the whole system with both soil and biochar ( $K_{d,tot}$ ). Sorption coefficients for the biochar only ( $K_{d,BC}$ ) were derived using a mass balance describing the percentage of biochar and soil in the column:

$$K_{d,tot} = K_{d,soil} \times 0.99 + K_{d,BC} \times 0.01 \quad (11)$$

Where the obtained  $K_d$  value for the unamended soil was used as  $K_{d,soil}$ .

When the two-compartment model was applied, two  $K_d$  values could be determined, one describing the rapid desorption ( $K_{d,soil}$ ) using  $k_{rap}$ , and one describing the slow desorption ( $K_{d,BC}$ ) using  $k_{slow}$ . Both fractions of desorption,  $F_{rapid}$  and  $F_{slow}$ , were used to determine an overall  $K_{d,tot}$ , since black carbon, organic matter or other fractions that might sorb PFAS, may have been in the soil (Cornelissen & Gustafsson, 2004). The fraction of slow desorption from the biochar,  $F_{slow}$ , was also used to adjust the  $K_{d,BC}$  when the two compartment model was applied.

### Freundlich Isotherm

The Freundlich sorption model describes the sorption for non-linear conditions, and is expressed as:

$$C_s = K_F \times C_w^{n_F} \quad (12)$$

Where  $C_s$  is the sorbed amount in  $\mu\text{g}/\text{kg}$ ,  $K_F$  is the Freundlich distribution coefficient in  $\text{L}/\text{kg}$ ,  $C_w$  is the concentration in the aqueous phase at equilibrium in  $\mu\text{g}/\text{L}$ , and  $n_F$  is the non-linearity coefficient. The equation predicts that adsorption strength will decrease with higher concentrations of adsorbate, leading to non-linear sorption. In contrast,  $K_d$  values describe linear adsorption, assuming infinite sorption sites on the sorbent, as given in equation ( 13 ). But as sorption to biochar is generally not linear (Krahn et al., 2023),  $K_d$  values will vary depending on the measured concentration in the aqueous phase. It is thus important to note that comparison should be done for  $K_d$  values measured at approximately the same concentrations. Moreover,  $K_d$  and  $K_F$  values for biochar sorption, can thus not be directly compared. Only if  $n_F$  equals 1, meaning that there is no competition for sorption sites,  $K_F = K_d$ .

$$K_d = \frac{C_s}{C_w} \quad (13)$$

In order to compare the distribution coefficients,  $K_d$ , determined in this thesis, to other studies presenting  $K_F$  values it was necessary to correct the  $K_F$  values to the specific concentration points used for calculation of the  $K_d$  values. However, as not one specific concentration point was used to calculate the  $K_d$  values using the model, it was decided to use the concentration at  $L/S$  0.1 for this purpose, as the water and solid concentrations was assumed to be in equilibrium at  $L/S$  0.1, after an equilibrium period of more than 5 days for the saturated columns. To correct the  $K_F$  values to the specific concentration points, equation ( 12 ) was inserted in ( 13 ) which yields:

$$K_d = \frac{K_F \times C_w^{n_F}}{C_w} \quad (14)$$

Simplifying the equation gives:

$$K_d = K_F \times C_w^{n_F-1} \quad (15)$$

Then the logarithm was taken on both sides:

$$\log K_d = \log K_F - (1 - n_F) \log C_w \quad (16)$$

A new log  $K_d$ , based on the log  $K_F$  could then be derived, describing the distribution ratio at the same concentration point as the log  $K_d$  values from this study. The concentration at L/S 0.1 was used as  $C_w$ , to determine the  $\log_{10}$  increase or decrease in concentration, compared to the concentration used for calculation of the  $K_F$ .

### 3.6.3 Groundwater infiltration based on L/S ratios

Based on the L/S ratios, a time scale could be estimated defining the period it would take before the soil was exposed to the same amount of water in nature, as during the column test (NGI, 2019). The equation is solely based on properties of the soil along with amount of annual precipitation and does therefore not take any contaminant properties into account.

$$L/S [L kg^{-1}] = \frac{N [mm yr^{-1}] \times t [yr]}{d [kg m^{-3}] \times h [m]} \quad (17)$$

L/S is the liquid to solid ratio, N is the annual precipitation, t is the time, d is the bulk density and h is the depth of the soil in the field. According to the different L/S ratios used in the experiment, the equation was solved for time, providing an estimated period of time before the same amount of water, as was used for the L/S ratios, has leached through the depth of the given soil.

## 3.7 Data handling

Raw data handling, statistical analysis and plotting were carried out using Microsoft Excel (version 2202).

## 3.8 Uncertainty

This section describes the uncertainties involved in the experiments and methods used in this study.

The many steps involved in the experiment, analyses, and data processing, all contributed to increase the uncertainties of the final results. The first factor of uncertainty was homogenisation and sampling of the soil. An insufficient homogenisation of the soil could lead to variations in PFAS and TOC concentrations among the 9 soil columns, as well as the differences in the total amount of soil in each column (about 1.3% uncertainty). Mixing and weighing of the biochar into the soil gave about 0.3% uncertainty among the columns. Heterogeneous flow through the column could be induced when packing the soil into the columns, possibly leading to less PFAS encountering the biochar. Uncertainty is also related to the equipment used during and after the



column test, where sorption of PFAS to the tubes, bottles and flasks could occur. Dilution of some of the leachate samples before analysis, in addition to splitting of samples, could cause less accurate results, the concentrations to be below detection level, or concentration variations in the split samples. Throughout the experiment, weighing of soil and leachate could also add some uncertainty in the mass and volume of samples. The resulting uncertainties of the column setup and dilution/splitting of samples could be estimated at ~ 10%.

Analytical uncertainty can be caused by numerous things during the sample preparation, detection and data processing. During sample preparation (SPE and LSE) and LC-MS/MS, target analytes could be lost, samples could be contaminated by used equipment or crossover from other samples could occur. Furthermore, insufficient extraction of analytes from the soil and/or biochar could cause faulty lower concentrations. Uncertainties could also be associated with the dilution of all samples followed by addition of new IS, before analysis by LC-MS/MS. This could have caused the signal on the IS to be higher than if it went through the SPE (overestimation of IS signal, because nothing was lost during SPE), which could give lower concentrations of the compounds in the sample when calculating the concentrations from the IS-calibration curve. The leachate samples, that were diluted the most, were corrected for this by dividing the concentrations with the absolute recovery of the compound. Peak integration, both done automatic and manually, in addition to the subsequent data processing, could cause further uncertainties in the results. Pipetting during sample preparation is also a cause of uncertainty. The uncertainties associated with sample preparation and detection of analytes could be estimated to be ~20-25%, resulting in an overall uncertainty of ~30-35%.

### 3.8.1 Relative standard deviation

Uncertainties of the experimental setup and the analyses were estimated by two sets of triplicates, which were used to identify the largest source of uncertainty. The experimental uncertainty was evaluated by triplicate columns amended with DWSS biochar, while the analytical uncertainty was evaluated by triplicate analysis of leachate samples from the column amended with CWC biochar, split in three. The analytical triplicates demonstrated the largest uncertainty for the PFAS analysis, and a relative standard deviation was computed on basis of these values. The relative standard deviation was applied to all of the presented concentrations, assuming that the measured uncertainty for one set of samples was representative for all of the samples. For the DOC analysis, the experimental triplicates (DWSS) demonstrated the largest uncertainties, and the relative standard deviation was based on these values instead.

A reason for the analytical uncertainty being the largest for the PFAS analysis, may be because this method requires many preparation steps and complicated data handling. In addition, it might also have to do with the difficulty of the instruments to resolve and quantify different PFAS in complex matrices, due to interferences. Furthermore, this method is not as established as other analyses (e.g., DOC and TOC), which also could lead to mistakes or uncertainties. In contrast, the DOC and TOC analysis uses a very established method, that requires fewer steps underway. Furthermore, these two analyses were carried out by a commercial lab, which performs these analyses on a regular basis and are expected to have low uncertainties on their results.

The relative standard deviation for different PFAS was highest for leachate sample L/S 0.1 and were generally decreasing with increasing L/S ratio. For PFBS, PFHxA, PFHpA, 6:2 FTS, PFHxS, PFOA, PFOS, 8:2 FTS (1H,2H-Perfluorodecan sulfonate (8:2)), PFOSA and diSAMPAP, the relative standard deviation for L/S 0.1 were ranging between 6.3% to 60%, but most were around 45-50%. This turned out to be higher than the anticipated 30-35% uncertainty. However, when looking at the relative standard deviation for samples of all L/S ratios, the uncertainty was on average between 22% and 39% for L/S 0.1, 0.2, 0.5 and 2, while the average uncertainty for L/S 1 and 5 was a bit higher with about 50% uncertainty. The uncertainty for the DOC analysis was, as mentioned very low, between 0.0% and 2.4% uncertainty for CWC triplicates, while DWSS triplicates showed uncertainties between 2.5% and 29%.

## 4 Results and discussion

In this chapter, the results from the leaching tests together with the different analyses performed on the data, are presented and discussed. Given that PFOS was the dominant compound in all samples, there will be focus on this compound throughout the chapter, in addition to 9 other PFAS (PFBS, PFHxA, PFHpA, 6:2 FTS, PFHxS, PFOA, 8:2 FTS, PFOSA and diSAMPAP) which were selected based on their concentration and chain length.

### 4.1 Biochar properties

This section presents selected properties of the 6 types of biochar used in the column tests, together with comparison of biochar pore diameter and molecular sizes of PFAS.

Selected properties for the 6 different biochars are presented in table 1. The biochar weight yield and ash content were highest for the three sludge biochars. These two properties are related as higher yield is observed with higher inorganic contents in the feedstock, which is indicated by relatively high ash content (Ahmad et al., 2014). This fits with the fact that sludge generally contains high inorganic contents (Zhang, C. et al., 2013). As expected, the aWT biochar had the lowest weight yield percent, caused by mass loss from the activation process. The two non-activated wood-based biochars had similar weight yields of 16.9% for CWC and 18.4% for WT. The three wood-based biochars had the highest carbon contents but lowest oxygen content, while the opposite was seen for the three sludge-based sorbents. Nitrogen content is feedstock dependent and often higher in sewage sludge-based biochars (Ahmad et al., 2014), but this was generally not the case here as the WT and aWT biochars contained higher amounts of N. O/C ratios increase with higher quantity of polar functional groups on the surface, while H/C ratios decreases with aromatization of the organic structure (Sajjadi et al., 2019). These ratios were highest for the three sludge-based biochars, indicating a higher amount of polar groups, but lower aromaticity than the wood-based biochars. A higher carbonization degree of the biochar result in reduction of the O/C, H/C and N/C ratios whereafter the amount of carboxylic, hydroxylic and amino groups are reduced (Sajjadi et al., 2019). This fits with the data in table 1, showing the lowest O/C, H/C and N/C ratios for CWC, WT and aWT biochars with the highest carbon contents. The stability of biochar is also indicated by low O/C and H/C ratios, implying high aromaticity which increases the time it can stay in soil without being degraded (Camps-Arbestain et al., 2015; Wang et al., 2022). As the lowest ratios of O/C and H/C were found in the two non-activated wood-based biochars, and presumably also the aWT biochar, these would have higher stability in soil, than the three sludge-based biochars.

**Table 1:** Properties for the biochar sorbents, including weight yield, ash, surface area (SA), pore volume (PV), elemental content and - ratio. The aWT biochar was not analysed for all the parameters given in the table.

Biochar sorbent	Biochar weight yield	Ash	CO <sub>2</sub> sorption (pores 0.3 – 1.5 nm)		N <sub>2</sub> sorption (pores > 1.5 nm)		Elemental content				Element ratio		
			DFT-SA	DFT-PV	BET-SA	BJH-PV	C	O	H	N	O/C	H/C	N/C
			%	%	m <sup>2</sup> /g	cm <sup>3</sup> /g	m <sup>2</sup> /g	cm <sup>3</sup> /g	%	%	%	%	
<b>CWC</b>	16.9	3.73	683	0.186	323	0.017	91.4	3.78	1.00	0.69	0.04	0.01	0.01
<b>DSS-1</b>	62.0	93.4	86.6	0.027	110	0.111	13.5	47.6	1.04	0.82	3.53	0.08	0.06
<b>DSS-2</b>	40.1	73.4	202	0.062	219	0.133	27.7	34.9	1.32	0.89	1.26	0.05	0.03
<b>DWSS</b>	33.7	93.4	171	0.050	128	0.126	29.6	48.9	1.24	1.13	1.65	0.04	0.04
<b>WT</b>	18.4	15.5	588	0.160	131	0.025	85.1	6.52	1.51	1.41	0.08	0.02	0.02
<b>aWT</b>	12.5	NA	850	0.257	617	0.429	89.5	NA	NA	1.16	NA	NA	0.01

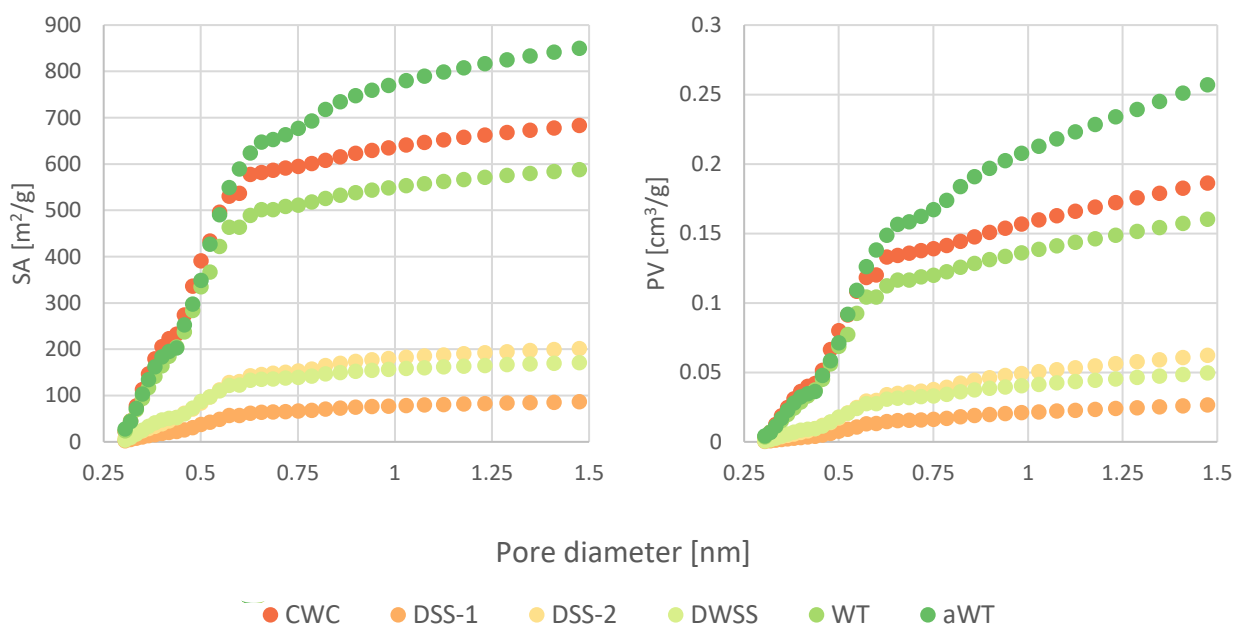
#### 4.1.1 Pore volume and surface area

Surface area (SA) and pore volume (PV) for the 6 biochar sorbents are also listed in table 1, and were determined by CO<sub>2</sub> gas adsorption and DFT data evaluation for pores 0.3-1.5 nm, while N<sub>2</sub> gas adsorption and BET- (for SA) and BJH (for PV) data evaluation were used for pores > 1.5 nm. Properties as surface area and pore volume in biochar have been shown to have great impact on the sorption capacity of different contaminants (Fabregat-Palau et al., 2022; Hale et al., 2016; Krahn et al., 2023). However, it should be kept in mind that PFAS molecules are quite big, and that pore sizes of about 1-1.5 nm are needed to accommodate most of the PFAS discussed in this thesis. Thus, it is important to take pore diameters into account, and not only the total pore volume of the sorbent. This relationship is further discussed later in this section. The aWT biochar showed highest cumulative SA for pores between 0.3 and 1.5 nm and for pores >1.5 nm of 850 m<sup>2</sup>/g and 617 m<sup>2</sup>/g, respectively. Furthermore, this biochar also showed highest PV of 0.257 cm<sup>3</sup>/g for pores between 0.3 and 1.5 nm, and 0.429 cm<sup>3</sup>/g, for pores >1.5 nm. CWC and WT biochars had the second and third highest SA and PV for pores between 0.3 and 1.5 nm but were in the lower end for pores >1.5 nm, except for the SA in CWC which also was the second highest after aWT. The three sludge biochars generally appeared to have the lowest SA and PV for both pores between 0.3 and 1.5 nm and > 1.5 nm. Wood-based biochar have been shown to exhibit higher surface area than biochar produced from animal litter and solid waste, possibly due to high carbon content and low ratios of H/C and O/C (Ahmad et al., 2014), which agree with the listed properties in table 1. Moreover, high surface area and microporosity (pores < 2 nm) lead to sorption of organic contaminants to the biochar

(Ahmad et al., 2014; Hale et al., 2016), which suggests that the three wood-based sorbents should be better sorbents of organic contaminants than the sludge-based sorbents.

### Distribution of pores 0.3-1.5 nm

Figure 6 illustrates the distribution of PV and SA for pores with diameter between 0.3-1.5 nm, in each of the 6 biochars. The three wood-based biochars (CWC, WT and aWT) stood out in terms of PV and SA among the three sludge biochars, as both parameters showed a steep increase in the smallest pores. More than 72% of the PV and 85% of SA in CWC and WT were located in ultra-micropores, which are pores with a diameter smaller than 0.7 nm (Bardestani et al., 2019). The aWT biochar documented somewhat lower percentages with 61.7% of PV and 76.8% of SA located in ultra-micropores. Even as the distribution of pore diameter in the three wood-based biochars looks very similar on figure 6, the reasonable higher cumulative SA and PV of aWT (given in table 1), can explain why the percentage of ultra-micropores was less dominating in this sorbent. In contrast, the sludge-based biochars (DSS-1, DSS-2 and DWSS) demonstrated a less steep and more continuous increase in SA and PV for pores between 0.3-1.5 nm.



**Figure 6:** Surface area (SA) given in  $\text{m}^2/\text{g}$  and pore volume (PV) in  $\text{cm}^3/\text{g}$  for pores between 0.3 and 1.5 nm, for each of the 6 biochar types.

The possibility of adsorption to ultra-micropores can be determined by the size of the PFAS molecules compared to the size of the pores in the biochar, as maximum adsorption only can be achieved if the dimensions of the two matches (Hale et al., 2016). The effective cross-sectional diameter ( $D_{\text{eff}}$ ) and maximum diameter ( $D_{\text{max}}$ ) of the 10 selected PFAS are shown in

table 2, and were determined based on values computed by Inoue et al. (2012). The  $D_{\text{eff}}$  ranges between 0.54 to 0.67 nm for CF-chain lengths 4 to 8 and 0.91 nm for CF16, while  $D_{\text{max}}$  ranges from 1.02 to 1.55 nm for CF4 to CF8 and 2.20 for CF16. This means that the majority of the pores in CWC and WT biochars were too small to accommodate the PFAS molecules. Despite from  $D_{\text{eff}}$  of the PFAS with CF-chain length 4 to 8 being below 0.7 nm, the PFAS molecules would have to be positioned exactly at the right angle to fit into the few pores with a diameter larger than the  $D_{\text{eff}}$ . A scenario which probably rarely takes place. diSAMPAP, with slightly larger  $D_{\text{eff}}$  and  $D_{\text{max}}$ , would not fit into any of the ultra-micropores, along with most of the micropores (< 2 nm) of all the 6 biochars.

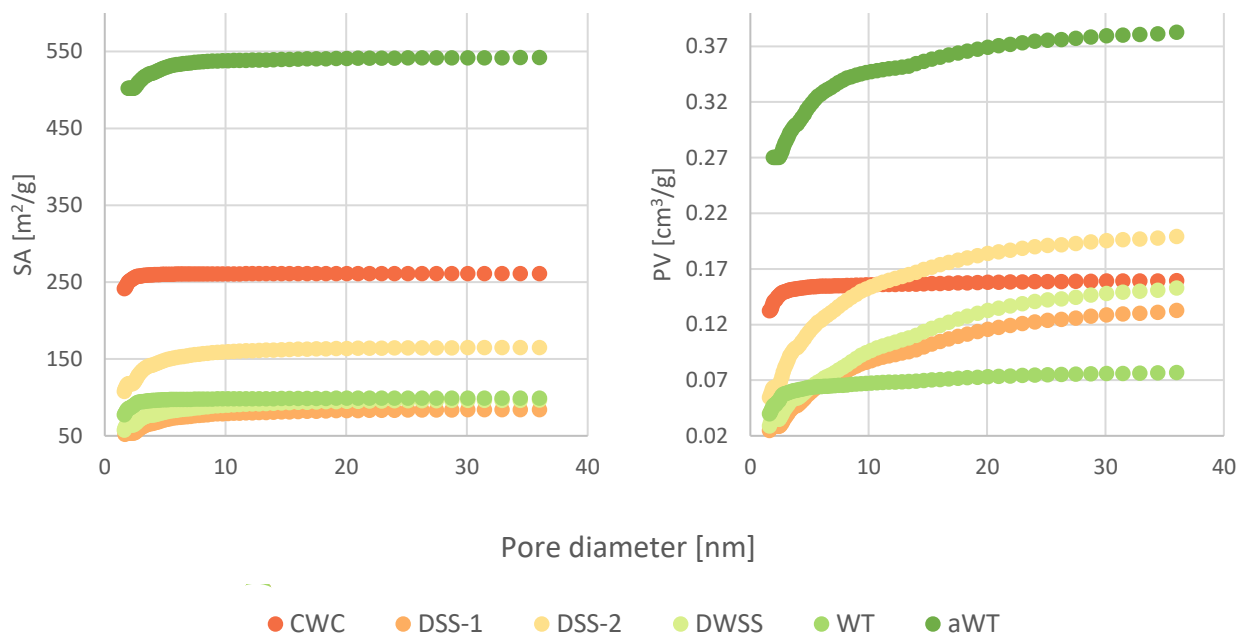
**Table 2:** Effective cross-sectional diameter ( $D_{\text{eff}}$ ) and maximum diameter ( $D_{\text{max}}$ ) of the 10 selected PFAS. Values were computed using interpolation and extrapolation by linear regression of  $D_{\text{eff}}$  and  $D_{\text{max}}$  for 6 PFAS calculated by Inoue et al. (2012). Perfluorotetradecanoic acid (PFTA) was excluded from the linear regression, obtaining a better  $R^2$  for the dataset. \* = value from Inoue et al. (2012).

Compound	CF-chain length	$D_{\text{eff}}$ [nm]	$D_{\text{max}}$ [nm]
PFBS	CF4	0.54	1.02
PFH <sub>x</sub> A	CF5	0.57	1.13
PFHpA	CF6	0.60	1.23
6:2 FTS	CF6		
PFH <sub>x</sub> S	CF6		
PFOA	CF7	0.61*	1.36*
PFOS	CF8	0.63*	1.55*
8:2 FTS	CF8	0.67	1.45
PFOSA	CF8		
diSAMPAP	CF16	0.91	2.20

### Distribution of pores > 1.5 nm

The SA and PV of pores larger than 1.5 nm showed large variations among the 6 sorbents, shown on figure 7. More than 90% of the SA and PV of the CWC biochar were located in pores smaller than 3 nm, the same applied for the SA of the WT biochar. The SA of the three sludge-based biochars was more evenly distributed over various pore sizes, however with over 80% located in pores below 5 nm in diameter. Furthermore, the distribution of PV on figure 7 demonstrated large variations. The PV of the WT biochar did not follow the CWC biochar as closely, as in the pores < 1.5 nm. 75% of the porosity in the WT was located in pores smaller than 3 nm, followed by a slightly increase up to pores sizes of 35 nm. The PV of DSS-1 and

DWSS biochars increased steadily up to pore sizes of 35 nm, whereas the DSS-2 biochar demonstrated a more rapid increase with over 75% of the porosity located in pores smaller than 10 nm. The SA and PV of the aWT biochar stood out among the other biochars on figure 7. The very high SA and PV were slowly increasing with larger pore sizes, indicating a high amount of both smaller and larger pores. Furthermore, more than 90% of PV was located in pores smaller than 10 nm, and nearly 98% of SA was located in pores smaller than 5 nm.



**Figure 7:** Surface area (SA) given in  $\text{m}^2/\text{g}$  and pore volume (PV) in  $\text{cm}^3/\text{g}$  for pores  $> 1.5$  nm, for each of the 6 biochar types.

Since the ultra-microporosity of the biochars were not essential for sorption of the PFAS listed in table 2, the SA and PV in pores  $> 1.5$  nm might have been crucial for differences in PFAS sorption to the biochar sorbents.

Overall, the highest amount of small pores was seen in the CWC biochar (90%  $< 3$  nm), followed by the WT biochar (75%  $< 3$  nm). The three sludge-based biochars (DSS-1, DSS-2 and DWSS) demonstrated similar patterns of SA and PV distribution in pores between 0.3 – 1.5 nm (SA of 86.6-202  $\text{m}^2/\text{g}$  and PV of 0.027-0.062  $\text{cm}^3/\text{g}$ ), also seen on figure 6, while for pores  $> 1.5$  nm greater variations were seen among the three. The DWSS and DSS-1 demonstrated very similar distribution of PV and SA (128  $\text{m}^2/\text{g}$  and 0.126  $\text{cm}^3/\text{g}$  for DWSS, and 110  $\text{m}^2/\text{g}$  and 0.111  $\text{cm}^3/\text{g}$  for DSS-1, respectively), while the SA and PV for DSS-2 (219  $\text{m}^2/\text{g}$  and 0.133  $\text{cm}^3/\text{g}$ ) was noticeable higher. The connection between biochar PV, SA and sorption of PFAS are discussed in section 4.2.1.

#### 4.1.2 Point of zero charge

Point of zero charge (PZC) describes the pH, at which the net charge of the surface on a sorbent is equal to zero. The PZC of a sorbent is determined with measurements of zeta potential at different pH points, which are extrapolated to find the pH at which the charge is zero. The zeta potential describes the electrical charge of particles at the interphase between solids and liquids. Measurements of zeta potential in mV at 5 different pH points were carried out for the 5 non-activated biochars. However, due to non-linearity of the measurements, no exact PZC values could be determined, although the PZC were predicted to be very low (below pH 1) for all 5 sorbents. A low PZC for the aWT biochar was also assumed. The very low PZC values mean that the biochars will have a negatively charged surface in natural soil conditions, even acidic ones of e.g. pH 4. This would also be the case in the columns, which imitated realistic environmental conditions. pH measurements of leachate samples are presented in table 3, and showed an average pH of around 7. The zeta potential at pH 7 for the 5 biochar sorbents are also presented in table 3, and were all negative and decreased in the following order: WT (-9.84 mV) > DSS-1 (-12.8 mV) > DWSS (-13.9 mV) > DSS-2 (-19.3 mV) > CWC (-19.7).

**Table 3:** Mean values  $\pm$  standard deviation of pH measured in all 6 leachate samples from each column. Zeta potential in mV at pH 7 for the 5 non-activated biochars.

Column	pH in leachate	Zeta potential at pH 7 [mV]
Control	6.9 $\pm$ 0.2	NA
CWC	7.1 $\pm$ 0.2	- 19.7
DSS-1	6.9 $\pm$ 0.2	-12.8
DSS-2	7.1 $\pm$ 0.1	-19.3
DWSS	6.9 $\pm$ 0.2	-13.9
WT	7.1 $\pm$ 0.2	-9.84
aWT	7.2 $\pm$ 0.2	NA

The negatively charged surfaces of the biochars will lead to electrostatic repulsion of PFAS with anionic functional groups, with the strongest repulsion by the CWC biochar, exhibiting the largest negative potential of -19.7 mV at pH 7. In contrast, the lowest repulsion was seen by the WT biochar of -9.84 mV also at pH 7. As PFAS with shorter CF-chain lengths are less hydrophobic, these will experience a relatively stronger electrostatic repulsion than longer chained PFAS. This is due to the repulsion of the anionic functional group of short-chain PFAS being less well compensated for by hydrophobic interactions with the chain. Electrostatic



repulsion by CWC biochar can therefore be assumed to be stronger for e.g., PFBS (CF<sub>4</sub>) than PFOS (CF<sub>8</sub>). These mechanisms are further explained in section 4.4.1.

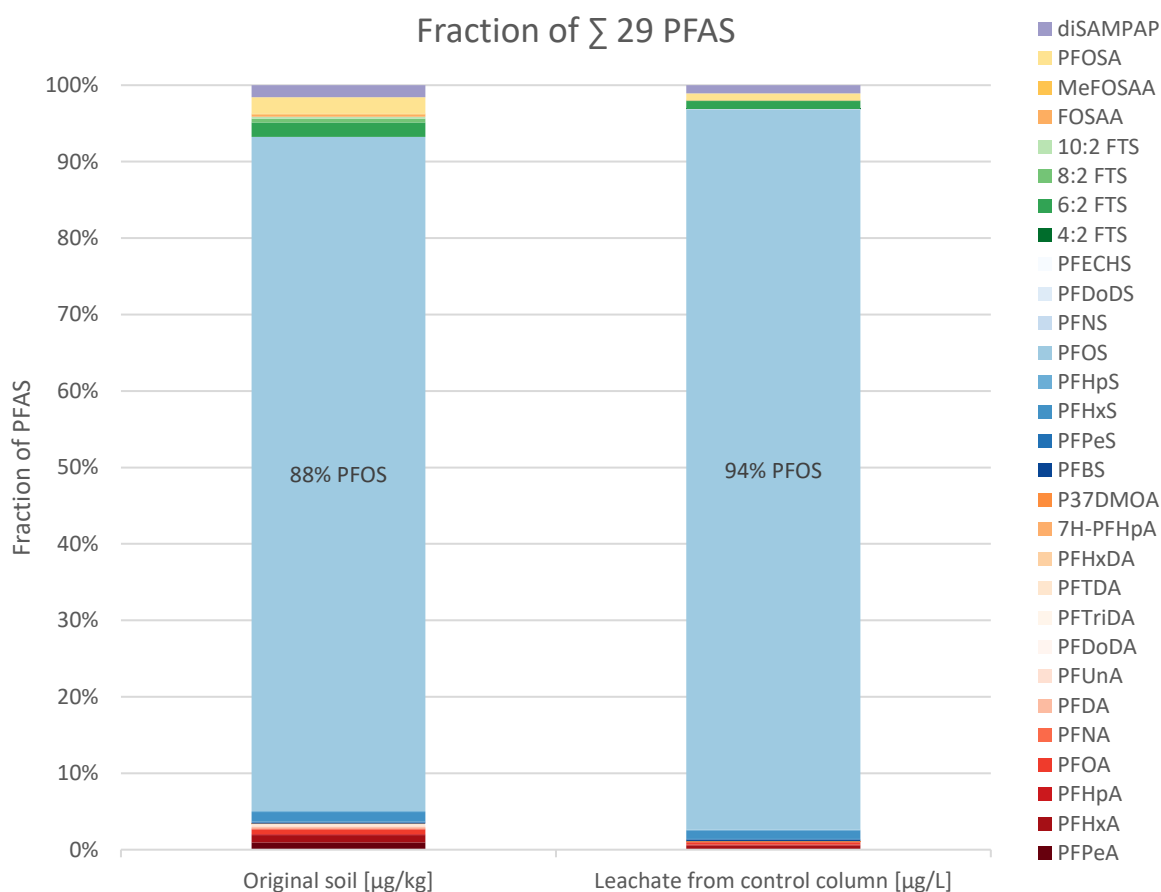
## 4.2 PFAS immobilisation by biochar amendment

This section presents the results from the leaching tests and discusses the effects of the different biochars on PFAS sorption.

A total of 29 different PFAS were detected in the leachate- and soil samples. 3 of these were only detected in the leachate samples (P37DMOA, PFECHS and 4:2 FTS), while 4 other PFAS only were detected in the soil samples (PFTDA, PFH<sub>x</sub>DA, 7H-PFH<sub>p</sub>A and PFDoDS). PFNS and PFDoDS were only detected in samples of soil used in columns, but not found in the original soil. PFOS represented 88% of the  $\sum 26$  quantified PFAS in the original soil, while 94% of the  $\sum 25$  quantified PFAS in the control column leachate was PFOS. Quantification of high PFOS concentrations corresponded to other analyses of AFFF-impacted soil (Hale et al., 2017; Høisæter et al., 2019; Høisæter & Breedveld, 2022). Figure 8 shows the fractions of the detected PFAS in the original soil and control column leachate. The total concentration of the 26 detected PFAS in the original soil was  $1333 \pm 46 \mu\text{g}/\text{kg}$  ( $n = 3$ ), while the total leachable concentration of the 25 detected PFAS in the control column leachate was more than double, with a concentration of  $3088 \mu\text{g}/\text{kg}$ . Large variations between unamended- and amended soil were also seen and led to not corresponding mass balances for PFOS. Even the  $M_{\text{tot,unamended}}$  for the original soil and the soil from the control column did not correspond, as the control column soil had a total mass of  $2664.9 \mu\text{g}$  PFOS, which was more than 1.5 times higher than the original soil with a total mass of  $998.8 \mu\text{g}$  PFOS. The  $M_{\text{tot,amended}}$  for the soil with different biochars were all lower than  $M_{\text{tot,unamended}}$  of the control column, but with large differences among the biochars. The  $M_{\text{tot,amended}}$  were  $1729.1 \pm 131.2 \mu\text{g}$  for CWC,  $551.5 \mu\text{g}$  for DSS-1,  $498.2 \mu\text{g}$  for DSS-2,  $545.6 \pm 165.1 \mu\text{g}$  for DWSS,  $1937.3 \mu\text{g}$  for WT and  $773.6 \mu\text{g}$  for aWT. Mass balances for other PFAS can be seen in Appendix E.3.

The main reason for the considerable differences between concentrations is suspected to be caused by non-representative samples of the original soil, leading to lower concentrations than in the control column, or due to insufficient extraction of PFAS during LSE of the soil. Extraction of PFAS from the soil matrix can be difficult, and other methods such as accelerated solvent extraction (ASE), offers higher extractions yields (Alzaga et al., 1998). Insufficient extraction could also lead to the variations in mass balances among the biochars, as the best biochar sorbents showed lower mass of PFOS than the poorest biochar sorbents and the control

column. The variation in detected PFAS from soil to leachate might be caused by precursors, which degraded to other PFAS during the experiment, or caused by insufficient extraction or uncertainty in the analyses, as the 7 compounds only detected in either soil or leachate, only were found in low concentrations ( $< 2.99 \mu\text{g}/\text{kg}$  and  $< 0.08 \mu\text{g}/\text{L}$ ). Furthermore, the tubes made of Teflon used in the column setup, could as well add PFAS to the leachate, causing higher concentrations in the leachate compared to the original soil. However, a simple study performed by Cox-Colvin & Assoc., Inc. showed that use of new Teflon tubing for groundwater sampling was not a significant source of PFAS cross-contamination, as detection of PFBA, PFHpA, PFPeA, PFOA and PFOSA only were detected at trace concentrations or below LOQ (Hunter, 2021). Thus, it is assumed that the Teflon tubes would not count as a considerable source of PFAS in the experiment.

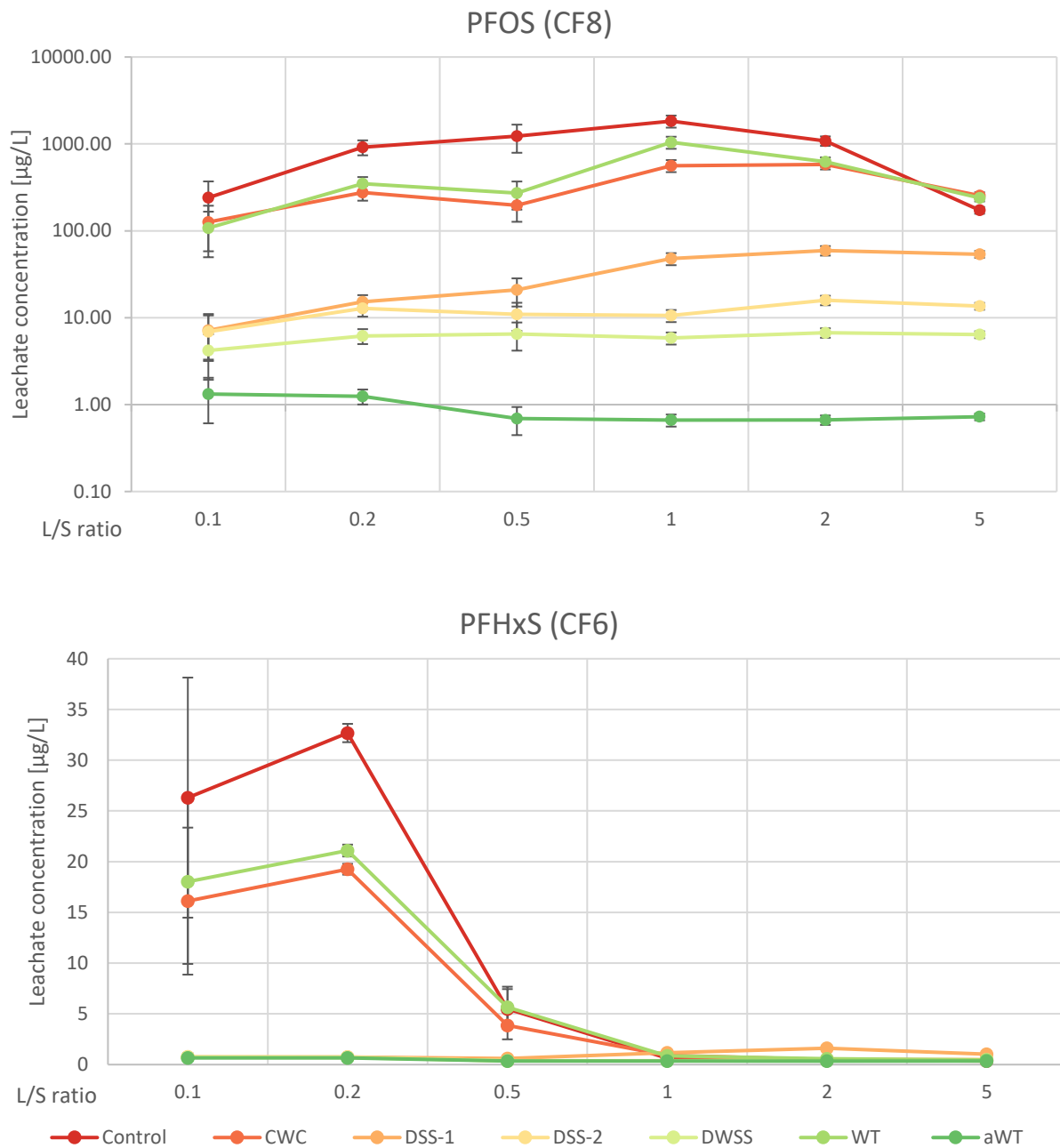


**Figure 8:** Fraction of the detected PFAS in the original soil and in the leachate from the control column. 88% of the total detected 26 PFAS in soil was PFOS, while 94% of the detected 25 PFAS in the control column leachate was PFOS. Fractions are based on concentrations in  $\mu\text{g}/\text{kg}$  for soil and  $\mu\text{g}/\text{L}$  in leachate.

The concentrations of PFOS and PFHxS in leachate over time, given as L/S ratios, can be seen on figure 9, while all leachate and soil concentrations can be seen in Appendix E. The analysis of leachate from the different columns demonstrated a big difference in PFAS sorption among

the biochar types. The concentration of PFOS was highest in the control column, as expected. A concentration of  $1828.9 \pm 289.7 \mu\text{g/L}$  PFOS was detected in the leachate of L/S 1 in the control column, as the highest concentration of all PFAS among all leachate samples analysed. The columns amended with WT and CWC biochar demonstrated the second and third highest PFOS concentrations of  $1044.3 \pm 165.4 \mu\text{g/L}$  at L/S 1 and  $580.1 \pm 72.1 \mu\text{g/L}$  at L/S 2, respectively. The highest leachate concentrations of PFOS from the rest of the columns were substantially lower and decreasing in the following order: DSS-1 ( $59.3 \pm 7.4 \mu\text{g/L}$  at L/S 2) > DSS-2 ( $15.9 \pm 2.0 \mu\text{g/L}$  at L/S 2) > DWSS ( $6.7 \pm 0.8 \mu\text{g/L}$  at L/S 2) > (aWT  $1.3 \pm 0.7 \mu\text{g/L}$  at L/S 0.1).

The PFOS desorption was not similar for all columns, but the overall pattern demonstrated an increase in PFOS leaching with peak concentrations at L/S 1 or 2, followed by a decrease in PFOS leaching. Only the aWT biochar seemed to increase the sorption of PFOS during the experiment, with decreasing concentrations over time. The same overall pattern of desorption as PFOS was only seen for PFOSA (CF8) and somewhat by 8:2 FTS (CF8), which generally showed a small dip in concentration at L/S 0.5 followed by a peak in concentration at L/S 1 or 2. Whereas PFHxS (CF6), 6:2 FTS (CF6), PFOA (CF7) demonstrated a different desorption pattern, with the highest concentrations observed at L/S 0.2 followed by rapid decrease. PFHpA (CF6) PFHxA (CF5) and PFBS (CF4) showed an even more rapid decrease in concentration over time, with the highest concentration at L/S 0.1 followed by rapid desorption. diSAMPAP (CF16) did not follow the pattern of the other long-chained PFAS, but instead decreased more slowly with stable concentrations at L/S 0.1 and 0.2. The diSAMPAP concentration in leachate from the control column stood out from this pattern, demonstrating a large peak in concentration ( $40.31 \pm 8.0 \mu\text{g/L}$ ) at L/S 0.2, before decreasing to somewhat same concentration as before ( $7.49 \pm 4.1 \mu\text{g/L}$ ).



**Figure 9:** Concentration in µg/L of PFOS and PFHxS in leachate from all columns. The y-axis for PFOS is given in log<sub>10</sub>, due to large variations among the concentrations in leachate samples. The x-axis is given as liquid to solid ratios (L/S). Relative standard deviations are applied to all concentrations, while mean values ± std are presented for the CWC (analytical triplicate) and DWSS (experimental triplicate). Points are discrete values, lines are only drawn for better visualization.

The different patterns of PFAS leaching, may be explained by the different functional groups and chain length. Both PFOS, PFOSA and 8:2 FTS have sulfonate/sulfonamide functional groups and a CF-chain length of 8. PFHxS, 6:2 FTS and PFOA may not all have the same functional group but are characterized as long-chain PFAS, however, with CF-chain lengths of 6 and 7, they are shorter than PFOS, PFOSA and 8:2 FTS. PFHpA, PFHxA and PFBS do not have the same chain lengths but are all characterised as short-chained PFAS. This trend shows that shorter chained PFAS are more mobile and will desorb more rapidly from soil, than PFAS

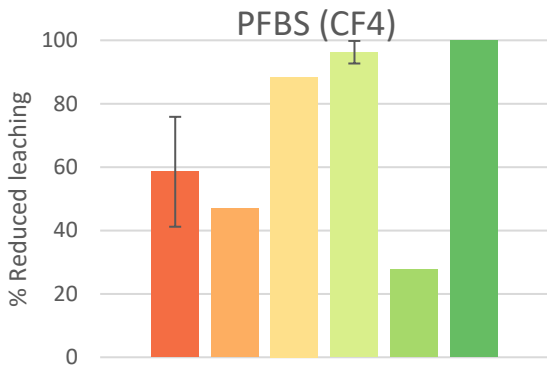
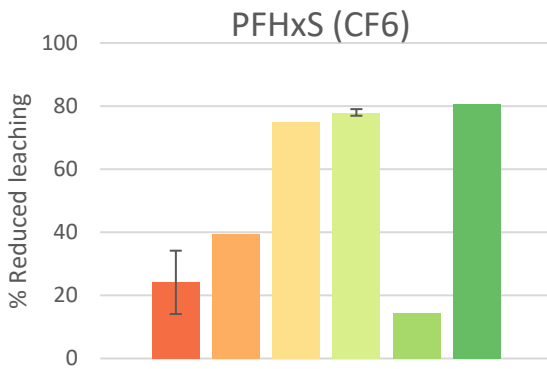
with longer CF-chains. Besides the chain length, the different leaching pattern of PFOS, PFOSA (and 8:2 FTS to some extent) may also be caused by their similar sulfonate/sulfonamide functional group, indicating that these long-chain sulfonates sorb more strongly to the soil and thus take longer to desorb. The influence of the functional groups on sorption is further discussed in section 4.4.1.

#### 4.2.1 Reduction of PFAS in leachate

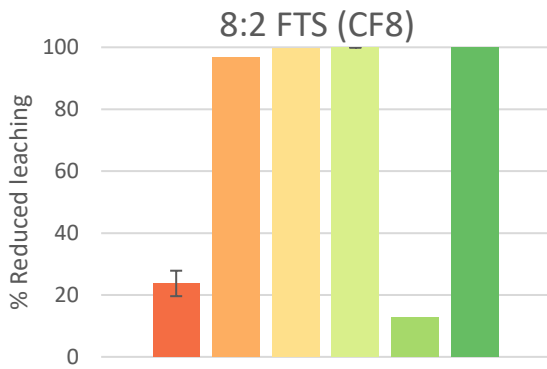
The reduced PFAS leaching due to biochar amendment, was computed for better comparison of the different biochar sorbents. Figure 10 shows the reduced leaching of 10 different PFAS, as a result of sorption to the biochar. The figure demonstrates again a great difference among the effect of the 6 biochar types tested in this study. The aWT biochar achieved the highest reduction of PFOS in the leachate of 99.9%, closely followed by the three sludge-based biochars with  $98.9 \pm 0.24\%$  (DWSS), 97.8% (DSS-2) and 91.6% (DSS-1). The two wood-based biochars demonstrated a much lower reduction of PFOS of  $42.4 \pm 5.1\%$  and 33.7% for CWC and WT, respectively. For the other 9 PFAS, the same overall trend was seen, with the aWT and sludge-based biochars showing the strongest PFAS sorption. The high reduction in PFAS leaching by the aWT biochar corresponds with the results on the same sorbent presented by Sørmo et al. (2021), reporting an almost complete reduction in PFAS leaching (> 99%) in batch tests with a low-TOC soil and varying doses (1-5%) of the aWT biochar.

When distinguishing between long- and short-chained PFAS, the trend was reversed between CWC and DSS-1 for the short-chained PFAS, as DSS-1 showed lower reduction percentages for PFHpA, PFHxA and PFBS, than the CWC biochar. Generally, the 10 selected PFAS showed that longer chained PFAS are retained better than the shorter chained PFAS, which also have been reported in other studies (Fabregat-Palau et al., 2022; Krahn et al., 2023; Sorengard et al., 2019), with exception for diSAMPAP and PFBS in this specific experiment. The very similar and low reduction percentage of diSAMPAP for all the 6 sorbents may be due to the peak concentration at L/S 0.2 in the control column being much higher than concentrations measured in any of the other leachate samples. Additionally, very similar concentrations were detected in all leachate samples from columns amended with biochar.

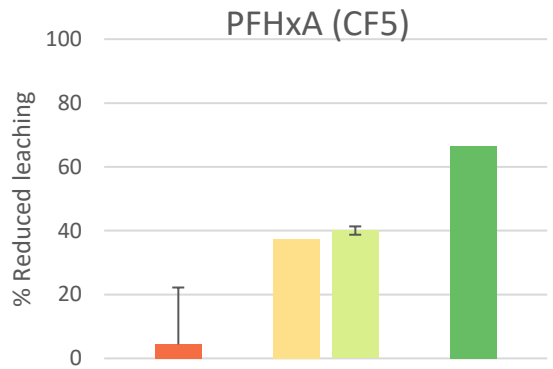
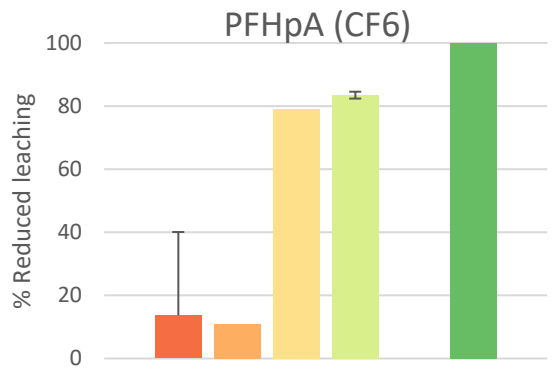
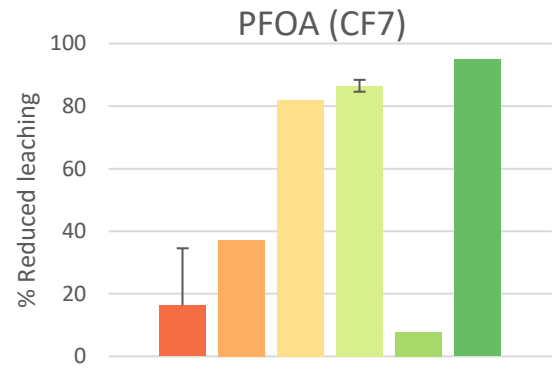
### Perfluoroalkyl sulfonates (PFSA)



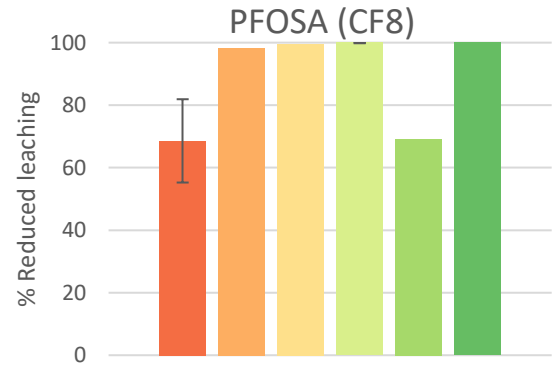
### Fluorotelomer sulfate (FTS)

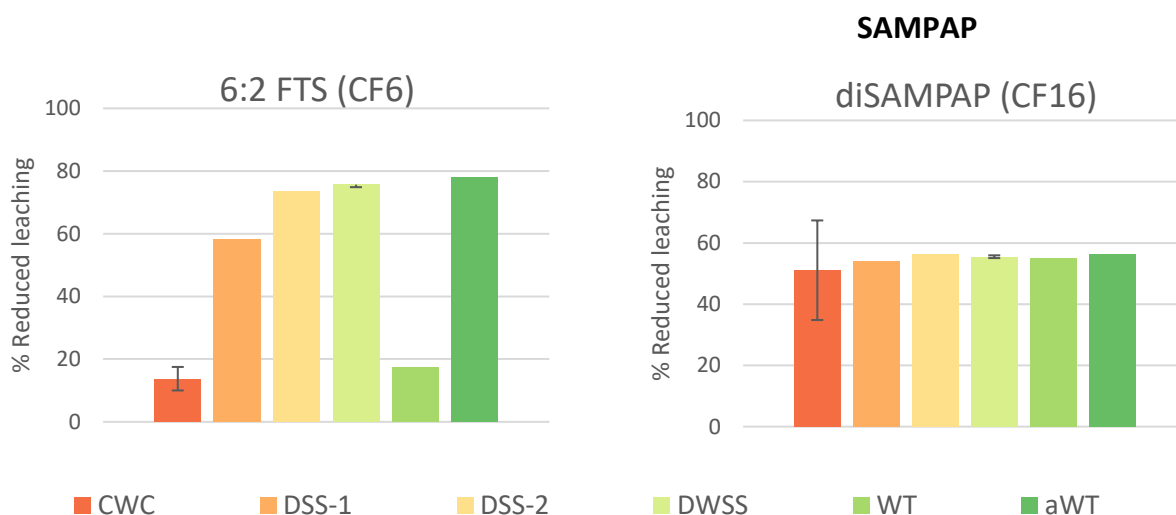


### Perfluorocarboxylic acids (PFCA)



### Perfluorooctanesulfonamides (FOSA)





**Figure 10:** Reduction [%] in leaching of PFAS by amendment with the 6 different biochar sorbents, relative to the control. The graphs are grouped by the PFAS functional group. Mean values  $\pm$  standard deviations are presented for the CWC (analytical triplicate) and DWSS (experimental triplicate).

The overall lower reduction in PFAS leaching by amendment with the CWC and WT biochar, might be explained by the majority of the pore volume being located in pores  $< 3$  nm (90% for CWC and 75% for WT), despite having some of the highest carbon contents (91.4% and 85.1%, respectively) of the 6 biochars. Even though the WT biochar contained 15% less pores  $< 3$  nm compared to the CWC biochar, the generally lower total SA and PV of the WT (131  $\text{m}^2/\text{g}$  and 0.025  $\text{cm}^3/\text{g}$  for WT, compared to 323 and 0.017 for CWC), in addition to  $\sim 6\%$  lower carbon content, might explain why the WT sorbent nevertheless demonstrated the lowest PFAS retention.

Despite the very similar distribution of PV and SA in the DSS-1, DSS-2 and DWSS biochars, DWSS still showed higher reduction in PFOS leaching ( $98.9 \pm 0.24\%$ ) compared to DSS-2 (97.8%) and DSS-1 (91.6%). This could be explained by DWSS having a slightly higher carbon content than DSS-2 and DSS-1 (29.6%, 27.7% and 13.5%, respectively), and the lowest percentage of smaller pores (62%, 65% and 76%  $< 10$  nm for DWSS, DSS-1 and DSS-2, respectively). However, higher SA and PV in the DSS-2 compared to the DWSS (219  $\text{m}^2/\text{g}$  and 0.133  $\text{cm}^3/\text{g}$ , compared to 128  $\text{m}^2/\text{g}$  and 0.126  $\text{cm}^3/\text{g}$ ), could have been expected to exhibit a higher PFAS sorption, although this was not the case.

The overall highest reduction in PFAS leaching was seen by aWT (99.9%), which similarly had the highest PV and SA, providing a large quantity of pores distributed at all pore diameters (illustrated on figure 6 and figure 7). Furthermore, this biochar showed the second highest carbon content (89.5%), leading to more effective adsorption of the hydrophobic PFAS CF-chain. It is also likely that this sorbent had the highest degree of aromaticity, as it was made at

the highest temperature, in addition to being activated. As these properties have shown to be important in PFAS sorption (Ahmad et al., 2014; Fabregat-Palau et al., 2022; Krahn et al., 2023), this can explain the high sorption strength of the aWT biochar.

The very high reduction in PFAS leaching by the DWSS biochar ( $98.9 \pm 0.24\%$  for PFOS) is also worth noting, as this biochar was made from PFAS contaminated sludge, originating from the WWTP located in the same area as the firefighting training facility. These results therefore document, that it is possible to effectively remediate contaminated soil with a sewage sludge-based biochar that originally was contaminated by PFAS from the same source that contaminated the soil.

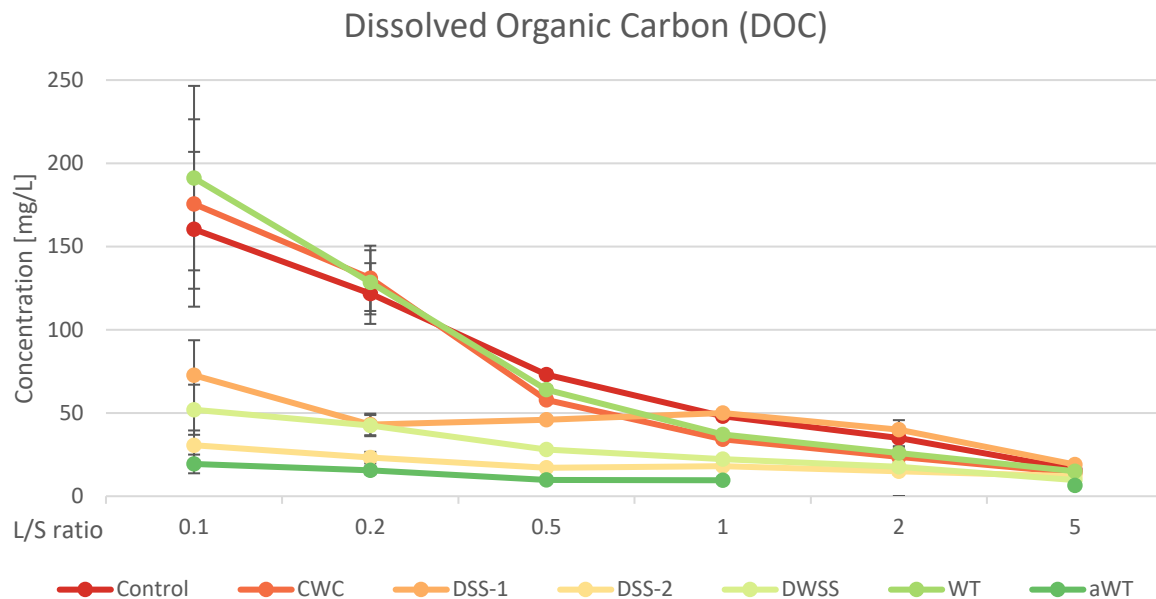
### 4.3 DOC-facilitated PFAS transport and TOC influence

This section presents the results from analyses of dissolved organic carbon (DOC) in the leachate and total organic carbon (TOC) in the soil, and discusses whether DOC and PFAS concentrations are correlated or not.

All leachate samples were analysed for DOC. Results from this analysis are illustrated on figure 11, and listed in Appendix C. DOC in leachate from the control column decreased linearly throughout the experiment ( $R^2 = 0.95$ ), with a concentration of  $160 \pm 47$  mg/L at L/S 0.1 and  $16 \pm 0.7$  mg/L at L/S 5. The unamended soil, along with soil amended with CWC and WT biochar, showed the highest DOC concentrations at most L/S ratios. DOC concentrations at L/S 0.1 decreased in the following order: WT ( $191 \pm 55$  mg/L) > CWC ( $176 \pm 51$  mg/L) > control ( $160 \pm 47$  mg/L) >> DSS-1 ( $73 \pm 21$  mg/L) > DWSS ( $52 \pm 15$  mg/L) > DSS-2 ( $31 \pm 8.9$  mg/L) > aWT ( $19 \pm 5.6$  mg/L) and followed roughly this order throughout the experiment.

The concentration of DOC in L/S 2 for aWT was excluded from the data set, due to the analysis showing an unlikely high concentration of 210 mg/L. Leachate from all columns were below 20 mg/L at L/S 5. Lower concentrations of DOC in soil amended with biochar compared to unamended soil have previously been documented, indicating sorption of dissolved organic material to biochar (Sørmo et al., 2021; Thies & Rillig, 2009). However, this was not the case for the CWC and WT biochar, which showed similar DOC concentrations as the unamended soil. Nevertheless, Tang et al. (2019) found the opposite trend, namely that DOC concentration increased with biochar amendment in soil, implying that amendment with biochar does not always signify lower DOC concentrations. Consequently, this connection might not be so straightforward, and are likely influenced by a number of biochar properties, such as surface area, pore volume and pore diameters, as described in section 4.1.1.

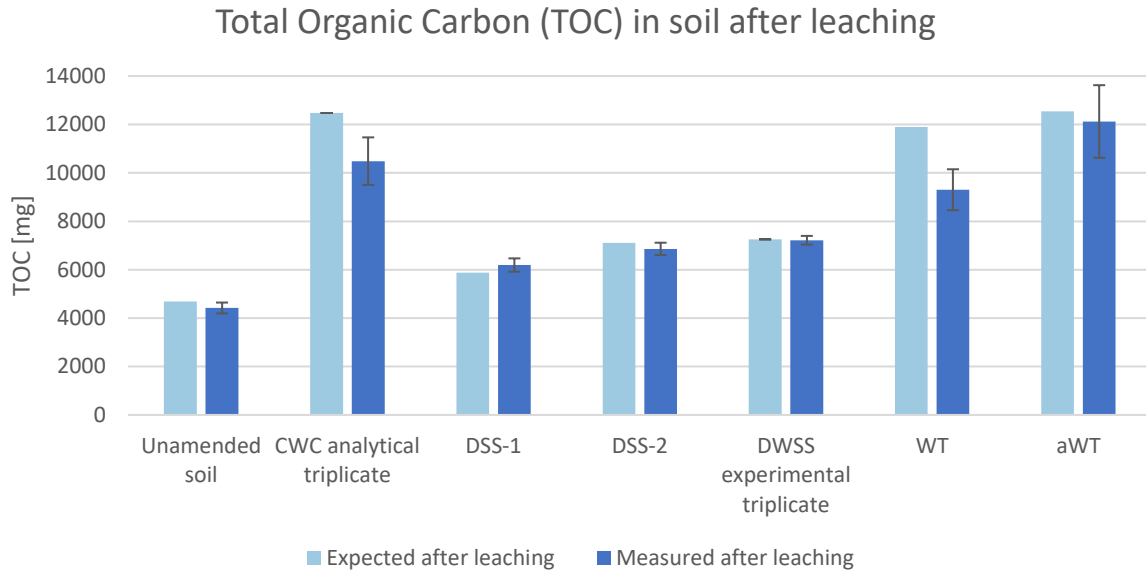




**Figure 11:** Dissolved organic carbon (DOC) [mg/L] in leachate from all columns. The x-axis is given as liquid to solid ratios (L/S). Relative standard deviations are applied to all concentrations, while mean values  $\pm$  std are presented for the CWC (analytical triplicate) and DWSS (experimental triplicate). Points are discrete values, lines are only drawn for better visualization.

Soil samples from each column and the original soil were analysed for total organic carbon (TOC) in triplicate, except for the three columns amended with DWSS biochar, where only one sample from each column was analysed. The original- and control column soil presented the lowest TOC contents of below 0.6%, while the soil amended with the wood-based sorbents presented the highest TOC contents above 1.1%, which is illustrated on figure 12 as "Measured after leaching". This corresponds with the higher carbon contents of the three wood-based biochars (91.4%, 89.5% and 85.1% for CWC, aWT and WT, respectively), which adds organic carbon to the soil, compared to the lower carbon content in the sludge-based sorbents (29.6%, 27.7% and 13.5% for DWSS, DSS-2 and DSS-1, respectively).

The higher TOC content seen in soil amended with biochar may contain some water-soluble carbon from the biochar as well as from the soil, which also can be released as DOC. This was studied by Smebye et al. (2016), which found that biochar amendment to soil could result in release of dissolved organic matter (DOM). Most of the released DOM was explained by an increase in pH upon the application of biochar, where an increase of 3.8 pH-units resulted in a 15-fold DOM increase. As the pH was neutral and generally did not increase following biochar amendment in this experiment (see pH of leachate samples in table 3 and Appendix A), a similarly increase in DOC could not be expected, although a smaller increase in DOC from biochar amendment could be likely.



**Figure 12:** Carbon mass balance for unamended soil and soil amended with biochar, shown for expected total organic carbon (TOC) [mg] in the soil after leaching and measured after leaching. TOC was analysed in triplicate samples of the soil after leaching, where the three columns amended with DWSS biochar provided one sample each. Mean values  $\pm$  std are presented for the CWC (analytical triplicate) and DWSS (experimental triplicate) for expected TOC after leaching.

Figure 12 shows a carbon mass balance for expected- and measured TOC in the soil with- and without biochar amendment, after the leaching test. The remaining TOC after leaching is the net of DOC adsorption to the biochar and DOC desorption from the biochar and soil. It was only a very small part of the TOC that leached out as DOC: 2.9% (unamended soil) > 1.6% (DSS-1) > 0.99% (WT) > 0.89% (CWC) > 0.88% (DWSS) > 0.84% (DSS-2) > 0.21% (aWT). The highest percent of leached DOC, from soils amended with biochar, were the WT (0.99%) and CWC (0.89%), only surpassed by the DSS-1 biochar (1.6%). However, the amount of leached DOC from the CWC and WT (118 mg and 111 mg, respectively) were still higher than the DSS-1 (91.6 mg), due to the low carbon content in the DSS-1 (13.5%). The amount of DOC leached from soils in mg followed the same order as given in percent otherwise. The overall highest percent of leached DOC was from the unamended soil, indicating that all 6 types of biochar sorb more DOC than are desorbed from them.

#### 4.3.1 PFAS and DOC correlation

A presumed correlation between DOC and PFAS was evaluated by performing a simple linear regression analysis in Excel, using the Data Analysis Tool.

The possibility of DOC-facilitated transport of PFAS in the aqueous phase, inhibits PFAS sorption to the biochar. This is due to the partitioning of PFAS into DOC, leading to formation of soluble complexes (Bolan et al., 2021). The link between DOC and concentration of PFOS

in batch test leachate was studied by Tang et al. (2017). The study found that DOC increased the solubility of PFOS in leachate, thereby enhancing the desorption of PFOS from soil. Furthermore, it was suggested that since the distribution of hydrophobic compounds in soil and sediment are influenced by DOC, the desorption of the PFOS may be related to hydrophobic adsorption and distribution functions. In another study, Fabregat-Palau et al. (2022) also reported that DOC content had a negative effect on PFAS adsorption to biochar, but contrasting Tang et al. (2017) it was instead suggested that the cause was competition between DOC and PFAS for sorption sites and blocking of pores.

The performed analysis was assessing whether DOC concentration was related to PFAS concentration in the leachate, with the following null hypothesis: The concentration of DOC has no effect on the concentration of PFAS in the leachate. The analysis was carried out with PFAS and DOC concentrations from all leachate samples, with a total of 66 observations. The regression analysis was carried out for PFBS, PFHxA, PFHpA, 6:2 FTS, PFHxS, PFOA, PFOS, 8:2 FTS, PFOSA and diSAMPAP.

**Table 4:** R<sup>2</sup> and p-values for linear regression of DOC and PFAS. Number of observations: 66.

<b>Compound</b>	<b>CF-chain length</b>	<b>R<sup>2</sup></b>	<b>p-value</b>
<b>PFBS</b>	CF4	0.54	< 0.05
<b>PFHxA</b>	CF5	0.68	< 0.05
<b>PFHpA</b>	CF6	0.74	< 0.05
<b>6:2 FTS</b>	CF6	0.73	< 0.05
<b>PFHxS</b>	CF6	0.75	< 0.05
<b>PFOA</b>	CF7	0.74	< 0.05
<b>PFOS</b>	CF8	0.02	0.31
<b>8:2 FTS</b>	CF8	0.03	0.19
<b>PFOSA</b>	CF8	0.01	0.50
<b>diSAMPAP</b>	CF16	0.25	< 0.05

R<sup>2</sup> and p-values of the linear regression analyses of DOC and different PFAS can be seen in table 4, and resulted in rejection of the null hypothesis for PFBS, PFHxA, PFHpA, 6:2 FTS, PFHxS, PFOA and diSAMPAP. This concluded that DOC concentrations were statistically significantly related to the concentrations of these 7 PFAS in the leachate. Although, the R<sup>2</sup> values indicated that not all the variance in the PFAS leaching concentrations were correlated

by the DOC concentrations in the leachate. In case DOC-facilitated transport was the cause of the relationship between PFAS and DOC, between 54% and 75% of the leachate concentrations could be due to DOC-facilitated transport for the 6 PFAS with CF-chain length 4 to 7, while for diSAMPAP maximally 25% could be explained by the DOC concentration.

The null hypothesis was not rejected for PFOS, 8:2 FTS and PFOSA, concluding no correlation between these three PFAS and DOC concentrations. This may be explained by the different leaching patterns of PFOS, 8:2 FTS and PFOSA compared to the other PFAS, which again might be due to longer CF-chain lengths, as mentioned in section 4.2. PFOS and PFOSA demonstrated peak concentrations at L/S 1 and 8:2 FTS at L/S 2, in contrast to the other PFAS, which showed peak concentrations at L/S 0.1 or 0.2. An exception was diSAMPAP with a CF-chain length of 16, which contrary to the three PFAS with CF-chain length of 8, showed relatively low retention by the sorbents and correlation with DOC in the leachate. This may be due to the larger molecular structure of this compound, leading to less pores in the biochars which could accommodate it. However, DOC may have a bigger impact on short-chained PFAS, as they both are less hydrophobic than long-chained PFAS, which also might be more tightly bound by the biochar or organic carbon in the solid phase. Thus, DOC-facilitated transport of long-chained PFAS is less prone to happen.

The results of the DOC analysis in leachate indicated a correlation between DOC and PFAS concentrations, suggesting that higher DOC concentration result in higher PFAS concentration in the leachate. Furthermore, the carbon mass balance demonstrated that all 6 biochars sorbed DOC, as the unamended soil leached more DOC (2.9%) than the soils amended with biochar ( $\leq 1.6\%$ ), with WT and CWC demonstrating highest amounts of DOC leaching. Considering that the regression analysis indicated a correlation between DOC and PFAS ( $< \text{CF}_8$ ) in leachate, the effect of DOC on PFAS mobilization could be twofold. First, as all 6 sorbents decrease the available DOC for PFAS desorption from the soil, less PFAS will be in the leachate. Second, less PFAS will leach if complexes of DOC and PFAS are sorbed to the biochar. As DOC-PFAS-complexes are quite big in size, this could be the reason that the effect of possible sorption of these complexes are higher in the aWT- and sludge-based sorbents, containing higher amounts of mesopores (2–50 nm) than the CWC and WT biochars.

#### 4.4 Distribution coefficients ( $K_d$ )

This section presents soil-water distribution coefficients of PFAS to the different biochars, and discusses the trends, variations, and dependency of different PFAS properties.

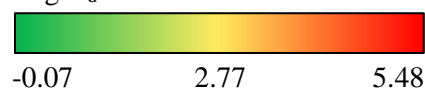
The solid-liquid distribution coefficients of PFBS, PFHxA, PFHpA, 6:2 FTS, PFHxS, PFOA, PFOS, 8:2 FTS, PFOSA and diSAMPAP to the CWC, DSS-1, DSS-2, DWSS, WT, aWT biochars and soil from the leaching test, are listed in table 5. A heatmap is incorporated in the table, indicating the weight of the value, with the lowest values being green and highest values being red. The distribution coefficients are given as a total value for the soil amended with biochar ( $K_{d,tot}$ ) and a value for the biochar only ( $K_{d,BC}$ ). Furthermore, distribution coefficients of PFAS to the unamended soil are also included in the table. All distribution coefficients are given in  $\log_{10}$ . Figure 13 illustrates the decrease in mass [ $\mu\text{g}$ ] of PFOS and PFHxS from the soil due to desorption, both as discrete points and modelled, which was used for calculating the  $K_d$  values.

Distribution coefficients in L/kg for the 10 different PFAS varied over 5 orders of magnitude with  $\log K_d$  values between 0.10 to 1.26 for the unamended soil, -0.07 to  $\geq 3.48$  for soil amended with biochar, and 0.26 to  $\geq 5.48$  for biochar only. Since  $K_d$  values are calculated for a specific substance concentration, it can be difficult to compare with other studies directly, without correcting for the concentration, as PFAS sorption to biochar generally not is linear (Hale et al., 2016; Krahn et al., 2023). Furthermore, the distribution coefficients in this study were calculated using a different method, compared to most other studies, which also might have an impact on the comparability. However, the distribution coefficients for unamended soil were generally higher than  $K_d$  values for PFAS with similar chain lengths reported by Hubert et al. (2023) and Høisæter and Breedveld (2022). Both studies presented  $K_d$  values for AFFF-impacted soil with similar concentrations of PFAS as the soil used in this study. However, the  $K_d$  values (not in  $\log_{10}$ ) for PFOS presented in the two studies were slightly higher (6.83 and 4.5-30 L/kg, respectively) than the one obtained in this study, of 1.25 L/kg, which might be due to some of the PFOS leachate concentrations used in their  $K_d$  calculations were less than half of the detected PFOS concentrations in the study.

**Table 5:** Log  $K_d$  values [L/kg] for the 6 different biochars and the control computed for 10 selected PFAS<sup>1</sup>. Log  $K_d$  were calculated for both the soil and biochar mixture ( $K_{d,tot}$ ), and for the biochar alone ( $K_{d,BC}$ ).  $K_d$  values for DWSS are given as mean values  $\pm$  standard deviation. \* = values computed using the 1<sup>st</sup> order two-compartment model. \*\* = mean value (n=2). NA =  $K_d$  could not be computed due to no detected PFAS concentration in leachate and/ or soil, or due to no significant/measurable sorption of  $F_{rap}$  in the model. Values given as " $\geq$ " were calculated (partly) with leaching concentration of LOD/2, as very little or no leaching was observed.

Biochar type		Control	CWC		DSS-1		DSS-2		DWSS		WT		aWT	
Compound	CF-chain length	Log $K_d$	Log $K_{d,tot}$	Log $K_{d,BC}$	Log $K_{d,tot}$	Log $K_{d,BC}$	Log $K_{d,tot}$	Log $K_{d,BC}$	Log $K_{d,tot}$ (mean, n=3)	Log $K_{d,BC}$ (mean, n=3)	Log $K_{d,tot}$	Log $K_{d,BC}$	Log $K_{d,tot}$	Log $K_{d,BC}$
PFBS	CF4	NA	NA	NA	$\geq -0.07$	NA	$\geq 1.48$	NA	$\geq 1.07^{**} \pm 0.20$	NA	NA	NA	NA	NA
PFHxA	CF5	$\geq 0.74^*$	NA	NA	$\geq 0.73$	NA	1.09	2.84	$1.16 \pm 0.12$	$2.94 \pm 0.20$	NA	NA	$\geq 1.29$	$\geq 3.15$
PFHpA	CF6	$0.29^*$	NA	NA	0.41	1.84	1.31	3.27	$1.80 \pm 0.36$	$3.78 \pm 0.37$	NA	NA	2.26	4.25
6:2 FTS	CF6	$1.26^*$	NA	$1.22^*$	1.34	2.61	1.59	3.33	$1.66 \pm 0.08$	$3.44 \pm 0.14$	NA	$1.36^*$	1.70	3.50
PFHxS	CF6	$0.72^*$	NA	$0.97^*$	0.95	2.58	1.47	3.38	$1.58 \pm 0.13$	$3.51 \pm 0.16$	NA	$0.97^*$	1.62	3.56
PFOA	CF7	$0.46^*$	NA	$0.26^*$	0.97	2.81	1.58	3.55	$1.92 \pm 0.10$	$3.91 \pm 0.10$	NA	$1.30^*$	2.26	4.26
PFOS	CF8	0.10	0.39	2.09	1.02	2.96	1.62	3.61	$2.11 \pm 0.11$	$4.10 \pm 0.11$	0.34	1.98	3.09	5.09
8:2 FTS	CF8	0.62	0.95	2.68	2.19	4.17	$\geq 2.84$	$\geq 4.84$	$\geq 2.84 \pm 0.13$	$\geq 4.83 \pm 0.13$	0.93	2.65	$\geq 2.86$	$\geq 4.85$
PFOSA	CF8	0.75	1.21	3.03	2.22	4.20	2.39	4.38	$\geq 3.22 \pm 0.52$	$\geq 5.22 \pm 0.52$	1.03	2.72	$\geq 3.48$	$\geq 5.48$
diSAMPAP	CF16	0.96	1.23	2.89	1.48	3.32	1.25	2.94	$1.40 \pm 0.07$	$3.20 \pm 0.11$	1.15	2.72	1.24	2.92

Log  $K_d$



<sup>1</sup> Only a few  $K_d$  values could be computed for PFBS, due to no detected concentration in any of the leachate and/ or soil samples, or complete desorption before the end of the experiment. In a few cases the  $K_{d,soil}$  or  $K_{d,BC}$  (not in  $\log_{10}$ ) ended up being negative when using the 1<sup>st</sup> order two-compartment model.  $K_{d,tot}$  for CWC and WT could therefore not be determined for 6:2 FTS, PFHxS and PFOA, as a negative  $K_d$  indicates no sorption of  $F_{rap}$  in the model.  $K_d$  for PFHpA and PFHxA sorption to CWC and WT biochars could not be determined either for the same reasons, or due to no noticeable adsorption effect to the biochar. A negative  $K_d$  could be due to analytical errors caused by the model predicting the rate constant ( $k_{rap}$  or  $k_{slow}$ ) to be lower than the actual water flow through the column. For the control column only, a  $K_{d,soil}$  value of 0 (no sorption) was used when calculating the  $K_{d,tot}$  instead.

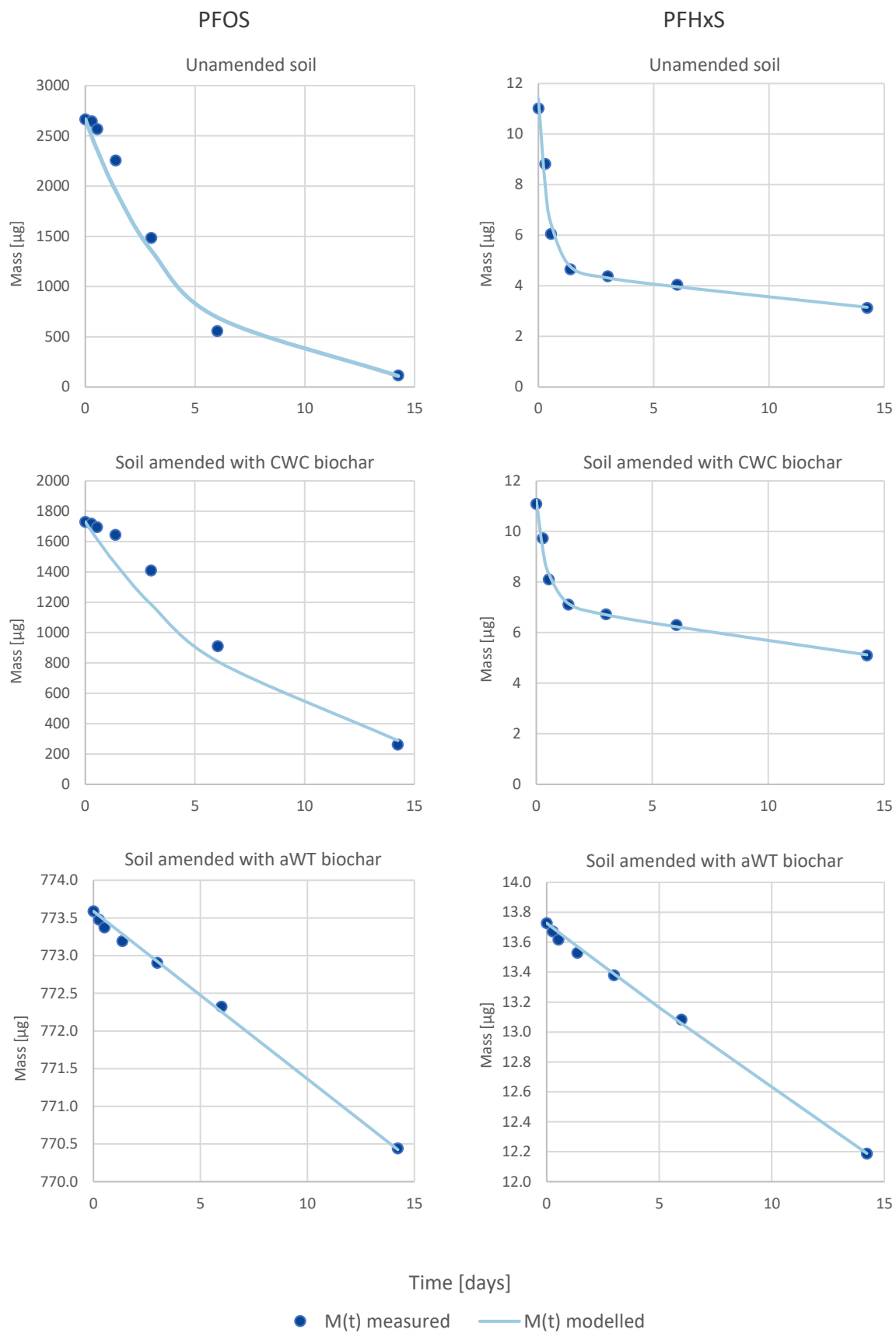
The log  $K_{d,BC}$  value for PFOS sorption to the aWT biochar (5.09) was found to be in the same range as the log  $K_d$  value presented by Sørmo et al. (2021) of  $5.7 \pm 0.6$ , using the same biochar sorbent in a batch test with a low-TOC soil and a normalized PFOS concentration of 1  $\mu\text{g/L}$ . The study also presented log  $K_d$  values for PFBS, PFHxA, PFHxS and PFOA sorption to the aWT biochar, ranging from  $5.4 \pm 0.7$  to  $6.2 \pm 0.7$ , which are higher than values presented for the same compounds in table 5. As the distribution coefficients determined by Sørmo et al. (2021) were obtained with normalized PFAS concentrations of either 1 ng/L or 1  $\mu\text{g/L}$ , it could be expected that the sorption to the biochar would be higher, leading to higher  $K_d$  values than in this study, as the leachate concentrations of PFAS generally was higher. Distribution coefficients for a biochar produced from the same feedstock as the WT biochar, but pyrolyzed at 900 °C, was also presented by Sørmo et al. (2021), exhibiting log  $K_d$  values of  $3.7 \pm 0.5$  to  $4.6 \pm 0.6$ , which overall compare well to the log  $K_{d,BC}$  values given in table 5, especially for the sludge-based biochars. Furthermore, the study by Krahn et al. (2023), also tested three of the same biochar sorbents as this study. The presented log  $K_d$  values, in the presence of soil and a mixture of PFAS, for PFHxA, PFHpA and PFOA sorption to the DSS-1 and DWSS (3.24 for only PFOA and 2.40 to 3.47, respectively), was generally in the same range the corresponding log  $K_{d,BC}$  from this study (1.84 to 2.81 for DSS-1 and 2.94 to 3.91 for DWSS). For the CWC biochar, the log  $K_d$  values presented by the study was considerably higher (2.19 to 2.73), than obtained in this study (0.26 for PFOA). Even though the studies by Sørmo et al. (2021) and Krahn et al. (2023) carried out batch tests with mixtures consisting of biochar (0.1 - 5% and 2%, respectively), soil and a mixture of PFAS, PFAS sorption to biochar can be expected to be lower in a soil column leaching test, imitating more realistic environmental conditions. While batch tests demonstrate optimal conditions for PFAS sorption to biochar, with the biochar and PFAS being able to be in contact for the whole duration of the test, this is not the case for column leaching tests. Although only the CWC biochar demonstrated considerably lower  $K_d$  values in the column tests compared to batch tests by Krahn et al. (2023), much higher concentrations of the three PFCA were used in the batch tests, compared to what was detected in the AFFF-impacted soil, indicating that the difference in setup of the tests may have a large influence on the sorption. Moreover, with only 1% of biochar added to the soil in this experiment, it is even further possible that less PFAS came in contact with the biochar, in addition to higher competition for sorption sites due to the lower amount of biochar compared to the two latter studies. Additionally, the possibility of inhomogeneous flow through the column may have restricted the contact even further.

Distribution coefficients for PFHxA, PFHpA 6:2 FTS, PFHxS, PFOA, PFOS, 8:2 FTS, PFOSA generally followed the same order, namely: WT < CWC < DSS-1 < DSS-2 < DWSS < aWT. diSAMPAP (CF16) showed strongest sorption to the DSS-1 and DWSS biochars, possibly caused by the greater proportion of larger pores in these two sorbents, making the large molecule fit easier into the pores, as proposed by Krahn et al. (2023). For the few  $K_d$  values calculated for PFBS, the order of increasing sorption was: DSS-1 < DWSS < DSS-2. Moreover, the few distribution coefficients and their values simply indicate the difficulty of retainment of short-chained PFAS. This trend of lower removal efficiency of short-chained PFAS by both AC and biochar was also found by e.g., Eschauzier et al. (2012), Ross et al. (2018) and Zhang and Liang (2022).

Log  $K_{d,BC}$  for the strongest sorbent, aWT, increased in the following order: diSAMPAP < PFHxA < 6:2 FTS < PFHxS < PFHpA < PFOA < 8:2 FTS < PFOS < PFOSA. The overall same order was followed for adsorption to the DWSS and DSS-2 biochars, with a few exceptions e.g., different order of the three CF8 PFAS: PFOS < 8:2 FTS < PFOSA. The aWT, DWSS and DSS-2 biochars showed strong retention of 8:2 FTS and PFOSA leading to concentration below LOD/LOQ or a few samples < 0.1  $\mu\text{g/L}$ . Thus, most of the  $K_d$  values for these compounds had to be calculated with a set concentration of LOD/2, and are marked with " $\geq$ " in table 5 for indication that the values might be higher, due to the strong sorption. A very strong sorption of PFAS to AC, leading to concentrations below detection level, was also seen by Kupryianchyk et al. (2016), which used the same method to calculate distribution coefficients.

The distribution coefficients calculated with the 1<sup>st</sup> order two-compartment model, marked with a "\*" in table 5, indicate a trend of rapid desorption of the PFAS with CF-chain lengths < 8, in unamended soil and soil amended with CWC and WT biochar. The two-compartment model was namely used when a rapid desorption in the beginning of the experiment was observed, as seen in figure 13 for PFHxS in unamended soil and soil amended with CWC. This further supports that these two non-activated wood-based biochars are poor sorbents, especially for the shorter chained PFAS.





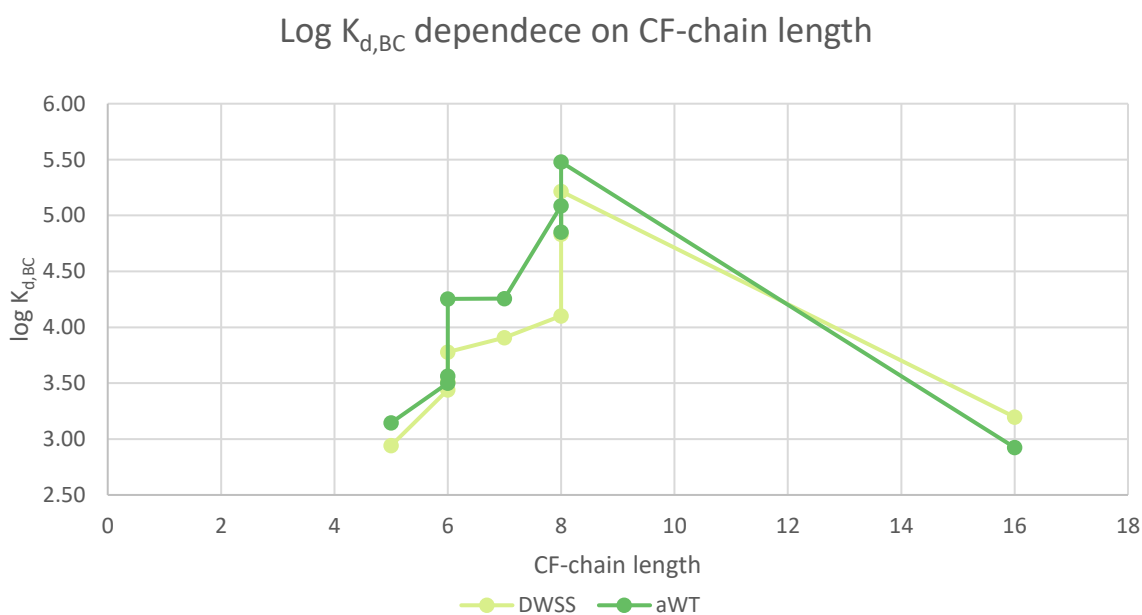
**Figure 13:** Mass [ $\mu\text{g}$ ] of PFOS and PFHxS in unamended soil, soil amended with CWC biochar and soil amended with aWT biochar over time. The mass is shown as measured discrete points and a modelled continuous line. The rate constant(s),  $k$ , for each modelled line was used for calculation of  $K_d$  values. The  $M(t)$  was modelled using the 1<sup>st</sup> order model, while PFHxS in unamended soil and soil amended with CWC biochar were modelled using the 1<sup>st</sup> order two-compartment model.

#### 4.4.1 Link between $K_d$ and PFAS properties

In this section, the relation between  $K_d$  values and different properties of the PFAS are discussed, mainly in connection with the CF-chain length and the functional groups.

##### CF-chain length and $K_d$

Generally, an increase in  $K_d$  with increasing CF-chain length was observed and are illustrated for the aWT and DWSS biochars on figure 14, which is in accordance with other studies (Fabregat-Palau et al., 2022; Higgins & Luthy, 2006; Hubert et al., 2023; Krahn et al., 2023; Söregård et al., 2020). This was even further evident when dividing into PFCA, PFSA and FTS, also demonstrated by Hubert et al. (2023). An exception was diSAMPAP (CF16) which deviated from this trend. The observation indicates hydrophobic interactions between PFAS and the biochar. PFAS generally show much lower van der Waals interaction energy per molecular contact, than other organic compounds of similar size (Goss & Bronner, 2006). This is caused by the energy required to create a cavity for a  $CF_2$  moiety in water, which is much greater than the energy that can be gained by van der Waals interactions between the  $CF_2$  moiety and neighbouring water molecules. Hence, dissolution in the water phase becomes more energetically unfavourable with each  $CF_2$  moiety, leading to higher adsorption onto the biochar surface (Du et al., 2014; Goss et al., 2006). In summary, this suggests that hydrophobic interactions had a very important role in sorption of PFAS onto the 6 types of biochar used in this study.



**Figure 14:** Log  $K_{d,BC}$  [L/kg] plotted against CF-chain length for the two strongest sorbents, aWT and DWSS. Points are discrete values, lines are only drawn for better visualization.

## Functional group and $K_d$

Electrostatic interactions based on the functional group should also be considered, as this can have a central role in sorption variations between PFAS with same chain lengths (Higgins & Luthy, 2006). Differences in sorption of PFSA and PFCA can be explained by the different properties of their acid functional group. In general, PFSA demonstrate stronger adsorption than PFCA, due to the stronger acidity of sulfonic acids compared to carboxylic acids, which leads to stronger ionic interactions with positively charged surfaces (Du et al., 2014; Zhang et al., 2021). The slightly larger size of the sulfonate functional group also requires greater cavity formation energy, resulting in larger hydrophobic effect (De Voogt et al., 2012). This could not be entirely confirmed by this study, as  $K_d$  values only were calculated for one pair of PFCA and PFSA of same CF-chain length (CF6), which showed the opposite for the two strongest sorbents (e.g.  $\log K_d$  for aWT of 4.25 and 3.56 for PFHpA and PFHxS, respectively), but were true for some of the other sorbents. On the other hand, this was true for PFOA (CF7) and PFOS (CF8) sorption to all biochars, which share the same carbon chain length, although this could also be caused by the slightly more hydrophobic chain of PFOS.

For all 6 biochars the PZC was very low, leading to negatively charged surfaces. Suppressed sorption from electrostatic repulsion may thus occur between the anionic biochar and anionic functional groups. A relatively stronger overall electrostatic repulsion will occur for shorter chains, as the hydrophobicity of the CF-chain will be less dominant. However, inorganic cations from mineral fractions, in especially the sewage sludge-based biochars with high ash content, may have contributed to divalent cation-bridging between negatively charged PFAS and biochar (Du et al., 2014; Tang et al., 2017; Zhou et al., 2010), contributing to stronger sorption of short-chain anionic PFAS to especially these three biochars.

A difference in sorption was observed between the three PFAS with the same CF-chain length of 8, with generally increasing  $K_{d,BC}$  values in the following order: PFOS < 8:2 FTS < PFOSA (e.g.  $\log K_{d,BC}$  for DWSS:  $4.10 \pm 0.11 < 4.83 \pm 0.13 < 5.22 \pm 0.52$ ). This order was observed for all distribution coefficients, both for  $K_{d,BC}$ ,  $K_{d,tot}$  and in the unamended soil, except for DSS-2 and aWT. For these two, the order was instead ( $\log K_{d,BC}$ ): PFOS (3.61) < PFOSA (4.38) < 8:2 FTS ( $\geq 4.84$ ) for DSS-2, and 8:2 FTS ( $\geq 4.85$ ) < PFOS (5.09) < PFOSA ( $\geq 5.48$ ) for aWT, which may be due to the use of concentrations of LOD/2 for some of the  $K_d$  values. Hubert et al. (2023) observed a similar order of increasing  $K_d$  values (PFOS < 8:2 FTS < PFOSA) and suggested that a stronger adsorption of the telomeric headgroup could be explained by its weaker negative charge compared to that of the sulfonic acid, leading to decrease in solubility

and increase in sorption of 8:2 FTS. The stronger anionic charge on PFOS, is caused by the stronger electron withdrawing effect of the perfluoroalkyl group on the sulfonic functional group, which is reduced by the ethylene spacer on the 8:2 FTS leading to a raise in  $pK_a$  (Jing et al., 2009). It was furthermore suggested by Hubert et al. (2023) that the sulfonamide group on PFOSA becomes partially neutral at environmental pHs, due to a high  $pK_a$ , leading to lower solubility and decreased electrostatic repulsion by negative charged surfaces. This could explain the stronger sorption of PFOSA and 8:2 FTS to the different biochar sorbents, compared to PFOS. Furthermore, the significant higher concentration of PFOS in the soil may also have influenced the higher leaching of PFOS compared to 8:2 FTS and PFOSA, leading to lower  $K_d$  values.

Fabregat-Palau et al. (2022) found that stronger sorption of PFAS to carbon-rich materials correlated with longer CF-chains, higher  $C_{org}/O$  molar ratio and surface area. Lower amounts of functional groups on the surface of the biochar are indicated by higher  $C_{org}/O$  ratios (opposite of O/C reported in table 1), resulting in less negative electrostatic repulsion of PFAS. It was therefore suggested that sorption mainly was controlled by hydrophobic interactions, while electrostatic interactions only played a minor role. The same could be assumed for this experiment, as the largest differences in  $K_d$  were observed between compounds with different tail lengths rather than between compounds with different functional groups. For PFAS with similar chain lengths,  $K_d$  was generally increasing in the following order: carboxylic acid < sulfonic acid < fluorotelomer < sulfonamide.

On average,  $\log K_d$  values were not as high as values presented in the studies by e.g. Krahn et al. (2023) and Sørmo et al. (2021), which could be expected for column tests, but did show the same trends as previously reported in the literature (Fabregat-Palau et al., 2022; Higgins & Luthy, 2006; Söregård et al., 2020).

#### 4.4.2 Attenuation factor

Attenuation is the reduced sorption strength of a sorbent, due to the presence of soil and/or other contaminants (Du et al., 2014). Sorption attenuation have been demonstrated for PFAS sorption to PAC with e.g. 87.1% lower PFOS sorption caused by effluent organic matter (Yu et al., 2012), attenuation of PFAS sorption to biochar by soil and other PFAS with factors of 8-6581 (Krahn et al., 2023), attenuation of PFAS to activated biochar by organic carbon with factors of 10-158 (Sørmo et al., 2021), as well as with other organic contaminants, e.g. attenuation by PAHs in phenanthrene sorption to black carbon, with a factor 5 decrease in sorption strength

(Cornelissen & Gustafsson, 2006), and attenuation by soil of pyrene and phenanthrene to sewage sludge-derived biochar with 4.7-11.2 times lower sorbate binding (Zielińska & Oleszczuk, 2016). As both presence of soil and other contaminants could influence the sorption strength of individual PFAS to the biochars, sorption attenuation was investigated.

Attenuation factors (AF) for individual PFAS to the biochar sorbents were determined using  $\log K_{d,BC-soil-mix}$  values (from the present work) calculated using concentrations at L/S 0.1 (sorption to biochar but corrected for direct impact of soil and a mixture of PFAS) and  $\log K_{d,BC-single}$  values (for clean biochar without soil and without other PFAS) calculated using  $\log K_{F,BC}$  (Freundlich isotherm for single PFAS in water) from Krahn et al. (2023).  $K_{F,BC}$  values from single PFAS-water batch tests at  $C_w$  of 1  $\mu\text{g/L}$  as presented by Krahn et al. (2023) were used to calculate  $K_{d,BC-single}$  values, and were corrected to apply for concentrations detected at L/S 0.1 in the column experiment. AF were calculated for PFHxA, PFHpA and PFOA to the CWC, DSS-1 and DWSS biochars, as these were tested in both studies:

$$AF = \frac{K_{d,BC-single} \text{ (Krahn et al., 2022)}}{K_{d,BC-soil-mix} \text{ (this work)}}$$

(18)

Attenuation factors thus represent how much weaker sorption is in the presence of soil and other PFAS as compared to sorption of single PFAS to clean biochar. AFs for PFAS sorption to the three different biochars impacted by presence of soil and a mixture of at least 26 (quantifiable) PFAS, are shown in table 6. AF for PFOA decreased in the following order: CWC (428) > DWSS (163) > DSS-1 (49.2). The same order applied for PFHpA and PFHxA. The most attenuation was observed for the CWC biochar, with AFs of 655 and 428 for PFHpA and PFOA, respectively. This means that this biochar was the most affected in sorption by presence of soil and competition of a mixture of other PFAS. The DWSS and DSS-1 biochars showed AFs less than half the values of CWC, but were lowest for the DSS-1 biochar, suggesting that these sorbents also demonstrate stronger sorption than the CWC in a natural soil environment with presence of other contaminants, as well as in a single PFAS-water batch test. A decrease in AF with shorter CF-chain was seen for DWSS and partly for DSS-1, but the chain length did not seem to have a considerable effect on attenuation. However, only three compounds with very similar chain lengths were evaluated, thus more data would be needed to test this relationship further.

**Table 6:** Attenuation factors (AF) [-] for sorption of PFAS to biochar under presence of soil and a mixture of PFAS, calculated using  $\log K_{d,BC\text{-soil-mix}}$  at L/S 0.1, and  $\log K_{d,BC\text{-single}}$  values both at the same  $C_w$  (also shown in the table).  $K_{d,BC\text{-single}}$  values were calculated from  $\log K_{F,BC}$  of single PFAS-water batch tests at  $C_w$  of 1  $\mu\text{g/L}$  from Krahn et al. (2023), and were corrected to apply for  $C_w$  detected at L/S 0.1.

Biochar type		CWC				DSS-1				DWSS			
Com-pound	CF-chain length	$C_w$ [ $\mu\text{g/L}$ ]	Log $K_{d,BC\text{-soil-mix}}$	Log $K_{d,BC\text{-single}}$	AF	$C_w$ [ $\mu\text{g/L}$ ]	Log $K_{d,BC\text{-soil-mix}}$	Log $K_{d,BC\text{-single}}$	AF	$C_w$ [ $\mu\text{g/L}$ ]	Log $K_{d,BC\text{-soil-mix}}$	Log $K_{d,BC\text{-single}}$	AF
PFHxA	CF5	18.0	1.53	NA	NA	1.62	2.88	3.32	2.78	1.17	3.04	4.75	52.3
PFHpA	CF6	3.40	1.41	4.22	655	0.04	3.56	5.27	51.8	0.03	3.75	5.86	129
PFOA	CF7	4.79	2.01	4.65	428	0.14	3.77	5.46	49.2	0.12	3.84	6.05	163

The AFs listed in table 6 were overall in the same range as the AFs presented by Krahn et al. (2023) in scenarios with soil and a mixture of PFAS. However, comparison of AFs for specific PFAS sorption to the biochars showed in some cases large variations. AFs reported by Krahn et al. (2023) were 55 for PFHxA, 6581 for PFHpA and 134 for PFOA sorption to DWSS biochar, while lower values were reported for CWC and DSS-1 biochars for the three PFCA. The AF of 6581 (PFHpA sorption to DWSS) was over 50 times higher than the AF obtained in this study of 129, while very similar values were obtained for PFHxA of 55 and 52.3 from Krahn et al. (2023) and this study, respectively. Moreover, the order of increasing attenuation factors was opposite from the observation in this study, with Krahn et al. (2023) presenting the following order of AFs for PFOA: DWSS (134)  $\gg$  DSS-1 (19)  $>$  CWC (8). The variation in some AFs might be due to the values not being directly comparable. In this study, attenuation was calculated using distribution coefficients for biochar impacted by a mixture of PFAS and soil organic matter, but with the direct impact of the soil organic matter corrected for. Furthermore, much lower concentration points (0.03-18  $\mu\text{g/L}$ ) were used for the  $K_{d,BC\text{-soil-mix}}$  in this study, than used by Krahn et al. (2023) ( $>283 \mu\text{g/L}$ ). As linear sorption is assumed for  $K_d$  values, the much higher concentrations used in the study by Krahn et al. (2023) leads to variations between the distribution coefficients reported in the study and the ones calculated in this study based on concentrations measured at L/S 0.1. Additionally, a different soil was used in the batch tests, which could lead to differences in attenuation, despite the soil also being low in TOC (1.3%).

The attenuation effect by competition from similar compounds could be assumed to be greater than the effect of the soil organic matter, as the TOC content in the soil was low ( $0.57 \pm 0.04\%$  for the original soil), implying less competition induced by organic matter. A larger attenuation

by presence of a mixture of PFAS was also suggested by Krahn et al. (2023), as the study compared attenuation of sorption to biochar in presence of a PFAS mixture (6 different PFAS) with and without soil. As the number of different PFAS that could compete for sorption sites were substantially higher in this study (at least 26), one could expect that this also would be the main aspect influencing sorption attenuation. Furthermore, the high concentration of PFOS strongly influenced the sorption of other PFAS to the biochar, while the opposite had a lower effect. Despite these observations, it cannot be conclusively defined which parameter had the most influence on attenuation, as they were not assessed in isolation from one another.

In summary, the presence of a PFAS mixture and soil organic matter had the largest impact on sorption to the CWC biochar, possibly due to a higher likelihood of pore clogging and saturation of the smaller pores of this sorbent.

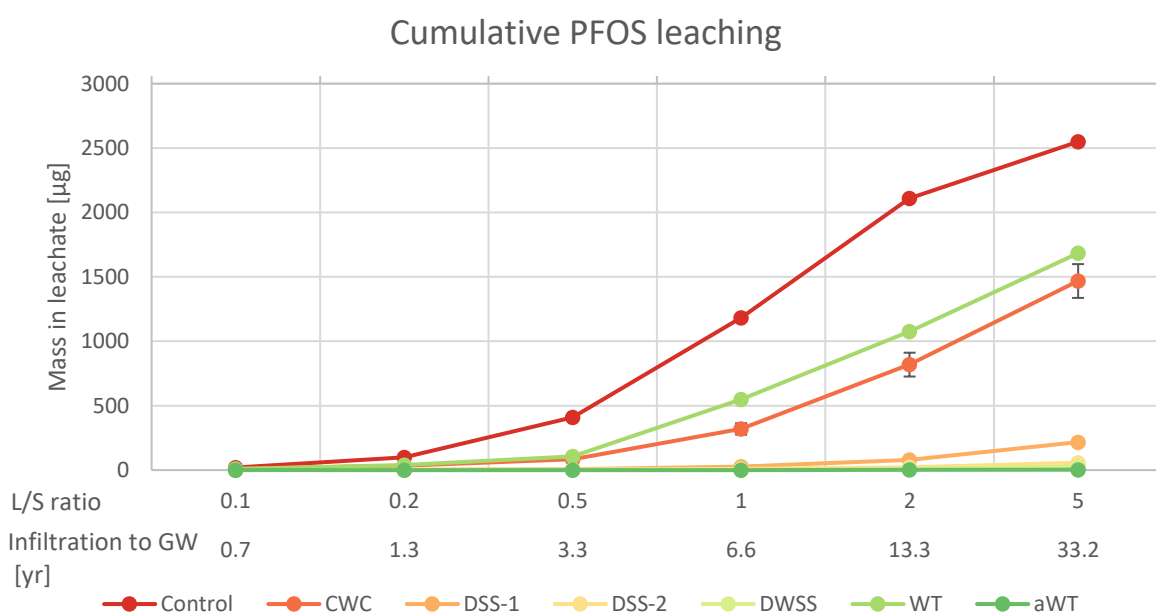
#### 4.5 Estimation of groundwater contamination with PFAS

Leaching of PFAS from the AFFF-affected soil may be a threat to the groundwater (GW) and the subsequent transport in the groundwater aquifer, possibly leading to contamination of drinking water. Based on the column tests and equation ( 17 ) a time scale was computed, describing the period it will take before the soil in field conditions is exposed to the same amount of water, as used for the 6 L/S ratios. The formula contained parameters of annual precipitation, bulk density, and height of the soil in field, yielding the estimated periods it would take water to infiltrate x m of soil. The groundwater level at the firefighting training facility, where the AFFF-affected soil originates from, is on average  $3.45 \pm 0.4$  m (n = 6) below the surface in vertical distance. Furthermore, the calculation was based on unamended soil in the control column, and an estimate of annual precipitation of 750 mm at the site was used (Statistisk sentralbyrå, 2014). In addition to the depth down to the GW level, the time scale for infiltrating 1 m of soil was also computed, which can be seen in table 7.

**Table 7:** Estimated time in year for water infiltration in field conditions, calculated based on L/S ratios, properties of the AFFF-impacted soil and annual precipitation.

	<b>Infiltration time [year] at different L/S ratios</b>					
<b>L/S ratio</b>	<b>0.1</b>	<b>0.2</b>	<b>0.5</b>	<b>1</b>	<b>2</b>	<b>5</b>
<b>1 m depth</b>	0.2	0.4	1.0	1.9	3.8	9.6
<b>3.45 m depth (GW level)</b>	0.7	1.3	3.3	6.6	13	33

As illustrated on figure 9, most of the PFOS had leached out from the soil at L/S 5. According to the calculation, it would take approximately 33 years for the amount of water required to get L/S 5, to have fallen on the soil and infiltrated down to the groundwater table, meaning that most of the PFOS would have reached the groundwater at this point. Figure 15 illustrates the cumulative leaching of PFOS in  $\mu\text{g}$  for the different L/S ratios and the estimated infiltration time for reaching the groundwater table. Both the unamended soil and soil amended with the different types of biochar are shown on the figure, to visualise how much PFOS is leaching over time, and how this process can be slowed down by the amendment with the different biochar sorbents.



**Figure 15:** Cumulative PFOS leaching in  $\mu\text{g}$  from the unamended soil and soil amended with biochar. The x-axis is given both in L/S ratios and the period of time in years it will take the amount of water, corresponding to the L/S ratio, to fall as rain and infiltrate to the groundwater. Mean values  $\pm$  standard deviations are presented for the CWC (analytical triplicate) and DWSS (experimental triplicate). Points are discrete values; lines are only drawn for better visualization.

Figure 9 also illustrates the concentration of PFHxS in the control column, which appeared to be leaching much faster than PFOS. At L/S 1,  $6.63 \mu\text{g}$  of PFHxS had leached from the soil, corresponding to 84% of the total leaching amount. According to table 7, it would take about 6 and a half years of rainfall and infiltration for almost complete leaching of PFHxS to the groundwater. Concentration of PFBS was dropping even faster, with nearly complete leaching of 98% of the total leaching amount at L/S 0.2, corresponding to roughly 3 years and 3 months of precipitation and infiltration to reach the groundwater table. With amendment of e.g. the two best sorbents for PFAS (aWT and DWSS), groundwater contamination could be prevented to a large degree. Figure 10 illustrated that PFOS leaching was almost completely prevented by



amendment with aWT and DWSS (99.9% and  $98.9 \pm 0.24\%$ , respectively), leading to a leachable concentration of only 3.63 and  $31.9 \pm 7.17$   $\mu\text{g}/\text{kg}$  soil, respectively. Moreover, the retardation of PFOS leaching due to amendment with the aWT biochar turned out to be over 4000, meaning that PFOS leaching was 4000 times slower than the flowrate of the water in the column. In contrast, amendment with DWSS biochar demonstrated a 10 times lower retardation factor of about 400 for PFOS. For short-chained PFAS, such as PFHxA, retardation by aWT and DWSS biochar were found to be much lower than for the long-chained PFAS, with retardation factors of 65 and  $47 \pm 12$ , respectively.

These observations indicate again the faster leaching of shorter chained PFAS to the groundwater. In addition to this, the model does not consider whether the infiltration takes place in the saturated or unsaturated zone. The columns imitated saturated conditions at the original site of the soil, while when using the formula to predict transport time for reaching the groundwater level, the transport is in the unsaturated zone. It has been reported that PFAS behave different in the vadose zone, compared to in saturated conditions, due to air-water interfacial adsorption, which impacts the transport and result in retention of PFAS (Brusseau et al., 2021). Increase in air-water partitioning coefficients with increase in carbon chain length of fluorotelomer alcohols were reported by Goss et al. (2006), as it becomes energetically less favourably for the molecule to be dissolved in water, with every additional  $\text{CF}_2$  moiety. Furthermore, a study by Brusseau et al. (2021) found that air-water interfacial adsorption was responsible for  $\sim 81\%$  of PFOA and  $\sim 83\%$  of PFOS retention in the unsaturated zone. This implies that the estimated time periods of infiltration given in table 7, may be longer for PFOS and other long-chained PFAS, while they might be more accurate for the shorter chained PFAS which are less hydrophobic. Furthermore, if the results were to be extrapolated to another PFAS contaminated site, differences in the soil composition and precipitation will also have an impact on PFAS retention and water infiltration. Either way, biochar amendment would serve as a beneficial method of retaining the PFAS from leaching into the groundwater at this specific site, as illustrated on figure 15. Especially the aWT and three sludge biochars (DSS-1, DSS-2 and DWSS) would be a suitable solution for remediation of the AFFF-contaminated soil.

## 5 Conclusion, implications and further work

The aim of this thesis was to study the effects of 6 different waste-based biochars on PFAS sorption in soil. The generated data led to promising results for especially the activated waste timber biochar (aWT) and de-watered raw sewage sludge biochar (DWSS), closely followed by the two digested sewage sludge biochars (DSS-2 and DSS-1), as all four biochars reduced the PFOS leaching from soil with more than 91% compared to the unamended soil, by addition of only 1% biochar.

Before summarizing the obtained results, the 5 hypotheses defined in the beginning of this thesis are restated:

- I.a Waste-based biochar produced from sewage sludge will reduce PFAS leaching more effectively than (non-activated) wood-based biochar. Effective PFAS treatment in water with sludge-based sorbents was seen by Krahn et al. (2023) and is expected to be similar for soil.
- II.a Biochar amendment will lead to lower DOC content in leachate, due to adsorption of DOC onto the biochar.
- II.b Following hypothesis II.a, reduced DOC content will result in less PFAS desorption from soil, thereby limiting complexation between PFAS and DOC, leading to less transport of PFAS in the water phase.
- I.b + II.c Activation of (waste-based) biochar will lead to higher sorption of PFAS and DOC than non-activated biochar, due to higher specific surface area and the creation of more and larger pore structures.
- III.a Attenuation of single PFAS sorption to biochar will occur in the presence of soil and a mixture of PFAS, as these will induce competition for sorption sites.
- IV.a Biochar amendment will have a smaller effect on sorption of PFAS with shorter chains, as water purification have been shown be to very challenging for short-chain PFAS (Appleman et al., 2014).

Hypotheses I.a and I.b were accepted on the basis of the high reduction in PFAS leaching of the three sludge-based biochars and the aWT biochar. The leaching of PFOS was reduced in the following order: aWT (99.9%) > DWSS (98.9 ± 0.24%) > DSS-2 (97.8%) > DSS-1 (91.6%) >> CWC (42.4 ± 5.1%) > WT (33.7%). The same order of reduction was overall followed by other PFAS detected in the leachate and soil. This clearly demonstrates that the three sludge-based biochars reduced the PFAS leaching with much higher efficiency than the two non-activated wood-based biochars (CWC and WT), while activation of the poorest sorbent WT

into aWT biochar, resulted in the highest sorption efficiency of all 6 biochars. Furthermore, this turned out to mainly be because the majority of the pores in the WT and CWC biochars were too small to accommodate the PFAS molecules. The aWT demonstrated both the highest surface area and pore volume of all 6 sorbents, which contributed to the high sorption strength.

Hypotheses II.a and II.b were only partly accepted, as these only were true for some of the biochar types. Amendment with DSS-1, DSS-2, DWSS and aWT lead to lower DOC in the leachate, while leachate from columns amended with CWC and WT biochar showed concentrations of DOC higher than or similar to the control column. A simple linear regression concluded that DOC concentrations were statistically significantly related to the concentrations of PFAS with CF-chain length of 4 to 7 in leachate, indicating that if the relationship is caused by DOC-facilitated transport, biochar amendment with DSS-1, DSS-2, DWSS and aWT will reduce the PFAS transport in the water-phase. Hypothesis II.c was accepted as the aWT effectively reduced the DOC concentration more than any of the other sorbents, due to its high sorption strength.

Hypotheses III.a and IV.a were both accepted. Attenuation by soil and a PFAS mixture was observed for single PFAS sorption to biochar, which lead to the acceptance of hypothesis III.a, although a high sorption strength still was maintained for many of the sorbents. The attenuation effect was highest for the CWC biochar, while the DSS-1 and DWSS biochar was considerably less affected. Competition between PFAS for sorption sites was assumed to cause the most attenuation, as 26 different PFAS were quantified in the samples. Furthermore, the high concentration of PFOS strongly influenced sorption of the other PFAS, whereas the influence of other PFAS on PFOS sorption was considerably lower.

Both water-biochar distribution coefficients ( $K_d$ ) and the reduction of PFAS in leachate demonstrated lower retention of short-chained PFAS, which contributed to accepting hypothesis IV.a.  $K_d$  values generally decreased with CF-chain length for all 6 biochar types, proving that short-chain PFAS are less effectively retained by biochar amendment.

Overall, the results show that application of waste/sludge-based biochar to contaminated soil can be a very effective remediation method, and a good alternative to e.g., fossil based activated carbon. This thesis also documented that PFAS contaminated sludge can be utilized for successful stabilization of soil contaminated with PFAS from the same contaminant source.

## 5.1 Wider implications

This section presents a wider overview of how the biochar sorbents can be used in-situ, in addition to what impacts and costs it might come with.

### 5.1.1 Remediation of the AFFF-affected site

The PFAS contaminated soil used in this thesis originated from a firefighting training facility, where it was posing a risk to the groundwater and surrounding area, due its high concentrations and low retention of the PFAS contamination. Some of the AFFF-impacted soil had been excavated and transported to a landfill. As this strategy is both costly, a burden to the natural environment of the area and roughly moves the problem from one site to another, biochar application at this site could be a good option.

The column experiment provided results for the soil amended with 1% (w/w) biochar, in saturated conditions. Although in-situ amendment of biochar to the soil would most likely help retain the PFAS from leaching into the groundwater, different conditions will influence the sorption mechanisms of PFAS in the unsaturated zone, as discussed in section 4.5. However, it has previously been shown that AC and biochar significantly reduced the root uptake of PCB when applied in-situ to a highly contaminated soil with a 2.8% (w/w) dose (Denyes et al., 2013). Although, it is still unknown how well PFAS will sorb to biochar in field conditions at this specific site, a similar dose of biochar (~3%) could be a better option for in-situ remediation. Furthermore, on basis of the results in this study, application of the DWSS or aWT biochar would lead to the best results.

Ex-situ remediation of the soil might also be an option, whereafter the soil could be returned to the site or brought to a landfill. This option may not be the best or most cost-effective, as it requires additional handling and transport.

### Cost-benefit

To estimate if remediation of this AFFF-contaminated site with biochar would be cost-effective, a cost-benefit analysis would be a good method to quantify the total costs and expected rewards. A rough estimate of the extent is here presented. The total area of the former firefighting training facility is about 25,000 m<sup>2</sup> with an average vertical distance of  $3.45 \pm 0.4$  m ( $n = 6$ ) to the groundwater level. Most of the firefighting foam has been used on platforms with a collection system to protect the groundwater, although some have spread to outside the platforms, leading to the contamination of the soil. Knowing this, it is believed that not the whole area is contaminated. Assuming only 30% of the area is affected, and that the upper 2 m of the soil in

the area is the most contaminated, it would result in 15,000 m<sup>3</sup> of contaminated soil, which is about 21,750 tonnes of soil (assuming the same bulk density as obtained from the soil used in the columns). Application of 3% biochar would result in 43.5 kg biochar per m<sup>3</sup>, equal to 652.5 tonnes of biochar for the 21,750 tonnes of soil.

The prices of biochar can vary a lot, depending on the price of the feedstock used to produce the biochar. A recent study presented prices from 17.15 USD/tonne biochar to 2,710 USD/tonne biochar (Campion et al., 2023). The price of sludge for feedstock can be assumed to be lower than most other feedstocks, and the prices for sludge-based biochar might therefore be in the lower end of this price range. Assuming a price of 100 USD/tonne for sludge-based biochar, this would result in a price of 65,250 USD, which is almost 700,000 Nok. Additional costs of excavation, mixing and handling of the soil and biochar could be estimated to 2000 Nok/hour. The total amount of time needed for the operation is difficult to estimate, as site specific conditions could change this. However, the use of 8 hours per day for 30 days would cost 510,000 Nok, resulting in a total of 1,210,000 Nok. To estimate if the use of biochar to remediate this site would be a cost-effective solution, the costs of excavation and landfilling should be higher than ~1,210,000 Nok. The approximated price for a landfill in Norway to take in 1 tonne of PFAS contaminated soil costs about 1000 Nok/tonne, but can vary depending on different factors, such as contamination degree. This would result in a price of 21,750,000 Nok, without the cost of excavation and transportation to the landfill. Assuming about the same cost for excavation and transport, as for handling and mixing with biochar, the price of landfilling would in total end up being 22,260,000 Nok, which is more than 18 times higher compared to remediation with biochar. Furthermore, costs associated with the possible purchase of new soil for the site, after landfilling, should also be added to the total costs. These estimated prices may vary largely depending on many factors. Furthermore, use of the aWT biochar could be assumed to be higher, as activation of the biochar would increase the price. However, this estimate indicates that in-situ remediation of the AFFF-affected site with biochar is much more cost-effective than excavation and landfilling.

## LCA

In addition to the cost-benefit analysis, a Life Cycle Assessment (LCA) could also be carried out, to estimate the environmental and resource impacts of remediating the site using biochar, compared to landfilling (or another remediation technology). An LCA for the biochar scenario would include the environmental impacts associated with the production of the biochar (e.g., materials for the pyrolysis unit, transportation of feedstock, electricity for the operation,

emissions during pyrolysis), the application (e.g., transport to the contaminated site, use of machinery for mixing with soil), the effectiveness of the remediation by biochar amendment, the anticipated residence time in the soil and contaminant retainment, and lastly the carbon sequestration. Ecological impacts on the surrounding area could also be included, for comparison with the area of the landfill. Inclusion of different biochar types, including activated and non-activated biochars, could also give a deeper insight of the environmental impacts of different feedstocks and pyrolysis temperatures, compared to the effect of the sorbents.

Ongoing work within the VOW project is carrying out an LCA of the 6 sorbents used in this study, assessing the environmental impacts attributed to pyrolysis of biowaste. The main goal is to compare the impacts of using different feedstocks and pyrolysis temperatures to produce waste-based biochar, and their effects as a remediation agent for PFAS contaminated soil. The functional unit of the LCA is the management of 1 kg carbon-rich waste in Norway. The system includes the collection and transportation of the biowaste to the pyrolysis unit (a fixed distance for all waste fractions), drying and pyrolysis of the biowaste, and remediation activities, where reduction of soil contamination and carbon storage are included as impact offsets. Impacts of generating the biowaste or using it for biochar production instead of e.g., biogas, are not considered within the system boundaries.

### Carbon sequestration

Sequestration of carbon is an additional benefit when biochar amendment is used for soil remediation. The challenges of climate change make biochar a more attractive option, as it helps mitigate climate change by locking up carbon, and for that reason only could be a better choice than many other remediation technologies on the market, when looking at environmental impacts. The application of biochar to contaminated soil, thus result in both remediation of the soil, and storage of the sequestered carbon for up to thousands of years, although strongly dependent on the stability of the biochar (Lehmann, 2007). The stability can be estimated from the H/C ratio of the biochar, where a lower ratio results in higher stability, which is achieved by higher pyrolysis temperatures (Camps-Arbestain et al., 2015; Smebye et al., 2017).

However, biochar can also be used to treat drinking water, although AC are more commonly used today (Rahman et al., 2014). Here, the carbonaceous material is used in filters to adsorb contaminants such as PFAS, which often are burned when the system is spent or exhausted (Xiao et al., 2020). Burning of the AC or biochar filters result in decomposition of the contaminants, but also release of the sequestered carbon from the pyrolysis process. A method

for maintaining both the carbon sequestration effect and the contaminant removal, could be regenerating the biochar/ AC by thermal reactivation or regeneration. Xiao et al. (2020) found that a 30 min thermal treatment of GAC at  $\geq 300$  °C removed  $\geq 99\%$  of PFCA, while for PFSA a higher temperature of  $\geq 500$  °C was needed for the same effect. These results demonstrate that it is possible to re-use biochar, even when used for drinking water treatment, to sustain the carbon sequestration effect achieved by pyrolysis.

## 5.2 Recommendations for further work

The presented results and conclusions of this thesis also led to rise of new questions for further research.

The 6 different biochars were tested in column experiments, imitating realistic environmental conditions. The results were promising and showed the same trends as Krahn et al. (2023) and Sørmo et al. (2021) presented from batch tests. Testing of these waste-based sorbents in-situ or in bigger columns, such as lysimeters, could thus be interesting for further investigations on soil remediation by sorbents made from waste fractions. Precipitation and natural infiltration are part of lysimeter tests, which could help study the effectiveness of biochar when applied to soil in unsaturated conditions. Furthermore, other soil types with higher organic carbon content should also be investigated, as this could lead to higher attenuation of the PFAS sorption to the biochars. A high organic carbon content also leads to higher PFAS sorption to the soil itself. In these cases, stronger sorbents are needed to increase the binding of PFAS to the biochar instead of the soil organic carbon. Higher dosages of biochar could also lead to stronger sorption, especially of the poorest sorbents (WT and CWC biochar) and should be tested. A similar column test, as conducted in this thesis, but carried out for higher liquid to solid ratios, could also help determine if more PFAS could be sorbed by the biochar. Not the whole amount of PFOS had leached from the unamended soil at L/S 5, indicating that more PFOS could leach or be adsorbed by biochar in the other columns. The correlation between DOC and PFAS concentrations evaluated by linear regression, indicated DOC-facilitated transport of PFAS in the columns, but as this simple test cannot conclusively determine this relationship, further research is needed on this important topic. Furthermore, investigation of the biochar stability in soil and retainment of contaminants are needed, as degradation of the biochar or desorption of contaminants at a later time, could have negative effects on the surrounding area. Even though biochar have been suggested to be stable in soil for hundreds to thousands of years (Lehmann, 2007), stability and possible contaminant release have not been extensively investigated. Long-term field- and laboratory trials could help cover this with more certainty.

## 8 Bibliography

- Ahmad, M., Rajapaksha, A. U., Lim, J. E., Zhang, M., Bolan, N., Mohan, D., Vithanage, M., Lee, S. S. & Ok, Y. S. (2014). Biochar as a sorbent for contaminant management in soil and water: A review. *Chemosphere*, 99: 19-33. doi: 10.1016/j.chemosphere.2013.10.071.
- Alzaga, R., Maldonado, C. & Bayona, J. M. (1998). Intercomparison among SFE, ASE, Soxhlet and sonication for the trialkylamine determination in sediment and sludge. *International Journal of Environmental Analytical Chemistry*, 72 (2): 99-111. doi: 10.1080/03067319808035882.
- Ambaye, T. G., Vaccari, M., Van Hullebusch, E. D., Amrane, A. & Rtimi, S. (2021). Mechanisms and adsorption capacities of biochar for the removal of organic and inorganic pollutants from industrial wastewater. *International Journal of Environmental Science and Technology*, 18 (10): 3273-3294. doi: 10.1007/s13762-020-03060-w.
- Amonette, J. E. & Joseph, S. (2009). Characteristics of Biochar: Microchemical Properties. In Lehmann, J. & Joseph, S. (eds) *Biochar for environmental management: Science and Technology*, pp. 33-52: Earthscan.
- Appleman, T. D., Higgins, C. P., Quiñones, O., Vanderford, B. J., Kolstad, C., Zeigler-Holady, J. C. & Dickenson, E. R. V. (2014). Treatment of poly- and perfluoroalkyl substances in U.S. full-scale water treatment systems. *Water Research*, 51: 246-255. doi: 10.1016/j.watres.2013.10.067.
- Arvaniti, O. S., Asimakopoulos, A. G., Dasenaki, M. E., Ventouri, E. I., Stasinakis, A. S. & Thomaidis, N. S. (2014). Simultaneous determination of eighteen perfluorinated compounds in dissolved and particulate phases of wastewater, and in sewage sludge by liquid chromatography-tandem mass spectrometry. *Analytical Methods*, 6 (5): 1341-1349. doi: 10.1039/c3ay42015a.
- Asimakopoulos, A. G., Wang, L., Thomaidis, N. S. & Kannan, K. (2014). A multi-class bioanalytical methodology for the determination of bisphenol A diglycidyl ethers, p-hydroxybenzoic acid esters, benzophenone-type ultraviolet filters, triclosan, and triclocarban in human urine by liquid chromatography-tandem mass spectrometry. *Journal of Chromatography A*, 1324: 141-148. doi: 10.1016/j.chroma.2013.11.031.
- Avinor. (2012). *Miljøprosjektet - DP 2, Miljøtekniske grunnundersøkelser ved Avinors lufthavner*. Available at: <https://avinor.no/konsern/miljo-og-samfunn/pfos-i-fokus/rapporter>.
- Bardestani, R., Patience, G. S. & Kaliaguine, S. (2019). Experimental methods in chemical engineering: specific surface area and pore size distribution measurements—BET, BJH, and DFT. *The Canadian Journal of Chemical Engineering*, 97 (11): 2781-2791. doi: 10.1002/cjce.23632.
- Benskin, J. P., Ikononou, M. G., Gobas, F. A. P. C., Woudneh, M. B. & Cosgrove, J. R. (2012). Observation of a Novel PFOS-Precursor, the Perfluorooctane Sulfonamido Ethanol-



- Based Phosphate (SAmPAP) Diester, in Marine Sediments. *Environmental Science & Technology*, 46 (12): 6505-6514. doi: 10.1021/es300823m.
- Bolan, N., Sarkar, B., Yan, Y., Li, Q., Wijesekara, H., Kannan, K., Tsang, D. C. W., Schauerte, M., Bosch, J., Noll, H., et al. (2021). Remediation of poly- and perfluoroalkyl substances (PFAS) contaminated soils – To mobilize or to immobilize or to degrade? *Journal of Hazardous Materials*, 401: 123892. doi: 10.1016/j.jhazmat.2020.123892.
- Brusseau, M. L., Guo, B., Huang, D., Yan, N. & Lyu, Y. (2021). Ideal versus Nonideal Transport of PFAS in Unsaturated Porous Media. *Water Research*, 202. doi: 10.1016/j.watres.2021.117405.
- Buck, R. C., Franklin, J., Berger, U., Conder, J. M., Cousins, I. T., De Voogt, P., Jensen, A. A., Kannan, K., Mabury, S. A. & Van Leeuwen, S. P. (2011). Perfluoroalkyl and polyfluoroalkyl substances in the environment: Terminology, classification, and origins. *Integrated Environmental Assessment and Management*, 7 (4): 513-541. doi: 10.1002/ieam.258.
- Busch, J., Ahrens, L., Sturm, R. & Ebinghaus, R. (2010). Polyfluoroalkyl compounds in landfill leachates. *Environmental Pollution*, 158 (5): 1467-1471. doi: 10.1016/j.envpol.2009.12.031.
- Campion, L., Bekchanova, M., Malina, R. & Kuppens, T. (2023). The costs and benefits of biochar production and use: A systematic review. *Journal of Cleaner Production*, 408. doi: 10.1016/j.jclepro.2023.137138.
- Camps-Arbestain, M., Amonette, J., Singh, B., Wang, T. & Schmidt, H.-P. (2015). A biochar classification system and associated test methods. In Lehmann, J. & Joseph, S. (eds) *Biochar for Environmental Management: Science and Technology*, pp. 165-194. London.
- Cornelissen, G., Van Noort, P. C. M., Parsons, J. R. & Govers, H. A. J. (1997). Temperature Dependence of Slow Adsorption and Desorption Kinetics of Organic Compounds in Sediments. *Environmental Science & Technology*, 31 (2): 454-460. doi: 10.1021/es960300+.
- Cornelissen, G., Rigterink, H., Ferdinandy, M. M. A. & Van Noort, P. C. M. (1998). Rapidly Desorbing Fractions of PAHs in Contaminated Sediments as a Predictor of the Extent of Bioremediation. *Environmental Science & Technology*, 32 (7): 966-970. doi: 10.1021/es9704038.
- Cornelissen, G. & Gustafsson, Ö. (2004). Sorption of Phenanthrene to Environmental Black Carbon in Sediment with and without Organic Matter and Native Sorbates. *Environmental Science & Technology*, 38 (1): 148-155. doi: 10.1021/es034776m.
- Cornelissen, G. & Gustafsson, Ö. (2006). Effects of added PAHs and precipitated humic acid coatings on phenanthrene sorption to environmental Black carbon. *Environmental Pollution*, 141 (3): 526-531. doi: 10.1016/j.envpol.2005.08.053.
- Dauchy, X., Boiteux, V., Bach, C., Rosin, C. & Munoz, J.-F. (2017). Per- and polyfluoroalkyl substances in firefighting foam concentrates and water samples collected near sites

- impacted by the use of these foams. *Chemosphere*, 183: 53-61. doi: 10.1016/j.chemosphere.2017.05.056.
- De Voogt, P., Zurano, L., Serné, P. & Haftka, J. J. H. (2012). Experimental hydrophobicity parameters of perfluorinated alkylated substances from reversed-phase high-performance liquid chromatography. *Environmental Chemistry*, 9 (6): 564. doi: 10.1071/en12132.
- Denyes, M. J., Rutter, A. & Zeeb, B. A. (2013). In situ application of activated carbon and biochar to PCB-contaminated soil and the effects of mixing regime. *Environmental Pollution*, 182: 201-208. doi: 10.1016/j.envpol.2013.07.016.
- Ding, G. & Peijnenburg, W. J. G. M. (2013). Physicochemical Properties and Aquatic Toxicity of Poly- and Perfluorinated Compounds. *Critical Reviews in Environmental Science and Technology*, 43 (6): 598-678. doi: 10.1080/10643389.2011.627016.
- Downie, A., Crosky, A. & Munroe, P. (2009). Physical Properties of Biochar. In Lehmann, J. & Joseph, S. (eds) *Biochar for environmental management: Science and Technology*, pp. 13-32: Earthscan.
- Du, Z., Deng, S., Bei, Y., Huang, Q., Wang, B., Huang, J. & Yu, G. (2014). Adsorption behavior and mechanism of perfluorinated compounds on various adsorbents - a review. *J Hazard Mater*, 274: 443-54. doi: 10.1016/j.jhazmat.2014.04.038.
- ECHA. (2023a). *Annex XV Restriction Report, Proposal for a Restriction: Per- and polyfluoroalkyl substances (PFASs)*.
- ECHA. (2023b). *Per- and polyfluoroalkyl substances (PFASs)* Available at: <https://echa.europa.eu/hot-topics/perfluoroalkyl-chemicals-pfas> (accessed: 16/01/2023).
- ECHA. (2023c). *Understanding POPs*. Available at: <https://echa.europa.eu/understanding-pops> (accessed: 16/01/2023).
- ECHA. (2023d). *Understanding the Drinking Water Directive*. Available at: <https://echa.europa.eu/understanding-dwd> (accessed: 24/01/2023).
- EFSA Panel on Contaminants in the Food Chain. (2018). Risk to human health related to the presence of perfluorooctane sulfonic acid and perfluorooctanoic acid in food. *EFSA Journal*, 16 (12). doi: 10.2903/j.efsa.2018.5194.
- EFSA Panel on Contaminants in the Food Chain. (2020). Risk to human health related to the presence of perfluoroalkyl substances in food. *EFSA Journal*, 18 (9). doi: 10.2903/j.efsa.2020.6223.
- Egge, J. H. (2021, 07/07/2021). Halvparten av sminkeproduktene i ny studie inneholdt giftstoffer. *NRK*. Available at: <https://www.nrk.no/trondelag/ny-sminkestudie-avslorer-giftstoffer-i-mer-enn-halvparten-av-de-testede-produktene-1.15561750>.
- EPA. (2021). PFAS Master List of PFAS Substances. In *United States Environmental Protection Agency*. Available at: <https://comptox.epa.gov/dashboard/chemical-lists/pfasmaster> (accessed: 28/04/2023).

- Eschauzier, C., Beerendonk, E., Scholte-Veenendaal, P. & De Voogt, P. (2012). Impact of Treatment Processes on the Removal of Perfluoroalkyl Acids from the Drinking Water Production Chain. *Environmental Science & Technology*, 46 (3): 1708-1715. doi: 10.1021/es201662b.
- European Union. (2020). *Directive (EU) 2020/2184 of the European Parliament and of the Council of 16 December 2020 on the quality of water intended for human consumption*.
- Fabregat-Palau, J., Vidal, M. & Rigol, A. (2022). Examining sorption of perfluoroalkyl substances (PFAS) in biochars and other carbon-rich materials. *Chemosphere*, 302. doi: 10.1016/j.chemosphere.2022.134733.
- Fromme, H., Tittlemier, S. A., Volkel, W., Wilhelm, M. & Twardella, D. (2009). Perfluorinated compounds - Exposure assessment for the general population in western countries. *International Journal of Hygiene and Environmental Health*, 212 (3): 239-270. doi: 10.1016/j.ijheh.2008.04.007.
- Goss, K.-U. & Bronner, G. (2006). What Is So Special about the Sorption Behavior of Highly Fluorinated Compounds? *The Journal of Physical Chemistry A*, 110 (30): 9518-9522. doi: 10.1021/jp062684o.
- Goss, K.-U., Bronner, G., Harner, T., Hertel, M. & Schmidt, T. C. (2006). The Partition Behavior of Fluorotelomer Alcohols and Olefins. *Environmental Science & Technology*, 40 (11): 3572-3577. doi: 10.1021/es060004p.
- Hagemann, N., Spokas, K., Schmidt, H.-P., Kägi, R., Böhler, M. & Bucheli, T. (2018). Activated Carbon, Biochar and Charcoal: Linkages and Synergies across Pyrogenic Carbon's ABCs. *Water*, 10 (2): 182. doi: 10.3390/w10020182.
- Hagemann, N., Schmidt, H. P., Kagi, R., Bohler, M., Sigmund, G., Maccagnan, A., McArdell, C. S. & Bucheli, T. D. (2020). Wood-based activated biochar to eliminate organic micropollutants from biologically treated wastewater. *Science of the Total Environment*, 730: 11. doi: 10.1016/j.scitotenv.2020.138417.
- Hale, S. E., Arp, H. P., Kupryianchyk, D. & Cornelissen, G. (2016). A synthesis of parameters related to the binding of neutral organic compounds to charcoal. *Chemosphere*, 144: 65-74. doi: 10.1016/j.chemosphere.2015.08.047.
- Hale, S. E., Arp, H. P. H., Slinde, G. A., Wade, E. J., Bjørseth, K., Breedveld, G. D., Straith, B. F., Moe, K. G., Jartun, M. & Høisæter, Å. (2017). Sorbent amendment as a remediation strategy to reduce PFAS mobility and leaching in a contaminated sandy soil from a Norwegian firefighting training facility. *Chemosphere*, 171: 9-18. doi: 10.1016/j.chemosphere.2016.12.057.
- Hale, S. E., Arp, H. P. H., Schliebner, I. & Neumann, M. (2020). Persistent, mobile and toxic (PMT) and very persistent and very mobile (vPvM) substances pose an equivalent level of concern to persistent, bioaccumulative and toxic (PBT) and very persistent and very bioaccumulative (vPvB) substances under REACH. *Environmental Sciences Europe*, 32 (1). doi: 10.1186/s12302-020-00440-4.

- Hale, S. E., Kalantzi, O. I. & Arp, H. P. H. (2022). Introducing the EU project ZeroPM: zero pollution of persistent, mobile substances. *Environmental Sciences Europe*, 34 (1). doi: 10.1186/s12302-022-00681-5.
- Higgins, C. P. & Luthy, R. G. (2006). Sorption of perfluorinated surfactants on sediments. *Environmental Science & Technology* 40 (23): 7251-7256. doi: 10.1021/es061000n.
- Høisæter, Å., Pfaff, A. & Breedveld, G. D. (2019). Leaching and transport of PFAS from aqueous film-forming foam (AFFF) in the unsaturated soil at a firefighting training facility under cold climatic conditions. *Journal of Contaminant Hydrology*, 222: 112-122. doi: 10.1016/j.jconhyd.2019.02.010.
- Høisæter, Å. & Breedveld, G. D. (2022). Leaching potential of per- and polyfluoroalkyl substances from source zones with historic contamination of aqueous film forming foam - a surfactant mixture problem. *Environmental Advances*, 8 (10022). doi: 10.1016/j.envadv.2022.100222.
- Hubert, M., Arp, H. P. H., Hansen, M. C., Castro, G., Meyn, T., Asimakopoulos, A. G. & Hale, S. E. (2023). Influence of grain size, organic carbon and fiber content on the sorption of PFAS to AFFF contaminated soils - implications for remediation via soil washing. *Science of the Total Environment*, 875. doi: 10.1016/j.scitotenv.2023.162668.
- Hunter, D. (2021). *Collecting Groundwater Samples for PFAS Analysis using Dedicated Teflon® Lined Tubing and Bladders*: Cox-Colvin & Assoc., Inc. Available at: <https://coxcolvin.com/articles/collecting-groundwater-samples-for-pfas-analysis-using-dedicated-teflon-lined-tubing-and-bladders/> (accessed: 25/04/2023).
- Inoue, Y., Hashizume, N., Yakata, N., Murakami, H., Suzuki, Y., Kikushima, E. & Otsuka, M. (2012). Unique Physicochemical Properties of Perfluorinated Compounds and Their Bioconcentration in Common Carp *Cyprinus carpio* L. *Archives of Environmental Contamination and Toxicology*, 62 (4): 672-680. doi: 10.1007/s00244-011-9730-7.
- International Biochar Initiative. (2015). Standardized product definition and product testing guidelines for biochar that is used in soil.
- ITRC. (2018). *Remediation Technologies and Methods for Per- and Polyfluoroalkyl Substances (PFAS)*: Interstate Technology & Regulatory Council.
- Jing, P., Rodgers, P. J. & Amemiya, S. (2009). High Lipophilicity of Perfluoroalkyl Carboxylate and Sulfonate: Implications for Their Membrane Permeability. *Journal of the American Chemical Society*, 131 (6): 2290-2296. doi: 10.1021/ja807961s.
- Kissa, E. (2001a). Liquid-Vapor and Liquid-Liquid Boundaries. Surface Tension. In Surfactant Science Series, *Fluorinated Surfactants and Repellents*, pp. 103-174.
- Kissa, E. (2001b). Physical and Chemical Properties. In Surfactant Science Series, *Fluorinated Surfactants and Repellents*, pp. 80-102.
- Knutsen, H., Mæhlum, T., Haarstad, K., Slinde, G. A. & Arp, H. P. H. (2019). Leachate emissions of short- and long-chain per- and polyfluoroalkyl substances (PFASs) from various Norwegian landfills. *Environmental Science: Processes & Impacts*, 21 (11): 1970-1979. doi: 10.1039/c9em00170k.

- Krafft, M. P. & Riess, J. G. (2015). Per- and polyfluorinated substances (PFASs): Environmental challenges. *Current Opinion in Colloid & Interface Science*, 20 (3): 192-212. doi: 10.1016/j.cocis.2015.07.004.
- Krahn, K. M., Cornelissen, G., Castro, G., Arp, H. P. H., Asimakopoulos, A. G., Wolf, R., Holmstrand, R., Zimmerman, A. R. & Sørmo, E. (2023). Sewage sludge biochars as effective PFAS-sorbents. *Journal of Hazardous Materials*, 445. doi: 10.1016/j.jhazmat.2022.130449.
- Krull, E. S., Baldock, J. A., Skjemstad, J. O. & Smernik, R. J. (2009). Characteristics of Biochar: Organo-chemical properties. In Lehmann, J. & Joseph, S. (eds) *Biochar for environmental management: Science and Technology*, pp. 53-65: Earthscan.
- Kupryianchyk, D., Hale, S. E., Breedveld, G. D. & Cornelissen, G. (2016). Treatment of sites contaminated with perfluorinated compounds using biochar amendment. *Chemosphere*, 142: 35-40. doi: 10.1016/j.chemosphere.2015.04.085.
- Lehmann, J. (2007). A handful of carbon. *Nature*, 447: 143-144. doi: 10.1038/447143a.
- Lehmann, J. & Joseph, S. (2009). Biochar for Environmental Mangement: An Introduction. In Lehmann, J. & Joseph, S. (eds) *Biochar for environmental management: Science and Technology*, pp. 1-12: Earthscan.
- Lovdata. (2004). *Forskrift om begrensning av forurensning (forurensningsforskriften)*: Lovdata.
- Mahinroosta, R. & Senevirathna, L. (2020). A review of the emerging treatment technologies for PFAS contaminated soils. *Journal of Environmental Management*, 255 (109896). doi: 10.1016/j.jenvman.2019.109896.
- Miljøstatus. (2023). *Forurenset grunn*. Available at: <https://miljostatus.miljodirektoratet.no/tema/forurensning/forurenset-grunn/> (accessed: 13/02/2023).
- NGI. (2016). *Fraksjonell ekstraksjon av fast stoff i kolonne (Kolonneforsøk – CEN/TS 14405)*. Haug, G. (ed.): Norwegian Geotechnical Institute.
- NGI. (2019). *Testing og karakterisering av materialer til gjenvinning*. In Okkenhaug, G. (ed.). NGI SP10 GEORCIRC: Norwegian Geotechnical Institute.
- NGI. (2020). *Proposal for new Normative Values for PFOS and PFOA in contaminated soil*. In Breedveld, G. (ed.): Norwegian Geotechnical Institute.
- NGI. (2021). *Grunnlagsrapport - Verktøy for å beregne spredning fra forurenset grunn*. In Breedveld, G. (ed.): Norwegian Geotechnical Institute.
- Norden. (2013). *Per- and polyfluorinated substances in the Nordic Countries; Use, occurrence and toxicology*: Nordic Council of Ministers.
- OECD. (2013). *Synthesis paper on per- and polyfluorinated chemicals (PFCs)*: OECD/ UNEP Global Group.

- OECD. (2021). *Reconciling Terminology of the Universe of Per- and Polyfluoroalkyl Substances: Recommendations and Practical Guidance*. OECD Series on Risk Management. Paris.
- Panwar, N. L. & Pawar, A. (2022). Influence of activation conditions on the physicochemical properties of activated biochar: a review. *Biomass Conversion and Biorefinery*, 12 (3): 925-947. doi: 10.1007/s13399-020-00870-3.
- Paul, A. G., Jones, K. C. & Sweetman, A. J. (2009). A First Global Production, Emission, And Environmental Inventory For Perfluorooctane Sulfonate. *Environmental Science & Technology*, 43 (2): 386-392. doi: 10.1021/es802216n.
- Prevedouros, K., Cousins, I. T., Buck, R. C. & Korzeniowski, S. H. (2006). Sources, Fate and Transport of Perfluorocarboxylates. *Environmental Science & Technology*, 40 (1): 32-44. doi: 10.1021/es0512475.
- Rahman, M. F., Peldszus, S. & Anderson, W. B. (2014). Behaviour and fate of perfluoroalkyl and polyfluoroalkyl substances (PFASs) in drinking water treatment: A review. *Water Research*, 50: 318-340. doi: 10.1016/j.watres.2013.10.045.
- Rayne, S. & Forest, K. (2009). Perfluoroalkyl sulfonic and carboxylic acids: A critical review of physicochemical properties, levels and patterns in waters and wastewaters, and treatment methods. *Journal of Environmental Science and Health*, 44 (12): 1145-1199. doi: 10.1080/10934520903139811.
- Regjeringen.no. (2023). *Drikkevansdirektivet 2020/2184*. Available at: <https://www.regjeringen.no/no/sub/eos-notatbasen/notatene/2018/sep/nytt-drikkevansdirektiv-2018-2019/id2615569/> (accessed: 24/01/2023).
- Ross, I., McDonough, J., Miles, J., Storch, P., Thelakkat Kochunarayanan, P., Kalve, E., Hurst, J., S. Dasgupta, S. & Burdick, J. (2018). A review of emerging technologies for remediation of PFASs. *Remediation Journal*, 28 (2): 101-126. doi: 10.1002/rem.21553.
- Sajjadi, B., Chen, W. Y. & Egiebor, N. O. (2019). A comprehensive review on physical activation of biochar for energy and environmental applications. *Reviews in Chemical Engineering*, 35 (6): 735-776. doi: 10.1515/revce-2017-0113.
- Salvidge, R. (2022, 08/02/2023). 'Forever chemicals': what are PFAS and what risk do they pose? *The Guardian*. Available at: <https://www.theguardian.com/environment/2022/feb/08/what-are-pfas-forever-chemicals-what-risk-toxicity>.
- Schaefer, T. H., Dlugogorski, B. Z. & Kennedy, E. M. (2008). Sealability Properties of Fluorine-Free Fire-Fighting Foams (FfreeF). *Fire Technology*, 44 (3): 297-309. doi: 10.1007/s10694-007-0030-8.
- Sigmund, G., Arp, H. P. H., Aumeier, B. M., Bucheli, T. D., Chefetz, B., Chen, W., Droge, S. T. J., Endo, S., Escher, B. I., Hale, S. E., et al. (2022). Sorption and Mobility of Charged Organic Compounds: How to Confront and Overcome Limitations in Their Assessment. *Environmental Science & Technology*, 56 (8): 4702-4710. doi: 10.1021/acs.est.2c00570.

- Smebye, A., Ailing, V., Vogt, R. D., Gadmar, T. C., Mulder, J., Cornelissen, G. & Hale, S. E. (2016). Biochar amendment to soil changes dissolved organic matter content and composition. *Chemosphere*, 142: 100-105. doi: 10.1016/j.chemosphere.2015.04.087.
- Smebye, A. B., Sparrevik, M., Schmidt, H. P. & Cornelissen, G. (2017). Life-cycle assessment of biochar production systems in tropical rural areas: Comparing flame curtain kilns to other production methods. *Biomass & Bioenergy*, 101: 35-43. doi: 10.1016/j.biombioe.2017.04.001.
- Smernik, R. J. (2009). Biochar and Sorption of Organic Compounds. In Lehmann, J. & Joseph, S. (eds) *Biochar for environmental management: Science and Technology*, pp. 289-300: Earthscan.
- Sorengard, M., Kleja, D. B. & Ahrens, L. (2019). Stabilization of per- and polyfluoroalkyl substances (PFASs) with colloidal activated carbon (PlumeStop (R)) as a function of soil clay and organic matter content. *Journal of Environmental Management*, 249: 7. doi: 10.1016/j.jenvman.2019.109345.
- Söregård, M., Kleja, D. B. & Ahrens, L. (2019). Stabilization and solidification remediation of soil contaminated with poly- and perfluoroalkyl substances (PFASs). *Journal of Hazardous Materials*, 367: 639-646. doi: 10.1016/j.jhazmat.2019.01.005.
- Söregård, M., Ostblom, E., Kohler, S. & Ahrens, L. (2020). Adsorption behavior of per- and polyfluoroalkyl substances (PFASs) to 44 inorganic and organic sorbents and use of dyes as proxies for PFAS sorption. *Journal of Environmental Chemical Engineering*, 8 (3): 8. doi: 10.1016/j.jece.2020.103744.
- Sørmo, E., Silvani, L., Thune, G., Gerber, H., Schmidt, H. P., Smebye, A. B. & Cornelissen, G. (2020). Waste timber pyrolysis in a medium-scale unit: Emission budgets and biochar quality. *Sci Total Environ*, 718: 137335. doi: 10.1016/j.scitotenv.2020.137335.
- Sørmo, E., Silvani, L., Bjerkli, N., Hagemann, N., Zimmerman, A. R., Hale, S. E., Hansen, C. B., Hartnik, T. & Cornelissen, G. (2021). Stabilization of PFAS-contaminated soil with activated biochar. *Science of the Total Environment*, 763. doi: 10.1016/j.scitotenv.2020.144034.
- Sørmo, E., Castro, G., Hubert, M., Licul-Kucera, V., Quintanilla, M., Asimakopoulos, A. G., Cornelissen, G. & Arp, H. P. H. (2023). The decomposition and emission factors of a wide range of PFAS in diverse, contaminated organic waste fractions undergoing dry pyrolysis. *Journal of Hazardous Materials*, 454. doi: 10.1016/j.jhazmat.2023.131447.
- Sparrevik, M., Saloranta, T., Cornelissen, G., Eek, E., Fet, A. M., Breedveld, G. D. & Linkov, I. (2011). Use of Life Cycle Assessments To Evaluate the Environmental Footprint of Contaminated Sediment Remediation. *Environmental Science & Technology*, 45 (10): 4235-4241. doi: 10.1021/es103925u.
- Statistisk sentralbyrå. (2014). *Tabell - Nedbør (SÅ 26) - SSB*. Available at: <https://www.ssb.no/233220/nedbor-sa-26> (accessed: 21/04/2023).
- Stockholm Convention. (2019). *The POPs*. Available at: <http://chm.pops.int/TheConvention/ThePOPs/AllPOPs/tabid/2509/Default.aspx> (accessed: 23/01/2023).

- Tang, J., Zhang, Y., Zha, Y., Li, X. & Fan, S. (2017). Oxalate Enhances Desorption of Perfluorooctane Sulfonate from Soils and Sediments. *Water Air Soil Pollution*. doi: 10.1007/s11270-017-3626-8.
- Tang, J., Cao, C., Gao, F. & Wang, W. (2019). Effects of biochar amendment on the availability of trace elements and the properties of dissolved organic matter in contaminated soils. *Environmental Technology & Innovation*, 16. doi: 10.1016/j.eti.2019.100492.
- Thies, J. E. & Rillig, M. C. (2009). Characteristics of Biochar: Biological Properties. In Lehmann, J. & Joseph, S. (eds) *Biochar for environmental management: Science and Technology*, pp. 85-106: Earthscan.
- Travar, I., Uwayezu, J. N., Kumpiene, J. & Yeung, L. W. Y. (2020). Challenges in the PFAS Remediation of Soil and Landfill Leachate: A Review. *Advances in Environmental and Engineering Research*, 02 (02): 1-1. doi: 10.21926/aeer.2102006.
- Tvede, I. & Bech, T. H. (2023, 13/04/2023). Skal PFAS forbydes i din stegepande og din ansigtscreme? I dag tager Folketinget stilling. *DR*. Available at: <https://www.dr.dk/nyheder/indland/skal-pfas-forbydes-i-din-stegepande-og-din-ansigtscreme-i-dag-tager-folketinget>.
- Vierke, L., Berger, U. & Cousins, I. T. (2013). Estimation of the Acid Dissociation Constant of Perfluoroalkyl Carboxylic Acids through an Experimental Investigation of their Water-to-Air Transport. *Environmental Science & Technology*, 47 (19): 11032-11039. doi: 10.1021/es402691z.
- Wang, H., Nan, Q., Waqas, M. & Wu, W. (2022). Stability of biochar in mineral soils: Assessment methods, influencing factors and potential problems. *Science of the Total Environment*, 809. doi: 10.1016/j.scitotenv.2021.150789.
- Xiao, F., Sasi, P. C., Yao, B., Kubátová, A., Golovko, S. A., Golovko, M. Y. & Soli, D. (2020). Thermal Stability and Decomposition of Perfluoroalkyl Substances on Spent Granular Activated Carbon. *Environmental Science & Technology Letters*, 7 (5): 343-350. doi: 10.1021/acs.estlett.0c00114.
- Yu, J., Lv, L., Lan, P., Zhang, S., Pan, B. & Zhang, W. (2012). Effect of effluent organic matter on the adsorption of perfluorinated compounds onto activated carbon. *Journal of Hazardous Materials*, 225-226: 99-106. doi: 10.1016/j.jhazmat.2012.04.073.
- Zhang, C., Yan, H., Li, F., Hu, X. & Zhou, Q. (2013). Sorption of short- and long-chain perfluoroalkyl surfactants on sewage sludges. *Journal of Hazardous Materials*, 260: 689-699. doi: 10.1016/j.jhazmat.2013.06.022.
- Zhang, D. Q., He, Q., Wang, M., Zhang, W. & Liang, Y. (2021). Sorption of perfluoroalkylated substances (PFASs) onto granular activated carbon and biochar. *Environmental Technology*, 42 (12): 1798-1809. doi: 10.1080/09593330.2019.1680744.
- Zhang, K., Huang, J., Yu, G., Zhang, Q., Deng, S. & Wang, B. (2013). Destruction of Perfluorooctane Sulfonate (PFOS) and Perfluorooctanoic Acid (PFOA) by Ball Milling. *Environmental Science & Technology*, 47 (12): 6471-6477. doi: 10.1021/es400346n.



- Zhang, W. & Liang, Y. (2022). Performance of different sorbents toward stabilizing per- and polyfluoroalkyl substances (PFAS) in soil. *Environmental Advances*, 8. doi: 10.1016/j.envadv.2022.100217.
- Zhou, Q., Deng, S., Zhang, Q., Fan, Q., Huang, J. & Yu, G. (2010). Sorption of perfluorooctane sulfonate and perfluorooctanoate on activated sludge. *Chemosphere*, 81 (4): 453-458. doi: 10.1016/j.chemosphere.2010.08.009.
- Zielińska, A. & Oleszczuk, P. (2016). Attenuation of phenanthrene and pyrene adsorption by sewage sludge-derived biochar in biochar-amended soils. *Environmental Science and Pollution Research*, 23 (21): 21822-21832. doi: 10.1007/s11356-016-7382-x.
- Zimmerman, A. R. & Mitra, S. (2017). Trial by Fire: On the Terminology and Methods Used in Pyrogenic Organic Carbon Research. *Frontiers in Earth Science*, 5: 8. doi: 10.3389/feart.2017.00095.

## Appendix A            pH and electrical conductivity

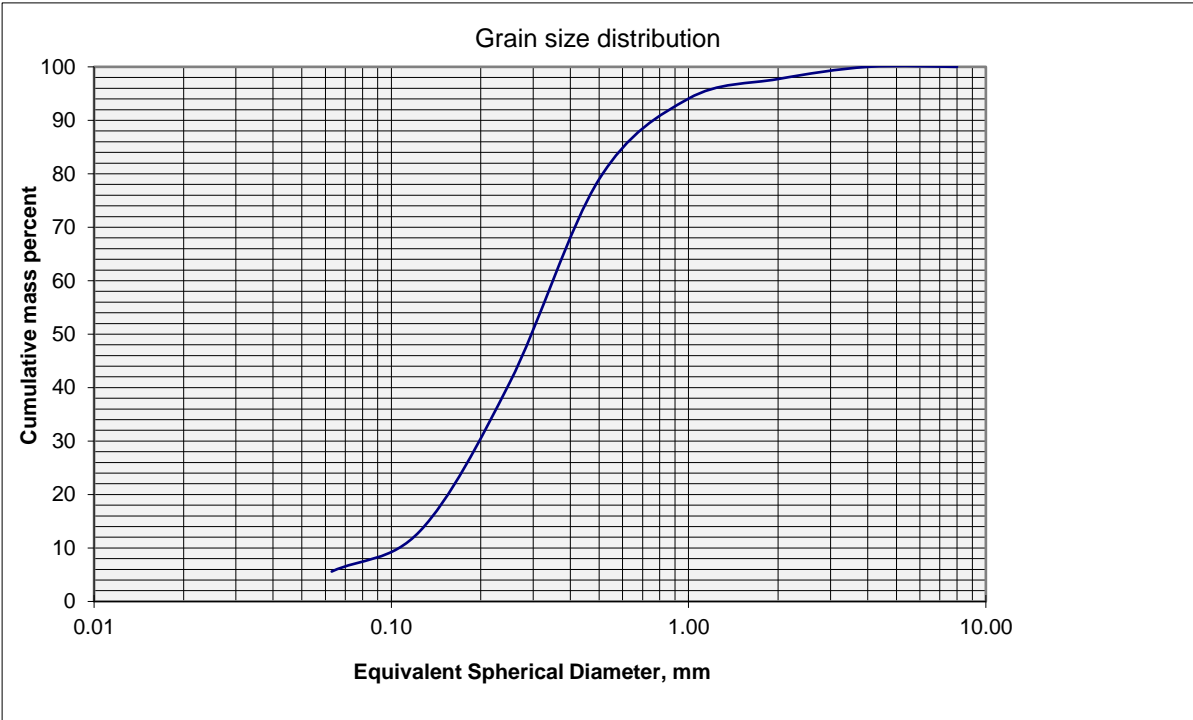
**Table A.1:** pH and electrical conductivity in  $\mu\text{S}/\text{cm}$  measured in all leachate samples.

Sample	pH	Conductivity [ $\mu\text{S}/\text{cm}$ ]	Sample	pH	Conductivity [ $\mu\text{S}/\text{cm}$ ]
Control L/S 0.1	6.724	3369.8	DWSS 2 L/S 0.1	6.875	2870.2
Control L/S 0.2	7.064	715.3	DWSS 2 L/S 0.2	7.126	861.1
Control L/S .5	6.753	320	DWSS 2 L/S 0.5	6.650	320
Control L/S 1	6.931	133.6	DWSS 2 L/S 1	6.785	316
Control L/S 2	6.901	86.8	DWSS 2 L/S 2	6.866	86.4
Control L/S 5	7.084	56.5	DWSS 2 L/S 5	6.342	60.1
CWC L/S 0.1	7.381	3538.4	DWSS 3 L/S 0.1	6.855	2512.0
CWCL/S 0.2	7.485	894.5	DWSS 3 L/S 0.2	7.131	720.7
CWC L/S 0.5	7.112	448.0	DWSS 3 L/S 0.5	6.761	305
CWC L/S 1	6.958	196.8	DWSS 3 L/S 1	6.880	146.8
CWC L/S 2	6.838	105.2	DWSS 3 L/S 2	6.997	79.2
CWC L/S 5	7.072	69.5	DWSS 3 L/S 5	7.155	57.6
DSS-1 L/S 0.1	6.997	3227.0	WT L/S 0.1	7.168	3195.3
DSS-1 L/S 0.2	7.241	857.1	WT L/S 0.2	7.310	811.3
DSS-1 L/S 0.5	6.669	359	WT L/S 0.5	7.019	415
DSS-1 L/S 1	6.823	157.6	WT L/S 1	7.029	196.1
DSS-1 L/S 2	6.811	83.5	WT L/S 2	6.918	111.2
DSS-1 L/S 5	6.993	64.7	WT L/S 5	6.925	60.3
DSS-2 L/S 0.1	7.028	3748.0	aWT L/S 0.1	7.338	2627.5
DSS-2 L/S 0.2	7.365	1630.6	aWT L/S 0.2	7.480	871.7
DSS-2 L/S 0.5	6.954	337	aWT L/S 0.5	7.066	410
DSS-2 L/S 1	7.176	287	aWT L/S 1	7.231	192
DSS-2 L/S 2	7.059	73.3	aWT L/S 2	7.098	94.8
DSS-2 L/S 5	7.200	61.3	aWT L/S 5	7.168	58.4
DWSS 1 L/S 0.1	6.786	2930.6			
DWSS 1 L/S 0.2	7.153	760.2			
DWSS 1 L/S 0.5	6.608	341			
DWSS 1 L/S 1	6.809	150.3			
DWSS 1 L/S 2	6.787	89.1			
DWSS 1 L/S 5	6.970	73.4			

# Appendix B Grain size distribution analysis

**Table B.1:** Grain size distribution analysis for soil from the control column, after end experiment.

<b>Sample no</b>	1: Control	<b>Date</b>	04/10/2022	
<b>Sample weight</b>		100.76	<b>gram</b>	
<b>Lost % in sieving</b>	0.62			
Mash size d mm	weight in sieve (g)	mass percentages	on curve	Cumulative mass percentages
8.000	0.00	0.00		100.00
4.000	0.00	0.00	8.000	100.00
2.000	2.28	2.28	4.000	100.00
1.000	3.66	3.65	2.000	97.72
0.500	15.11	15.09	1.000	94.07
0.250	38.12	38.07	0.500	78.98
0.125	27.75	27.71	0.250	40.91
0.063	7.61	7.60	0.125	13.20
Pan	5.61	5.60	0.063	5.60
Sum	100.14	100.00		



**Figure B.1:** Grain size distribution of soil from the control column after end experiment.

## Appendix C DOC and TOC analysis

**Table C.1:** Dissolved organic carbon (DOC) analysis carried out 14/12/2022 by ALS Laboratory Group in Oslo. \* = excluded from dataset due to unlikely high concentration.

<b>Dissolved organic carbon (DOC)</b>					
<b>Sample</b>	<b>mg/L</b>	<b>Sample</b>	<b>mg/L</b>	<b>Sample</b>	<b>mg/L</b>
<b>Control</b>		<b>DSS-1</b>		<b>DWSS 3</b>	
L/S 0.1	160	L/S 0.1	73	L/S 0.1	62
L/S 0.2	122	L/S 0.2	43	L/S 0.2	35
L/S 0.5	73	L/S 0.5	46	L/S 0.5	27
L/S 1	48	L/S 1	50	L/S 1	23
L/S 2	35	L/S 2	40	L/S 2	20
L/S 5	16	L/S 5	19	L/S 5	10
<b>CWC #1</b>		<b>DSS-2</b>		<b>WT</b>	
L/S 0.1	176	L/S 0.1	31	L/S 0.1	191
L/S 0.2	131	L/S 0.2	23	L/S 0.2	129
L/S 0.5	58	L/S 0.5	17	L/S 0.5	64
L/S 1	34	L/S 1	18	L/S 1	37
L/S 2	23	L/S 2	15	L/S 2	26
L/S 5	14	L/S 5	12	L/S 5	15
<b>CWC #2</b>		<b>DWSS 1</b>		<b>aWT</b>	
L/S 0.1	176	L/S 0.1	59	L/S 0.1	19.4
L/S 0.2	131	L/S 0.2	48	L/S 0.2	15.5
L/S 0.5	58	L/S 0.5	28	L/S 0.5	9.8
L/S 1	34	L/S 1	22	L/S 1	9.5
L/S 2	24	L/S 2	15	L/S 2	210*
L/S 5	14	L/S 5	9.2	L/S 5	6.5
<b>CWC #3</b>		<b>DWSS 2</b>		<b>Blank</b>	
L/S 0.1	176	L/S 0.1	35	#1	0.9
L/S 0.2	131	L/S 0.2	44		
L/S 0.5	58	L/S 0.5	29		
L/S 1	34	L/S 1	22		
L/S 2	24	L/S 2	18		
L/S 5	14	L/S 5	9.9		

**Table C.2:** Total organic carbon (TOC) analysis carried out 14/12/2022 by ALS Laboratory Group in Oslo

	<b>Dry matter at 105 °C</b>	<b>Total organic carbon (TOC)</b>
<b>Sample</b>	<b>%</b>	<b>% dryweight</b>
Original soil #1	99.4	0.53
Original soil #2	99.5	0.57
Original soil #3	99.2	0.6
Control #1	100	0.51
Control #2	100	0.5
Control #3	99.7	0.55
CWC #1	99.5	1.3
CWC #2	100	1.3
CWC #3	99.8	1.1
DSS-1 #1	99.6	0.71
DSS-1 #2	99.6	0.76
DSS-1 #3	99.8	0.7
DSS-2 #1	99.6	0.84
DSS-2 #2	99.8	0.78
DSS-2 #3	100	0.81
DWSS 1	99.6	0.87
DWSS 2	99.8	0.83
DWSS 3	99.8	0.86
WT #1	100	1.2
WT #2	100	1.1
WT #3	99.6	1
aWT #1	99.8	1.6
aWT #2	99.8	1.3
aWT #3	99.8	1.3

## Appendix D LC-MS/MS

### D.1 QA/QC and instrument parameters

**Table D.1:** Quality assurance and quality controls were prepared in the same way for both water- and soil samples. \* = Injected every 8-29 samples.

Code (no. of samples)	Sample matrix	Addition pre-extraction		Addition post-extraction		Solvent MQ:MeOH
		TA	IS	TA	IS	
Procedure blank (4)	NO		x			50:50
Blank (2)	YES		x			50:50
Spike (3) 20 ppb	YES	x	x			50:50
Matrix matched (2) 20 ppb	YES			x	x	50:50
Quality control (2) 20 ppb	YES	x	x			50:50
Solvent blank*	NO					0:100
Calibration 0 ppb	NO				x	43:57
Calibration 0.01 ppb	NO			x	x	43:57
Calibration 0.02 ppb	NO			x	x	36:64
Calibration 0.05 ppb	NO			x	x	46:54
Calibration 0.1 ppb	NO			x	x	43:57
Calibration 0.2 ppb	NO			x	x	36:64
Calibration 0.5 ppb	NO			x	x	46:54
Calibration 1 ppb	NO			x	x	43:57
Calibration 2 ppb	NO			x	x	36:64
Calibration 5 ppb*	NO			x	x	46:54
Calibration 10 ppb	NO			x	x	43:57
Calibration 20 ppb	NO			x	x	36:64
Calibration 50 ppb	NO			x	x	45:55
Calibration 100 ppb	NO			x	x	42:58

**Table D.2:** Gradient between the mobile phases used for the LC-MS/MS. Water phase (A) was water with 2 mM ammonium acetate, while the organic phase (B) was methanol.

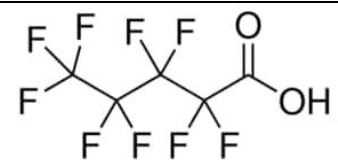
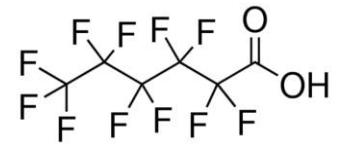
Gradient				
Time (min)	Flow	% A	% B	Step
Init	0.25	80	20	Init
0.1	0.25	80	20	6
0.2	0.25	50	50	6
0.8	0.25	30	70	6
1.5	0.25	20	80	6
2.8	0.25	15	85	5
4.5	0.25	0	100	6
5.5	0.25	0	100	6
5.6	0.25	80	20	6
6	0.25	80	20	6

**Table D.3:** Tune parameters for electrospray ionization source (ESI) in negative used for the UPLC-Xevo TQS instrument.

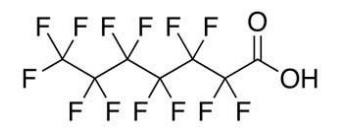
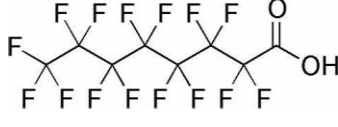
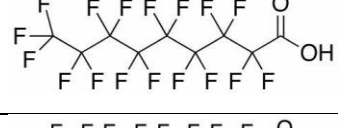
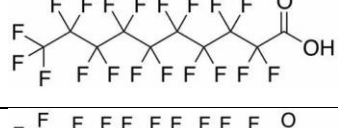
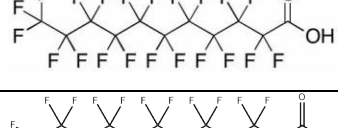
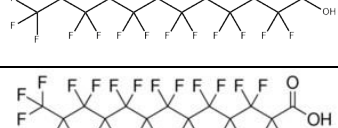
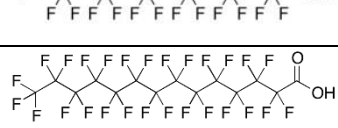
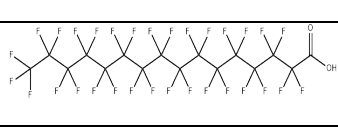

<b>ESI (-)</b>	
Capillary (kV)	2
Cone (V)	25
Source Offset (V)	40
Desolvation temperature (°C)	450
Desolvation Gas flow (L/h)	650
Cone (L/h)	150
Nebuliser (Bar)	6
Source temperature (°C)	150

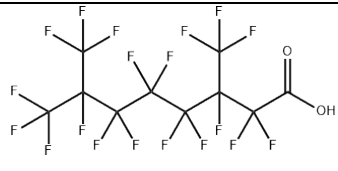
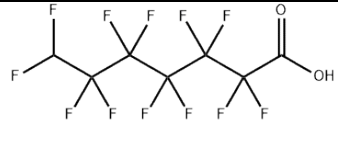
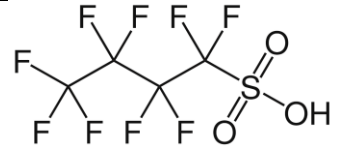
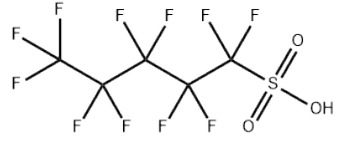
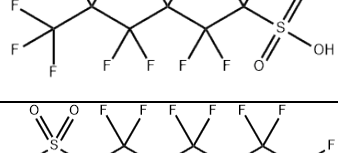
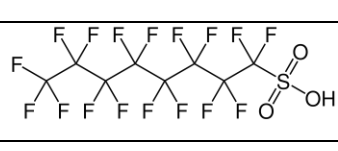

## D.2 List of analysed PFAS

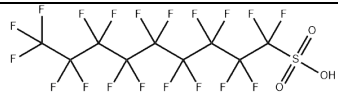
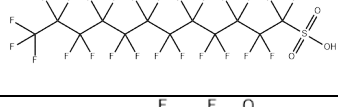
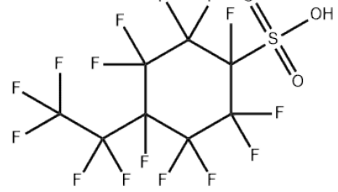

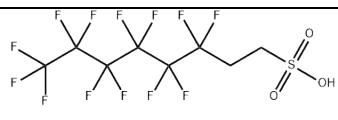
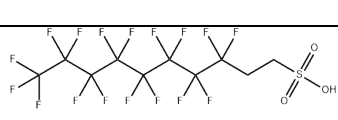
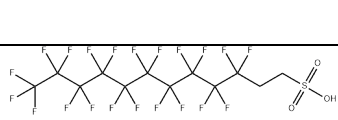
**Table D.4:** Complete list of the three internal standards (IS) and all PFAS analysed for in the LC-MS/MS, including structure, CAS-number, formula, molecular weight (MW), molecular weight of parent compound, cone in V and transitions in CE.


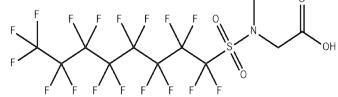
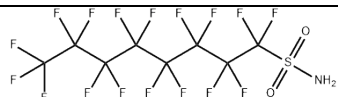
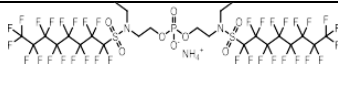
Compound	Name	Structure	CAS	Formula	MW	Parent	Cone [V]	Transitions [CE]
<i>Internal standards (IS)</i>								
PFOA - <sup>13</sup> C <sub>8</sub>	Perfluorooctanoic acid <sup>13</sup> C <sub>8</sub>			<sup>13</sup> C <sub>8</sub> HF <sub>15</sub> O <sub>2</sub>	422.01	420.9	16	420.90 → 171.86 (16)
								420.90 → 222.84 (16)
PFOS - <sup>13</sup> C <sub>8</sub>	Perfluorooctanesulfonate <sup>13</sup> C <sub>8</sub> sodium salt			<sup>13</sup> C <sub>8</sub> F <sub>17</sub> O <sub>3</sub> S	507.06	506.9	56	506.90 → 79.87 (46)
								506.90 → 171.85 (32)
6:2 FTS - <sup>13</sup> C <sub>2</sub>	<sup>1</sup> H, <sup>2</sup> H-Perfluorooctane sulfonate (6:2) <sup>13</sup> C <sub>2</sub>			C <sub>6</sub> <sup>13</sup> C <sub>2</sub> H <sub>5</sub> F <sub>13</sub> O <sub>3</sub> S	432	432.96	26	432.96 → 411.959 (24)
								432.96 → 81.901 (30)
<i>Perfluorocarboxylic Acids (PFCA)</i>								
PFPeA	Perfluoropentanoic acid		2706-90-3	C <sub>5</sub> HF <sub>9</sub> O <sub>2</sub>	264.05	262.97	20	262.97 → 219 (8)
PFH <sub>x</sub> A	Perfluorohexanoic acid		307-24-4	C <sub>6</sub> HF <sub>11</sub> O <sub>2</sub>	314.05	312.97	10	312.97 → 118.95 (18)
								312.97 → 269 (8)



PFHpA	Perfluoroheptanoic acid		375-85-9	$C_7HF_{13}O_2$	364	362.96	6	362.96 → 119.00 (22)
								362.96 → 168.97 (18)
PFOA	Perfluorooctanoic acid		335-67-1	$C_8HF_{15}O_2$	414.07	412.97	20	412.97 → 168.90 (18)
								412.97 → 369.00 (8)
PFNA	Perfluorononanoic acid		375-95-1	$C_9HF_{17}O_2$	464.08	462.99	20	462.99 → 219 (16)
								462.99 → 419 (10)
PFDA	Perfluorodecanoic acid		335-76-2	$C_{10}HF_{19}O_2$	514.09	513.1	10	513.10 → 219.01 (18)
								513.10 → 269.04 (16)
PFUnA	Perfluoroundecanoic acid		2058-94-8	$C_{11}HF_{21}O_2$	564.09	562.96	12	562.96 → 268.92 (18)
								562.96 → 518.98 (10)
PFDoDA	Perfluorododecanoic acid		307-55-1	$C_{12}HF_{23}O_2$	614.1	612.95	26	612.95 → 168.93 (26)
								612.95 → 568.90 (12)
PFTriDA	Perfluorotridecanoic acid		72629-94-8	$C_{13}HF_{25}O_2$	664.11	662.93	6	662.93 → 168.90 (24)
								662.93 → 618.90 (10)
PFTDA	Perfluorotetradecanoic acid		376-06-7	$C_{14}HF_{27}O_2$	714.12	712.92	20	712.92 → 168.96 (30)
								712.92 → 668.92 (14)
PFHxDA	Perfluorohexadecanoic acid		67905-19-5	$C_{16}HF_{31}O_2$	814.13	813.03	36	813.03 → 168.96 (34)
								813.03 → 218.99 (24)

P37DMOA	Perfluoro-3,7-dimethyloctanoic acid		172155-07-6	$C_{10}HF_{19}O_2$	514	469	44	469 → 218.7 (24)
								469 → 269.03 (24)
7H-PFHpA	7H-Dodecafluoroheptanoic acid		1546-95-8	$C_7H_2F_{12}O_2$	346.07	345.03	8	345.03 → 131.03 (24)
								345.03 → 281.06 (10)
<b>Perfluoroalkyl Sulfonates (PFSA)</b>								
PFBS	Perfluorobutane sulfonic acid		375-73-5	$C_4HF_9O_3S$	299.09	298.68	42	298.90 → 79.86 (26)
								298.90 → 98.96 (28)
								298.90 → 82.95 (26)
PFPeS	Perfluoropentane sulfonic acid		2706-91-4	$C_5HF_{11}O_3S$	350	348.98	20	348.98 → 79.96 (30)
								348.98 → 98.96 (26)
PFHxS	Perfluorohexane sulfonic acid		355-46-4	$C_6HF_{13}O_3S$	390	398.9	5	398.9 → 79.97 (30)
								398.9 → 98.97 (30)
PFHpS	Perfluoroheptane sulfonic acid		375-92-8	$C_7HF_{15}O_3S$	449.12	448.97	2	448.97 → 79.95 (34)
								448.97 → 98.95 (34)
PFOS	Perfluorooctano sulfonic acid		1763-23-1	$C_8HF_{17}O_3S$	500.13	498.97	20	498.97 → 79.96 (20)
								498.97 → 98.96 (38)

PFNS	Perfluorononane sulfonic acid		68259-12-1	$C_9HF_{19}O_3S$	550	548.9	10	548.9 → 79.97 (40)
								548.90 → 98.97 (10)
PFDods	Perfluorododecane sulfonic acid		79780-39-5	$C_{12}HF_{25}O_3S$	700	698.9	15	698.9 → 79.96 (10)
								698.90 → 98.91 (40)
PFECHS	Perfluoroethylcyclohexane sulfonic acid		646-83-3	$C_8HF_{15}O_3S$	461	460.97	34	460.97 → 98.95 (28)
								460.97 → 119.00 (40)
								460.97 → 381.00 (26)
<b>Fluorotelomer Sulfonates (FTS)</b>								
4:2 FTS	1H,2H-Perfluorohexane sulfonate (4:2)		757124-72-4	$C_6H_5F_9O_3S$	328.15	327.1	34	327.1 → 80.80 (26)
								327.1 → 307.15 (18)
6:2 FTS	1H,2H-Perfluorooctane sulfonate (6:2)		27619-97-2	$C_8H_5F_{13}O_3S$	428.17	427.1	24	427.10 → 80.93 (26)
								427.10 → 407.18 (24)
8:2 FTS	1H,2H-Perfluorodecan sulfonate (8:2)		39108-34-4	$C_{10}H_5F_{17}O_3S$	528.18	527.16	40	527.16 → 80.93 (28)
								527.16 → 507.13 (26)
10:2 FTS	1H,2H-Perfluorododecan sulfonate (10:2)		120226-60-0	$C_{12}H_5F_{21}O_3S$	628.2	627.03	8	627.03 → 80.86 (32)
								627.03 → 607.07 (32)

<b>Perfluorooctanesulfonamidoacetic Acids (FPSAA)</b>								
FOSAA	Perfluoro-1-octanesulfonamidoacetic acid		2806-24-8	C <sub>10</sub> H <sub>4</sub> F <sub>17</sub> NO <sub>4</sub> S	557.18	555.97	12	555.97 → 419.05 (24)
								555.97 → 497.98 (28)
MeFOSAA	2-(N-methylPerfluoro-1-octanesulfonamido)acetic acid		2355-31-9	C <sub>11</sub> H <sub>6</sub> F <sub>17</sub> NO <sub>4</sub> S	571.21	569.99	6	569.99 → 419.03 (18)
								569.99 → 483.00 (16)
<b>Perfluorooctanesulfonamides (FOSA)</b>								
PFOSA	Perfluorooctane sulfonamide		754-91-6	C <sub>8</sub> H <sub>2</sub> F <sub>17</sub> NO <sub>2</sub> S	499.14	497.97	12	497.97 → 77.89 (28)
								497.97 → 477.58 (26)
<b>SaMPAP</b>								
diSAMPAP	bis[2-(N-ethylperfluorooctane-1-sulfonamido)ethyl] phosphate		30381-98-7	C <sub>24</sub> H <sub>22</sub> F <sub>34</sub> N <sub>3</sub> O <sub>8</sub> P S <sub>2</sub>	1221.50	1203.22	92	1203.22 → 169.02 (66)
								1203.22 → 526.09 (40)

# Appendix E PFAS concentrations in leachate and soil

## E.1 PFAS leachate concentrations

**Table E.1:** PFAS concentrations in µg/L for all leachate samples from the 9 columns, including the experimental- and analytical triplicates, blanks and LOD/ LOQ for all PFAS. Blank spaces indicate no detection of the compound. Short-chained PFAS are marked in blue.

Leachate [µg/L]		Control						CWC #1 (analytical triplicate)					
Compound + CF chain length		L/S 0.1	L/S 0.2	L/S 0.5	L/S 1	L/S 2	L/S 5	L/S 0.1	L/S 0.2	L/S 0.5	L/S 1	L/S 2	L/S 5
<b>Perfluoroalkyl Carboxylic Acids (PFCA)</b>													
PFPeA	4	2.84	0.21		< LOD	< LOD	< LOD	0.91	< LOD				
PFHxA	5	23.40	4.02	0.62	0.39	0.38	0.38	8.59	4.37	0.83	0.49	0.41	0.43
PFHpA	6	4.91	1.37	0.12	0.01	< LOQ	< LOQ	1.47	1.33	0.08	0.03	0.02	0.01
PFOA	7	6.87	9.19	2.49	0.16	0.07	0.05	2.13	6.33	1.39	0.31	0.10	0.08
PFNA	8	0.27	0.32	0.28	0.17	< LOD	< LOD	0.06	0.27	0.15	0.33	0.07	< LOD
PFDA	9	0.22	0.68	0.97	1.68	0.65	0.16	< LOD	< LOD	0.04	0.22	0.28	0.16
PFUnA	10	< LOQ	< LOD	0.39	0.47	0.35	0.07		< LOD	< LOD	0.04	0.15	0.09
PFDoDA	11	0.08	0.30		0.20	< LOQ	< LOD	< LOD	< LOD	< LOD	< LOD	< LOD	< LOD
PFTriDA	12	< LOQ		0.28	0.39	< LOQ	< LOD	< LOD		< LOD			< LOD
P37DMOA	9						0.02	< LOD	< LOD	< LOQ			
<b>Perfluoroalkane Sulfonic Acids (PFSA)</b>													
PFBS	4	9.47	0.98	0.09			< LOD	1.60	0.50	0.01	0.03	< LOD	< LOD
PFPeS	5	5.16	1.35	0.09	< LOD		< LOD	0.86	0.70	0.04	< LOD	< LOQ	0.01
PFHxS	6	26.31	32.68	5.49	0.64	0.40	0.36	7.75	19.19	3.24	0.98	0.47	0.48
PFHpS	7	0.56	1.78	1.38	0.33	< LOQ	< LOD	< LOQ	0.99	0.33	0.57	< LOQ	< LOQ
PFOS	8	240.35	918.62	1228.67	1828.91	1084.32	172.73	51.05	213.93	157.81	495.87	522.04	250.79
PFNS	9	0.65	1.04			1.90							
PFECHS	8	< LOD	< LOD	< LOD	< LOD	< LOD	< LOD	< LOD	< LOD	< LOQ	< LOD	< LOD	< LOD
<b>Fluorotelomer sulfates (FTS)</b>													
4:2 FTS	4		0.03				< LOD	0.04	< LOD	< LOQ	< LOD	< LOQ	< LOQ
6:2 FTS	6	24.31	31.38	5.42	0.58	0.51	0.51	7.88	19.74	4.10	0.98	0.59	1.00
8:2 FTS	8	0.22	0.71	0.82	0.98	1.01	0.45	< LOD	0.49	0.17	0.50	0.59	0.49
10:2 FTS	10	< LOD	0.08	0.34	0.16	0.06	0.04	< LOD	< LOD	< LOD	0.04	< LOD	0.05
<b>Perfluorooctanesulfonamidoacetic Acids (FOSAA)</b>													
FOSAA	8	< LOD	< LOD	0.75	0.65	0.72	0.25	< LOD	< LOD	0.05	0.11	0.21	0.19
MeFOSAA	8	0.08				0.06	0.01	0.10	< LOD	< LOD	0.04	0.03	0.04
<b>Perfluorooctanesulfonamides (FOSA)</b>													
PFOSA	8	3.31	7.49	13.30	14.09	10.10	2.85	< LOD	< LOD	0.99	2.77	3.40	2.64
<b>SaMPAP</b>													
diSAMPAP	16	4.45	40.31	7.49	4.52	2.27	1.78	8.14	8.34	2.81	1.93	1.57	
<b>∑ 25 PFAS</b>													
		353.47	1052.54	1268.97	1854.33	1102.82	179.67	90.58	276.20	172.05	505.24	529.92	256.45

Leachate [ $\mu\text{g/L}$ ]		CWC #2 (analytical triplicate)						CWC #3 (analytical triplicate)					
Compound + CF chain length		L/S 0.1	L/S 0.2	L/S 0.5	L/S 1	L/S 2	L/S 5	L/S 0.1	L/S 0.2	L/S 0.5	L/S 1	L/S 2	L/S 5
<b>Perfluoroalkyl Carboxylic Acids (PFCA)</b>													
PFPeA	4	3.67	< LOD				< LOD	3.45	0.97	< LOD		< LOD	
PFHxA	5	22.95	4.50	1.02	0.48	0.42	0.42	22.37	4.48	0.82	0.50	0.41	0.41
PFHpA	6	4.27	1.14	0.20	0.02	0.02	0.02	4.46	1.24	0.10	0.03	0.02	0.01
PFOA	7	6.30	6.83	2.84	0.35	0.11	0.09	5.93	6.04	1.40	0.30	0.11	0.09
PFNA	8	0.26	0.33	0.28	0.44	0.08	< LOD	0.30	0.28	0.14	0.31	0.06	< LOD
PFDA	9	< LOQ	< LOQ	0.07	0.17	0.32	0.16	< LOQ	< LOQ	0.06	0.15	0.18	0.15
PFUnA	10	< LOD		< LOD	< LOQ	0.13	0.06		< LOD	< LOD	0.07	0.05	0.04
PFDoDA	11		< LOD	< LOD	< LOD	< LOD	< LOD	< LOD	< LOD	< LOD	< LOQ	< LOD	< LOD
PFTriDA	12		< LOD					< LOD					
P37DMOA	9	< LOD	< LOD					< LOD	< LOD	< LOD	0.02		
<b>Perfluoroalkane Sulfonic Acids (PFSA)</b>													
PFBS	4	4.67	0.53	0.07	< LOQ	0.01	< LOD	4.88	0.54	0.01	< LOQ	< LOD	< LOD
PFPeS	5	3.66	0.83	0.10	0.02	0.01	0.01	3.40	0.96	0.05	0.01	0.01	< LOD
PFHxS	6	20.42	18.76	5.43	0.89	0.52	0.47	20.16	19.82	2.91	0.90	0.50	0.45
PFHpS	7	0.79	0.70	0.69	0.63	0.09	< LOD	0.90	0.50	0.46	0.62	0.09	< LOQ
PFOS	8	183.89	304.85	278.40	527.99	660.86	279.10	143.91	309.81	155.54	663.72	557.47	234.01
PFNS	9												
PFECBS	8	< LOQ	< LOD	0.02	< LOD	< LOD	< LOQ	< LOD	< LOQ	< LOQ	< LOD	< LOD	< LOD
<b>Fluorotelomer sulfates (FTS)</b>													
4:2 FTS	4	0.04	< LOD	< LOQ		< LOQ	< LOQ	0.07		0.02	< LOD		
6:2 FTS	6	17.07	18.48	7.29	1.03	0.66	0.56	18.62	22.04	3.93	1.10	0.55	0.52
8:2 FTS	8	0.16	0.46	0.33	0.52	0.62	0.51	0.21	0.57	0.21	0.45	0.59	0.45
10:2 FTS	10	< LOD	< LOD	< LOD	< LOD	< LOQ	< LOQ	< LOD	< LOD	< LOD	< LOD	< LOD	< LOD
<b>Perfluorooctanesulfonamidoacetic Acids (FOSAA)</b>													
FOSAA	8	< LOD	< LOD	0.08	0.10	0.16	0.18	< LOD	< LOD	0.03	0.09	0.11	0.10
MeFOSAA	8	< LOD	< LOD	< LOD	< LOD	0.09	< LOQ	< LOD	< LOD	< LOQ	0.03	0.03	
<b>Perfluorooctanesulfonamides (FOSA)</b>													
PFOSA	8	0.52	0.94	1.42	2.03	3.31	1.99	< LOQ	0.77	0.71	1.94	1.38	0.82
<b>SaMPAP</b>													
diSAMPAP	16	9.02	8.72	2.85	1.87	1.73	1.58	8.08	8.20	2.73	1.89	1.47	1.47
<b><math>\Sigma</math> 25 PFAS</b>													
		277.68	367.08	301.10	536.55	669.15	285.14	236.74	376.21	169.12	672.12	563.03	238.52

Leachate [ $\mu\text{g/L}$ ]		DSS-1						DSS-2					
Compound + CF chain length		L/S 0.1	L/S 0.2	L/S 0.5	L/S 1	L/S 2	L/S 5	L/S 0.1	L/S 0.2	L/S 0.5	L/S 1	L/S 2	L/S 5
<b>Perfluoroalkyl Carboxylic Acids (PFCA)</b>													
PFPeA	4	5.94	4.08	1.05	< LOQ	< LOD	< LOD	1.69	< LOQ	< LOQ	0.18	0.23	0.21
PFHxA	5	1.62	2.09	2.28	1.92	1.14	0.54	0.90	0.82	0.41	0.43	0.51	0.62
PFHpA	6	0.04	0.06	0.11	0.20	0.20	0.08	0.02	< LOQ	0.01	0.01	0.02	0.04
PFOA	7	0.14	0.12	0.16	0.28	0.32	0.37	0.14	0.11	0.05	0.05	0.07	0.11
PFNA	8	< LOD	< LOD	< LOD	0.01	0.01	0.03	< LOD	< LOD		< LOD	< LOD	< LOD
PFDA	9		< LOD	< LOQ	0.02	< LOQ	< LOQ		< LOD	< LOQ	< LOD	< LOD	< LOD
PFUnA	10				< LOD	< LOD	< LOD				< LOD	< LOD	< LOD
PFDoDA	11	< LOD	< LOD	< LOD		< LOD	< LOD		< LOD	< LOD	< LOD	< LOD	< LOD
PFTriDA	12						< LOD	< LOD		< LOD			
P37DMOA	9								< LOD	< LOD			
<b>Perfluoroalkane Sulfonic Acids (PFSA)</b>													
PFBS	4	0.03	0.11	0.28	0.37	0.20	0.03	< LOD	< LOD	< LOD	< LOD	0.01	0.04
PFPeS	5	< LOQ	0.01	0.07	0.17	0.20	0.07	< LOD	< LOD	< LOD	< LOD	< LOQ	0.02
PFHxS	6	0.76	0.75	0.60	1.15	1.61	1.03	0.77	0.75	0.37	0.38	0.45	0.48
PFHpS	7	< LOQ	< LOD	< LOQ	< LOQ	0.08	< LOQ	< LOQ	< LOD	< LOD	< LOQ	< LOQ	< LOQ
PFOS	8	7.16	15.22	20.91	47.79	59.28	53.80	6.91	12.79	10.96	10.58	15.90	13.58
PFNS	9		< LOD	0.04	0.16	0.26	0.18					0.10	
PFECHS	8	< LOD		< LOD		< LOD	< LOD						< LOD
<b>Fluorotelomer sulfates (FTS)</b>													
4:2 FTS	4	< LOD		< LOD						< LOD	< LOD		
6:2 FTS	6	0.90	0.83	0.53	0.71	0.83	0.81	0.89	0.88	0.43	0.43	0.49	0.50
8:2 FTS	8		< LOD	0.03	0.05	0.02	0.02	< LOD	< LOQ	0.03	< LOD	< LOQ	< LOD
10:2 FTS	10			< LOD	< LOD	< LOD	< LOD		< LOD	< LOD		< LOD	< LOD
<b>Perfluorooctanesulfonamidoacetic Acids (FOSAA)</b>													
FOSAA	8		< LOD	< LOD	< LOQ	< LOD	< LOD	< LOD	< LOD	< LOD	< LOQ	< LOQ	< LOD
MeFOSAA	8	< LOD	< LOD		< LOD		< LOD			< LOD		< LOD	< LOD
<b>Perfluorooctanesulfonamides (FOSA)</b>													
PFOSA	8	< LOD	< LOD	0.09	0.15	< LOD	0.14	< LOD	< LOD	0.07	0.09	0.07	0.00
<b>SaMPAP</b>													
diSAMPAP	16	2.77	2.74	1.47	1.46	1.46	1.47	2.69	2.92	1.39	1.40	1.39	1.40
<b><math>\Sigma</math> 25 PFAS</b>													
		19.35	26.01	27.62	54.46	65.61	58.57	14.00	18.26	13.72	13.56	19.25	17.01

Leachate [ $\mu\text{g/L}$ ]		DWSS 1 (experimental triplicate)						DWSS 2 (experimental triplicate)					
Compound + CF chain length		L/S 0.1	L/S 0.2	L/S 0.5	L/S 1	L/S 2	L/S 5	L/S 0.1	L/S 0.2	L/S 0.5	L/S 1	L/S 2	L/S 5
<b>Perfluoroalkyl Carboxylic Acids (PFCA)</b>													
PFPeA	4	1.79	0.39	< LOQ	< LOQ	< LOQ	< LOQ	2.78	0.68	0.17	< LOQ	< LOQ	< LOQ
PFHxA	5	1.10	0.84	0.49	0.51	0.53	0.55	1.42	0.94	0.54	0.51	0.53	0.54
PFHpA	6	0.02	0.02	0.01	0.01	0.02	0.02	0.05	0.03	0.02	0.01	0.02	0.03
PFOA	7	0.14	0.08	0.05	0.04	0.06	0.06	0.13	0.10	0.06	0.06	0.07	0.09
PFNA	8	< LOD	< LOD	< LOD	< LOD		< LOD	< LOD	< LOD	< LOD	< LOD	< LOD	< LOD
PFDA	9	< LOD	< LOD	< LOD	< LOD	< LOD	< LOD	< LOD	< LOD	< LOD	< LOQ	< LOQ	< LOD
PFUnA	10					< LOD			< LOD	< LOD	< LOD	< LOD	< LOD
PFDoDA	11	< LOD	< LOD	< LOD	< LOD	< LOD	< LOD	< LOD	< LOD	< LOD	< LOD	< LOD	< LOD
PFTriDA	12				< LOD	< LOD	< LOD			< LOD	< LOD		
P37DMOA	9				< LOD								
<b>Perfluoroalkane Sulfonic Acids (PFSA)</b>													
PFBS	4	< LOD	< LOD	< LOD	< LOD	< LOD	< LOD	< LOQ	< LOD	< LOD	< LOD	0.01	0.01
PFPeS	5	< LOD	< LOD	< LOD	< LOD	< LOD	< LOD	< LOD	< LOD	< LOD	< LOD	< LOD	< LOQ
PFHxS	6	0.75	0.69	0.37	0.35	0.37	0.38	0.74	0.70	0.37	0.37	0.40	0.43
PFHpS	7	< LOD	< LOD		< LOD	< LOD		< LOD	< LOD	< LOQ	< LOD	< LOQ	< LOQ
PFOS	8	6.23	8.50	6.57	4.28	5.69	4.75	3.51	5.57	5.48	8.53	7.79	8.26
PFNS	9	< LOD	< LOD			0.03	0.02			< LOQ	0.02	0.00	0.05
PFECHS	8			< LOD			< LOD		< LOD			< LOD	< LOD
<b>Fluorotelomer sulfates (FTS)</b>													
4:2 FTS	4												< LOD
6:2 FTS	6	0.88	0.80	0.43	0.41	0.43	0.44	0.88	0.84	0.45	0.45	0.45	0.46
8:2 FTS	8	< LOD	< LOD	0.01	< LOD	< LOD	< LOD	< LOD	< LOD	< LOD	< LOD	< LOD	< LOD
10:2 FTS	10					< LOD	< LOD		< LOD			< LOD	< LOD
<b>Perfluorooctanesulfonamidoacetic Acids (FOSAA)</b>													
FOSAA	8	< LOD		< LOD	< LOD	< LOD	< LOD		< LOD	< LOD	< LOD	< LOD	< LOD
MeFOSAA	8		< LOD	< LOD	< LOD								
<b>Perfluorooctanesulfonamides (FOSA)</b>													
PFOSA	8	< LOD	< LOD	< LOD	< LOD	0.07	< LOD	< LOD		< LOD	< LOQ	< LOQ	< LOD
<b>SaMPAP</b>													
diSAMPAP	16	2.70	2.74	1.44	1.42	1.43	1.43	2.73	2.70	1.43	1.43	1.42	1.42
<b><math>\Sigma</math> 25 PFAS</b>													
		13.60	14.05	9.36	7.03	8.63	7.66	12.23	11.56	8.52	11.39	10.68	11.28



Leachate [ $\mu\text{g/L}$ ]		DWSS 3 (experimental triplicate)						WT					
Compound + CF chain length		L/S 0.1	L/S 0.2	L/S 0.5	L/S 1	L/S 2	L/S 5	L/S 0.1	L/S 0.2	L/S 0.5	L/S 1	L/S 2	L/S 5
<b>Perfluoroalkyl Carboxylic Acids (PFCA)</b>													
PFPeA	4	2.37	0.70	0.35	0.20	0.17	< LOQ	9.01	0.88	< LOQ		< LOD	< LOD
PFHxA	5	1.00	0.86	0.54	0.49	0.53	0.53	25.40	4.00	0.86	0.45	0.41	0.39
PFHpA	6	0.03	0.02	0.01	0.01	0.02	0.02	4.17	1.62	0.19	0.02	0.02	0.01
PFOA	7	0.10	0.10	0.06	0.05	0.06	0.07	4.67	6.06	2.80	0.32	0.13	0.08
PFNA	8	< LOD	< LOD	< LOD	< LOD	< LOD	< LOD	0.16	0.28	0.30	0.32	0.05	< LOD
PFDA	9		< LOD	< LOD	< LOD	< LOD	< LOD	< LOD	0.03	0.15	0.21	0.20	0.15
PFUnA	10			< LOD			< LOD		< LOD	0.03	0.11	0.10	0.06
PFDoDA	11	< LOD	< LOD	< LOD	< LOD	< LOD	< LOD			< LOD	< LOD	< LOD	< LOD
PFTriDA	12							< LOD	< LOD				
P37DMOA	9												
<b>Perfluoroalkane Sulfonic Acids (PFSA)</b>													
PFBS	4	< LOD	< LOD	< LOD	< LOD	0.01	0.02	6.37	0.92	0.12	< LOQ	< LOD	< LOD
PFPeS	5		< LOD	< LOD	< LOQ	< LOD	0.01	3.89	1.35	0.16	0.02	< LOQ	< LOD
PFHxS	6	0.70	0.66	0.37	0.38	0.40	0.41	18.02	21.10	5.67	0.86	0.57	0.46
PFHpS	7				< LOD	< LOQ	< LOQ	0.35	0.81	0.73	0.53	< LOQ	< LOQ
PFOS	8	2.84	4.48	7.44	4.70	6.68	6.18	107.84	347.46	272.42	1044.33	622.01	239.39
PFNS	9	< LOD		< LOD		0.03	0.03			0.48			
PFECHS	8	< LOD			< LOD	< LOD		< LOD		< LOD			< LOD
<b>Fluorotelomer sulfates (FTS)</b>													
4:2 FTS	4			< LOD				0.03				< LOD	
6:2 FTS	6	0.82	0.78	0.44	0.44	0.44	0.44	15.31	19.05	5.46	1.12	0.65	0.52
8:2 FTS	8	< LOD	< LOD	< LOD	< LOD	< LOD	< LOD	0.13	0.38	0.32	0.57	0.76	0.53
10:2 FTS	10					< LOD	< LOD					< LOD	< LOD
<b>Perfluorooctanesulfonamidoacetic Acids (FOSAA)</b>													
FOSAA	8	< LOD	< LOD	< LOD	< LOD	< LOD	< LOD		< LOQ	< LOD	0.29	0.12	0.18
MeFOSAA	8		< LOD								< LOD	< LOD	< LOD
<b>Perfluorooctanesulfonamides (FOSA)</b>													
PFOSA	8	< LOD	< LOD	< LOD	< LOD	< LOD	< LOD	0.14	1.03	1.66	4.34	1.93	1.59
<b>SaMPAP</b>													
diSaMPAP	16	2.70	2.67	1.40	1.40	1.41	1.41	2.83	2.83	1.40	1.65	1.44	1.40
<b><math>\Sigma</math> 25 PFAS</b>													
		10.56	10.26	10.60	7.66	9.75	9.13	198.33	407.78	292.74	1055.14	628.40	244.77

Leachate [µg/L]		aWT						Blank			
Compound + CF chain length		L/S 0.1	L/S 0.2	L/S 0.5	L/S 1	L/S 2	L/S 5	#1	#2	LOD	LOQ
<b>Perfluoroalkyl Carboxylic Acids (PFCA)</b>											
PFPeA	4	< LOD	< LOD	< LOD	< LOD	< LOD	< LOD	< LOD	< LOD	0.05	0.165
PFHxA	5	0.71	0.71	0.37	0.37		0.37	0.37	0.37	0.01	0.033
PFHpA	6			< LOQ	< LOQ		< LOQ		< LOQ	0.01	0.033
PFOA	7		0.06	0.04	0.03		0.03	0.04	0.04	0.01	0.033
PFNA	8	< LOD	< LOD	< LOD	< LOD	< LOD	< LOD	< LOD	< LOD	0.01	0.033
PFDA	9		< LOD	< LOD						0.01	0.033
PFUnA	10						< LOD			0.02	0.066
PFDoDA	11	< LOD	< LOD	< LOD	< LOD	< LOD	< LOD	< LOD	< LOD	0.01	0.033
PFTriDA	12			< LOD	< LOD					0.05	0.165
P37DMOA	9									0.01	0.033
<b>Perfluoroalkane Sulfonic Acids (PFSA)</b>											
PFBS	4					< LOD			< LOD	0.01	0.033
PFPeS	5				< LOD	< LOD		< LOD		0.01	0.033
PFHxS	6	0.66	0.65	0.34	0.35	0.34	0.34	0.34	0.34	0.05	0.165
PFHpS	7									0.1	0.33
PFOS	8	1.32	1.25	0.69	0.66	0.67	0.73			0.01	0.033
PFNS	9									0.01	0.033
PFECHS	8					< LOD	< LOD			0.01	0.033
<b>Fluorotelomer sulfates (FTS)</b>											
4:2 FTS	4					< LOD				0.01	0.033
6:2 FTS	6	0.79	0.77	0.40	0.41	0.41	0.40	0.40	0.41	0.01	0.033
8:2 FTS	8		< LOD	< LOD		< LOD		< LOD	< LOD	0.01	0.033
10:2 FTS	10			< LOD						0.01	0.033
<b>Perfluorooctanesulfonamidoacetic Acids (FOSAA)</b>											
FOSAA	8			< LOD	< LOD		< LOD		< LOD	0.01	0.033
MeFOSAA	8	< LOD								0.01	0.033
<b>Perfluorooctanesulfonamides (FOSA)</b>											
PFOSA	8				< LOD				< LOD	0.01	0.033
<b>SaMPAP</b>											
diSAMPAP	16	2.73	2.67	1.39	1.40	1.41	1.39	1.39	1.39	0.5	1.65
<b>∑ 25 PFAS</b>											
		6.20	6.12	3.23	3.22	2.82	3.27	2.54	2.54		

## E.2 PFAS soil concentrations

**Table E.2:** PFAS concentrations in µg/kg for all soil samples from the 9 columns, the reference soil, and LOD/ LOQ for all PFAS. Blank spaces indicate no detection of the compound. Short-chained PFAS are marked in blue.

Soil [µg/kg]	Original soil			Control			CWC			DSS-1			
Compound + CF chain length	#1	#2	#3	#1	#2	#3	#1	#2	#3	#1	#2	#3	
<b>Perfluorocarboxylic Acids (PFCA)</b>													
PFPeA	4	14.63	11.90	10.72		1.26		1.26	1.91	1.62	4.30	4.04	
PFHxA	5	14.35	12.28	12.73	3.60	1.95	2.28	3.96	3.46	3.93	3.05	5.66	2.51
PFHpA	6	1.53	1.06	1.74				0.55	< LOD		< LOD	0.36	< LOD
PFOA	7	7.42	9.85	8.23	0.74	0.69		1.05	< LOQ	< LOQ	1.81	3.33	1.44
PFNA	8	< LOQ	1.56	< LOQ	< LOQ			< LOD	< LOD		< LOD	< LOQ	< LOQ
PFDA	9	1.92	2.93	2.57		0.39	< LOQ	0.67	0.81	0.55	0.82	0.65	0.47
PFUnA	10	2.31	4.61	3.09	3.30	4.65	1.95	2.74	3.32	3.00	1.62	1.68	1.59
PFDoDA	11	< LOQ	0.34	0.38	< LOQ	0.30	< LOQ	0.31	0.53	0.81		< LOQ	< LOQ
PFTriDA	12	< LOD	0.93	0.90	< LOD	0.82		< LOD	1.92	0.96			0.97
PFTDA	13	0.65					< LOQ		0.58	0.52		0.76	< LOQ
PFHxDA	15	0.69	0.54	0.62			0.59		< LOQ	0.72		< LOQ	0.58
7H-PFHpA	6	0.39		< LOQ	< LOQ	< LOQ	< LOQ	< LOQ	< LOQ	< LOQ	< LOQ	< LOQ	0.34
<b>Perfluoroalkyl Sulfonates (PFSA)</b>													
PFBS	4	1.49	< LOQ	< LOQ	< LOD	< LOD	< LOD	< LOD	< LOD	< LOD	< LOD	< LOD	< LOD
PFPeS	5	1.97	1.80	1.57	< LOQ	< LOQ	< LOD	< LOD	< LOQ	< LOQ	< LOD	< LOD	< LOQ
PFHxS	6	17.78	15.67	15.76	4.79	2.58	3.66	7.36	4.50	6.14	7.24	6.35	9.12
PFHpS	7	1.99	1.81	1.48	< LOD	0.95	< LOQ	0.85	0.82	< LOD	< LOQ	< LOQ	1.66
PFOS	8	1123.34	1192.50	1210.43	102.16	187.19	119.83	343.20	312.54	265.69	417.62	329.56	425.29
PFNS	9				9.62	11.94	10.51	13.04	14.39	10.27	6.58	5.79	6.39
PFDoDS	12						< LOQ		2.98	1.79		< LOD	
<b>Fluorotelomer sulfates (FTS)</b>													
6:2 FTS	6	26.83	26.44	22.19	11.78	10.65	13.05	12.84	14.10	11.71	17.27	15.46	12.87
8:2 FTS	8	4.89	8.10	6.67	0.93	1.83	1.79	3.44	3.78	2.25	2.81	2.99	4.12
10:2 FTS	10	1.64	3.79	4.35	2.47	3.75	2.84	2.80	4.03	2.95	1.41	0.78	2.22
<b>Perfluorooctanesulfonamidoacetic Acids (FOSAA)</b>													
FOSAA	8	3.50	3.99	4.80	2.84	3.64	2.68	2.76	2.72	2.55	0.77	1.26	1.44
MeFOSAA	8	1.26	1.05	1.45	1.00	1.26	0.71	0.72	1.23	0.91	0.54	0.79	0.72
<b>Perfluorooctanesulfonamides (FOSA)</b>													
PFOSA	8	24.47	30.07	31.52	17.98	35.87	24.86	27.78	26.32	24.94	16.09	9.94	19.34
<b>SaMPAP</b>													
diSaMPAP	16	23.14	19.65	20.06	31.06	26.14	26.81	25.22	26.93	28.67	53.13	41.85	31.38
<b>∑ 26 PFAS</b>													
		1276.20	1350.88	1361.28	192.27	295.87	211.56	450.55	426.87	369.97	535.05	431.24	522.43

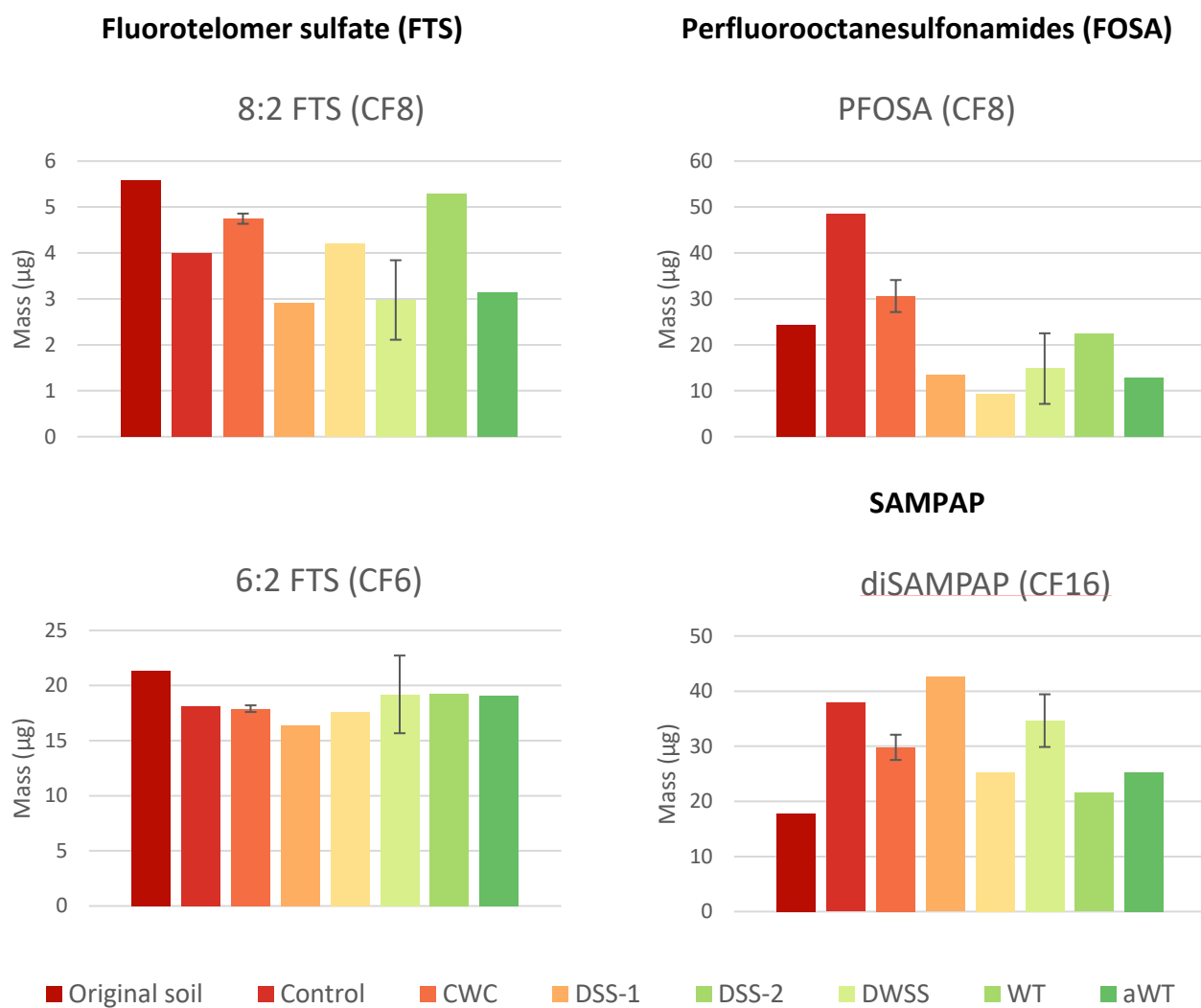
Soil [ $\mu\text{g}/\text{kg}$ ]		DSS-2			DWSS	DWSS	DWSS	WT			aWT		
Compound + CF chain length		#1	#2	#3	1	2	3	#1	#2	#3	#1	#2	#3
<b>Perfluorocarboxylic Acids (PFCA)</b>													
PFPeA	4	1.65	3.51	2.65	4.33	4.34	2.87		1.95	1.73	5.80	5.07	3.01
PFHxA	5	4.67	7.39	4.91	4.62	8.94	7.16	5.58	3.18	4.18	5.61	6.10	7.95
PFHpA	6	0.85	< LOD	0.49	1.86	2.30	0.43	< LOD			1.07	1.16	0.49
PFOA	7	2.85	2.55	4.12	5.34	7.54	4.27	4.18	1.17	1.79	5.89	4.65	3.16
PFNA	8	< LOQ	< LOQ	< LOQ	< LOD	< LOQ	1.59	< LOD	< LOQ		< LOQ	< LOD	< LOD
PFDA	9	1.57	2.22	0.47	0.83	1.71	1.20		0.40	< LOQ	2.08	1.20	1.45
PFUnA	10	1.73	3.62	1.81	3.26	2.10	2.76	6.78	2.86	2.80	1.63	1.97	1.97
PFDoDA	11	< LOQ	1.21	0.33	< LOQ	< LOQ	0.59	0.58	0.56	< LOQ	0.56	0.52	0.40
PFTriDA	12	< LOD	0.99	< LOQ	< LOQ	0.66	< LOD	2.27	1.20	< LOQ	0.62	< LOD	< LOD
PFTDA	13		0.72	< LOQ	< LOQ		< LOQ		1.30		< LOQ	1.08	
PFHxDA	15	< LOQ			0.60	< LOQ	< LOQ	0.64	0.61	< LOQ		< LOQ	< LOQ
7H-PFHpA	6		< LOQ	< LOQ	< LOQ	< LOQ		< LOQ		< LOQ	< LOQ		< LOQ
<b>Perfluoroalkyl Sulfonates (PFSA)</b>													
PFBS	4	< LOQ	< LOD	< LOQ	< LOD	< LOQ	< LOQ	< LOD	< LOD	< LOD	< LOQ	< LOD	< LOD
PFPeS	5	< LOD	< LOD	1.09	0.58	0.76	1.46	< LOD	< LOD	< LOD	1.06	< LOD	1.33
PFHxS	6	14.28	9.67	13.17	9.54	16.54	19.19	8.13	5.00	5.65	15.81	12.06	14.34
PFHpS	7	1.00	1.73	1.42	1.99	0.70	1.70	0.87	< LOQ	0.65	2.07	1.66	1.93
PFOS	8	513.19	576.75	472.78	621.27	760.84	998.32	396.19	244.80	259.63	1048.89	776.26	843.81
PFNS	9					11.84	15.63	15.07	7.92	7.63		8.74	
PFDoDS	12				1.88	3.43		2.98	1.67				
<b>Fluorotelomer sulfates (FTS)</b>													
6:2 FTS	6	20.89	18.71	15.40	15.76	21.94	23.46	17.67	13.10	14.01	20.51	16.72	22.51
8:2 FTS	8	4.22	5.86	4.76	2.52	4.57	3.46	5.13	2.14	3.17	4.66	3.29	2.94
10:2 FTS	10	2.80	3.20	1.50	2.53	1.87	2.20	7.24	4.00	2.89	3.41	1.11	2.13
<b>Perfluorooctanesulfonamidoacetic Acids (FOSAA)</b>													
FOSAA	8	1.22	2.10	1.33	1.41	3.08	1.11	5.34	3.48	2.15			
MeFOSAA	8	< LOQ	0.51	0.45	0.87	1.06	0.74	1.67	1.00	0.34			
<b>Perfluorooctanesulfonamides (FOSA)</b>													
PFOSA	8	12.80	7.99	11.60	8.72	16.94	26.80	26.74	13.07	11.01			
<b>SaMPAP</b>													
diSAMPAP	16	28.49	20.44	18.87	35.99	27.14	37.61	19.61	15.42	19.05			
<b><math>\Sigma</math> 26 PFAS</b>													
		612.22	669.18	557.14	723.90	898.29	1152.56	526.65	324.85	336.70			

Soil [ $\mu\text{g}/\text{kg}$ ]		Reference soil			
Compound + CF chain length		#1	#2	LOD	LOQ
<b>Perfluorocarboxylic Acids (PFCA)</b>					
PFPeA	4	116.66	119.01	0.033	0.01
PFHxA	5	21.76	33.27	0.033	0.01
PFHpA	6	17.69		0.033	0.01
PFOA	7	32.93	28.53	0.066	0.02
PFNA	8	5.32	4.02	0.165	0.05
PFDA	9	3.12	5.04	0.033	0.01
PFUnA	10	1.54	1.53	0.066	0.02
PFDoDA	11		0.54	0.033	0.01
PFTriDA	12		< LOD	0.066	0.02
PFTDA	13		0.29	0.033	0.01
PFHxDA	15			0.066	0.02
7H-PFHpA	6			0.033	0.01
<b>Perfluoroalkyl Sulfonates (PFSA)</b>					
PFBS	4			0.165	0.05
PFPeS	5	3.61		0.066	0.02
PFHxS	6	3.91	4.11	0.066	0.02
PFHpS	7			0.066	0.02
PFOS	8	192.40	224.80	0.033	0.01
PFNS	9	7.23	8.93	0.33	0.1
PFDoDS	12			0.165	0.05
<b>Fluorotelomer sulfates (FTS)</b>					
6:2 FTS	6	1.71	2.60	0.033	0.01
8:2 FTS	8	3.70	5.28	0.033	0.01
10:2 FTS	10		1.74	0.033	0.01
<b>Perfluorooctanesulfonamidoacetic Acids (FOSAA)</b>					
FOSAA	8	1.21	1.71	0.033	0.01
MeFOSAA	8	20.69	21.59	0.033	0.01
<b>Perfluorooctanesulfonamides (FOSA)</b>					
PFOSA	8	< LOD	< LOD	0.033	0.01
<b>SaMPAP</b>					
diSAMPAP	16	14.57	19.90	0.033	0.01
<b><math>\Sigma</math> 26 PFAS</b>					
		448.05	482.88		

### E.3 PFAS mass balances

Mass balances for 10 selected PFAS in the original soil, unamended soil and soil amended with biochar.





**Figure E.1:** Mass balance for PFOS, PFHxS, PFBS, PFOA, PFHpA, PFHxA, 8:2 FTS, 6:2 FTS, PFOSA and diSAMPAP for the original soil, unamended soil and soil amended with biochar. Mean values  $\pm$  standard deviations are presented for the CWC (analytical triplicate) and DWSS (experimental triplicate).

# Appendix F Recovery test

**Table F.1:** Absolute recovery (AR), relative recovery (RR) for each internal standard (IS), matrix effect (ME), and the IS used for calibration of each PFAS. Recoveries are given for the three spiked samples (SP), and as a mean value  $\pm$  std.

Absolute Recovery %											
Compound + CF chain length		Water					Soil				
		SP1	SP2	SP3	Mean	STD	SP1	SP2	SP3	Mean	STD
<b>Internal Standard</b>											
PFOA - <sup>13</sup> C <sub>8</sub>		94.1	86.4	99.4	93.3	6.6	71.1	97.3	77.6	82.0	13.7
PFOS - <sup>13</sup> C <sub>8</sub>		67.7	65.6	91.6	75.0	14.4	69.9	104.9	72.3	82.4	19.6
6:2 FTS - <sup>13</sup> C <sub>2</sub>		120.9	109.1	121.2	117.1	6.9	68.6	99.3	81.0	83.0	15.5
<b>Perfluorocarboxylic Acids (PFCA)</b>											
PFPeA	4	270.4	175.4	287.0	244.2	60.2	40.2	78.5	47.9	55.5	20.2
PFHxA	5	138.8	116.6	173.8	143.1	28.9	49.9	88.3	57.9	65.4	20.3
PFHpA	6	141.7	137.2	143.5	140.8	3.3	50.7	89.8	59.8	66.8	20.5
PFOA	7	135.3	120.2	119.4	125.0	8.9	53.0	92.2	60.2	68.5	20.9
PFNA	8	99.7	93.5	92.2	95.1	4.0	53.3	88.0	59.6	67.0	18.4
PFDA	9	72.7	75.9	78.0	75.5	2.6	61.0	92.3	69.9	74.4	16.1
PFUnA	10	48.4	46.9	61.8	52.4	8.2	73.6	92.6	70.5	78.9	12.0
PFDODA	11	26.1	25.1	39.7	30.3	8.2	78.5	92.8	78.0	83.1	8.4
PFTriDA	12	12.6	12.9	26.4	17.3	7.9	67.9	81.0	71.7	73.5	6.7
PFTDA	13	7.1	7.1	16.6	10.3	5.5	44.4	66.3	66.4	59.1	12.7
PFHxDA	15	2.5	1.8	4.2	2.8	1.2	19.3	36.9	38.6	31.6	10.7
P37DMOA	9	67.0	58.7	64.3	63.3	4.2	67.5	95.2	74.7	79.1	14.4
7H-PFHpA	6	103.1	102.8	116.9	107.6	8.1	64.6	101.5	73.9	80.0	19.2
<b>Perfluoroalkyl Sulfonates (PFAS)</b>											
PFBS	4	156.8	149.9	142.1	149.6	7.4	48.5	82.2	61.7	64.1	17.0
PFPeS	5	162.7	183.5	174.3	173.5	10.4	52.8	95.6	68.4	72.3	21.7
PFHxS	6	393.0	514.4	383.1	430.1	73.1	57.2	95.8	76.4	76.5	19.3
PFHpS	7	125.8	108.1	118.6	117.5	8.9	56.7	81.3	71.2	69.7	12.4
PFOS	8	75.1	48.0	31.6	51.6	22.0	-215.7	-179.3	-102.1	-165.7	58.0
PFNS	9	83.3	89.9	109.9	94.4	13.8	55.8	77.7	67.8	67.1	11.0
PFDODS	12	20.7	15.3	36.7	24.2	11.1	61.2	76.9	74.6	70.9	8.5
PFECHS	8	117.8	103.5	113.4	111.6	7.3	64.8	86.0	73.8	74.9	10.6
<b>Fluorotelomer sulfates (FTS)</b>											
4:2 FTS	4	129.1	136.3	142.1	135.9	6.5	61.8	101.1	73.9	78.9	20.1
6:2 FTS	6	323.4	280.0	273.5	292.3	27.1	87.1	121.5	88.9	99.2	19.4
8:2 FTS	8	100.5	104.3	98.3	101.0	3.0	59.7	114.7	94.3	89.5	27.8
10:2 FTS	10	44.7	45.5	70.0	53.4	14.4	94.0	105.7	81.6	93.8	12.0
<b>Perfluorooctanesulfonamidoacetic Acids (FOSAA)</b>											
FOSAA	8	68.1	67.1	78.8	71.4	6.5	60.6	85.0	73.2	72.9	12.2
MeFOSAA	8	36.8	37.5	43.3	39.2	3.6	74.3	93.0	79.7	82.3	9.6
<b>Perfluorooctanesulfonamides (FOSA)</b>											
PFOSA	8	14.6	14.3	13.0	14.0	0.9	95.4	98.0	64.8	86.1	18.5



SaMPAP											
diSAMPAP	16	7.4	6.2	16.3	10.0	5.5	15.9	45.8	44.3	35.4	16.8

Relative Recovery % PFOA - <sup>13</sup> C <sub>8</sub>											
Compound + CF chain length	Water					Soil					
	SP1	SP2	SP3	Mean	STD	SP1	SP2	SP3	Mean	STD	
<b>Perfluorocarboxylic Acids (PFCA)</b>											
PFPeA	4	287.4	202.9	288.6	259.6	49.1	56.6	80.6	61.7	66.3	12.7
PFHxA	5	147.6	134.9	174.8	152.4	20.4	70.2	90.7	74.7	78.5	10.8
PFHpA	6	150.6	158.8	144.3	151.2	7.3	71.3	92.3	77.1	80.2	10.8
PFOA	7	143.8	139.2	120.1	134.4	12.6	74.5	94.7	77.7	82.3	10.9
PFNA	8	106.0	108.2	92.7	102.3	8.4	75.1	90.4	76.8	80.7	8.4
PFDA	9	77.3	87.9	78.4	81.2	5.8	85.9	94.8	90.0	90.2	4.4
PFUnA	10	51.4	54.3	62.1	55.9	5.6	103.5	95.1	90.9	96.5	6.4
PFDoDA	11	27.7	29.0	40.0	32.2	6.7	110.5	95.3	100.5	102.1	7.7
PFTriDA	12	13.4	14.9	26.5	18.3	7.2	95.5	83.2	92.5	90.4	6.4
PFTDA	13	7.5	8.3	16.7	10.8	5.1	62.5	68.1	85.6	72.1	12.1
PFHxDA	15	2.6	2.1	4.2	3.0	1.1	27.2	37.9	49.8	38.3	11.3
P37DMOA	9	71.2	67.9	64.7	67.9	3.3	95.0	97.8	96.2	96.3	1.4
7H-PFHpA	6	109.6	118.9	117.5	115.4	5.0	90.9	104.3	95.3	96.8	6.8
<b>Perfluoroalkyl Sulfonates (PFAS)</b>											
PFBS	4	166.7	173.5	142.9	161.0	16.1	68.2	84.5	79.5	77.4	8.3
PFPeS	5	173.0	212.4	175.3	186.9	22.1	74.4	98.2	88.1	86.9	12.0
PFHxS	6	417.8	595.4	385.2	466.1	113.1	80.5	98.4	98.4	92.5	10.4
PFHpS	7	133.7	125.1	119.2	126.0	7.3	79.8	83.5	91.7	85.0	6.1
PFOS	8	79.9	55.5	31.8	55.7	24.1	-303.4	-184.2	-131.5	-206.4	88.1
PFNS	9	88.6	104.1	110.5	101.0	11.3	78.5	79.8	87.4	81.9	4.8
PFDoDS	12	22.0	17.8	36.9	25.5	10.0	86.1	79.0	96.1	87.1	8.6
PFECHS	8	125.2	119.8	114.0	119.7	5.6	91.2	88.3	95.1	91.5	3.4
<b>Fluorotelomer sulfates (FTS)</b>											
4:2 FTS	4	137.2	157.8	142.9	146.0	10.6	86.9	103.8	95.2	95.3	8.5
6:2 FTS	6	343.8	324.1	275.0	314.3	35.4	122.5	124.9	114.5	120.6	5.4
8:2 FTS	8	106.8	120.7	98.9	108.8	11.0	84.0	117.8	121.5	107.8	20.7
10:2 FTS	10	47.5	52.7	70.4	56.9	12.0	132.3	108.6	105.2	115.4	14.8
<b>Perfluorooctanesulfonamidoacetic Acids (FOSAA)</b>											
FOSAA	8	72.4	77.7	79.3	76.5	3.6	85.2	87.3	94.3	88.9	4.7
MeFOSAA	8	39.1	43.4	43.6	42.0	2.5	104.5	95.5	102.8	100.9	4.8
<b>Perfluorooctanesulfonamides (FOSA)</b>											
PFOSA	8	15.6	16.6	13.0	15.1	1.8	134.3	100.7	83.5	106.2	25.8
<b>SaMPAP</b>											
diSAMPAP	16	7.8	7.2	16.4	10.5	5.1	22.4	47.1	57.1	42.2	17.9

Relative Recovery % PFOS - <sup>13</sup> C <sub>8</sub>											
Compound + CF chain length		Water					Soil				
		SP1	SP2	SP3	Mean	STD	SP1	SP2	SP3	Mean	STD
<b>Perfluorocarboxylic Acids (PFCA)</b>											
PFPeA	4	399.3	267.2	313.4	326.7	67.0	57.5	74.8	66.2	66.2	8.6
PFHxA	5	205.0	177.6	189.8	190.8	13.7	71.3	84.2	80.2	78.6	6.6
PFHpA	6	209.3	209.0	156.7	191.7	30.3	72.5	85.6	82.7	80.3	6.9
PFOA	7	199.8	183.2	130.4	171.2	36.2	75.8	87.9	83.4	82.3	6.1
PFNA	8	147.3	142.5	100.7	130.2	25.7	76.3	83.8	82.4	80.9	4.0
PFDA	9	107.4	115.7	85.1	102.7	15.8	87.3	87.9	96.7	90.6	5.2
PFUnA	10	71.4	71.5	67.5	70.1	2.3	105.2	88.3	97.6	97.0	8.5
PFDoDA	11	38.5	38.2	43.4	40.0	2.9	112.3	88.4	107.8	102.9	12.7
PFTriDA	12	18.6	19.7	28.8	22.3	5.6	97.0	77.2	99.3	91.2	12.2
PFTDA	13	10.4	10.9	18.2	13.2	4.3	63.5	63.2	91.9	72.9	16.5
PFHxDA	15	3.6	2.8	4.6	3.7	0.9	27.6	35.2	53.4	38.8	13.3
P37DMOA	9	98.9	89.4	70.2	86.2	14.6	96.5	90.7	103.3	96.9	6.3
7H-PFHpA	6	152.3	156.6	127.7	145.5	15.6	92.4	96.7	102.3	97.1	4.9
<b>Perfluoroalkyl Sulfonates (PFAS)</b>											
PFBS	4	231.6	228.4	155.2	205.1	43.2	69.3	78.4	85.3	77.7	8.0
PFPeS	5	240.4	279.7	190.4	236.8	44.8	75.6	91.2	94.6	87.1	10.1
PFHxS	6	580.4	783.9	418.4	594.2	183.2	81.8	91.3	105.6	92.9	12.0
PFHpS	7	185.7	164.7	129.5	160.0	28.4	81.1	77.5	98.4	85.7	11.2
PFOS	8	111.0	73.1	34.5	72.9	38.2	-308.4	-170.9	-141.2	-206.9	89.2
PFNS	9	123.0	137.0	120.0	126.7	9.1	79.8	74.1	93.8	82.6	10.2
PFDoDS	12	30.5	23.4	40.1	31.3	8.4	87.5	73.3	103.2	88.0	15.0
PFECHS	8	173.9	157.8	123.9	151.9	25.5	92.7	82.0	102.0	92.2	10.0
<b>Fluorotelomer sulfates (FTS)</b>											
4:2 FTS	4	190.7	207.8	155.2	184.6	26.8	88.4	96.4	102.2	95.6	7.0
6:2 FTS	6	477.6	426.7	298.7	401.0	92.2	124.5	115.9	122.9	121.1	4.6
8:2 FTS	8	148.4	158.9	107.4	138.2	27.2	85.4	109.3	130.4	108.4	22.5
10:2 FTS	10	66.0	69.4	76.5	70.6	5.4	134.5	100.7	112.9	116.0	17.1
<b>Perfluorooctanesulfonamidoacetic Acids (FOSAA)</b>											
FOSAA	8	100.6	102.3	86.1	96.3	8.9	86.6	81.0	101.2	89.6	10.4
MeFOSAA	8	54.4	57.2	47.3	53.0	5.1	106.2	88.6	110.3	101.7	11.5
<b>Perfluorooctanesulfonamides (FOSA)</b>											
PFOSA	8	21.6	21.9	14.2	19.2	4.4	136.5	93.5	89.6	106.5	26.0
<b>SaMPAP</b>											
diSAMPAP	16	10.9	9.5	17.8	12.7	4.5	22.8	43.7	61.3	42.6	19.3

Relative Recovery % 6:2 FTS - <sup>13</sup> C <sub>2</sub>											
Compound + CF chain length		Water					Soil				
		SP1	SP2	SP3	Mean	STD	SP1	SP2	SP3	Mean	STD
<b>Perfluorocarboxylic Acids (PFCA)</b>											
PFPeA	4	223.6	160.7	236.7	207.0	40.6	58.6	79.0	59.1	65.6	11.6
PFHxA	5	114.8	106.8	143.4	121.7	19.2	72.7	88.9	71.5	77.7	9.7
PFHpA	6	117.2	125.7	118.4	120.4	4.6	73.9	90.4	73.8	79.4	9.6
PFOA	7	111.9	110.2	98.5	106.9	7.3	77.2	92.8	74.4	81.5	9.9
PFNA	8	82.5	85.7	76.0	81.4	4.9	77.8	88.6	73.5	80.0	7.8
PFDA	9	60.1	69.6	64.3	64.7	4.7	89.0	92.9	86.2	89.4	3.4
PFUnA	10	40.0	43.0	51.0	44.6	5.7	107.3	93.3	87.1	95.9	10.3
PFDoDA	11	21.6	23.0	32.8	25.8	6.1	114.5	93.4	96.2	101.4	11.5
PFTriDA	12	10.4	11.8	21.8	14.7	6.2	98.9	81.5	88.5	89.7	8.8
PFTDA	13	5.8	6.5	13.7	8.7	4.4	64.8	66.8	82.0	71.2	9.4
PFHxDA	15	2.0	1.7	3.5	2.4	0.9	28.2	37.2	47.7	37.7	9.8
P37DMOA	9	55.4	53.8	53.0	54.1	1.2	98.4	95.9	92.2	95.5	3.1
7H-PFHpA	6	85.3	94.2	96.4	92.0	5.9	94.2	102.2	91.2	95.9	5.7
<b>Perfluoroalkyl Sulfonates (PFAS)</b>											
PFBS	4	129.7	137.4	117.2	128.1	10.2	70.7	82.8	76.1	76.5	6.1
PFPeS	5	134.6	168.2	143.8	148.9	17.4	77.1	96.3	84.4	85.9	9.7
PFHxS	6	325.0	471.5	316.0	370.8	87.3	83.4	96.5	94.2	91.4	7.0
PFHpS	7	104.0	99.1	97.8	100.3	3.3	82.6	81.9	87.8	84.1	3.2
PFOS	8	62.1	44.0	26.1	44.1	18.0	-314.5	-180.6	-126.0	-207.0	97.0
PFNS	9	68.9	82.4	90.6	80.7	11.0	81.4	78.2	83.7	81.1	2.7
PFDoDS	12	17.1	14.1	30.3	20.5	8.6	89.2	77.4	92.1	86.2	7.8
PFECHS	8	97.4	94.9	93.6	95.3	1.9	94.5	86.6	91.0	90.7	4.0
<b>Fluorotelomer sulfates (FTS)</b>											
4:2 FTS	4	106.8	125.0	117.2	116.3	9.1	90.1	101.8	91.2	94.4	6.5
6:2 FTS	6	267.4	256.7	225.6	249.9	21.7	127.0	122.4	109.7	119.7	9.0
8:2 FTS	8	83.1	95.6	81.1	86.6	7.8	87.1	115.5	116.3	106.3	16.7
10:2 FTS	10	36.9	41.7	57.8	45.5	10.9	137.1	106.4	100.7	114.8	19.6
<b>Perfluorooctanesulfonamidoacetic Acids (FOSAA)</b>											
FOSAA	8	56.3	61.5	65.0	61.0	4.4	88.3	85.6	90.3	88.1	2.4
MeFOSAA	8	30.5	34.4	35.7	33.5	2.8	106.2	88.6	110.3	101.7	11.5
<b>Perfluorooctanesulfonamides (FOSA)</b>											
PFOSA	8	12.1	13.1	10.7	12.0	1.2	136.5	93.5	89.6	106.5	26.0
<b>SaMPAP</b>											
diSAMPAP	16	6.1	5.7	13.5	8.4	4.4	22.8	43.7	61.3	42.6	19.3

Compound + CF chain length		Matrix effect %		IS used for calibration	
		Water	Soil	Water	Soil
<b>Internal Standard</b>					
PFOA - <sup>13</sup> C <sub>8</sub>		-103.5	-103.3		
PFOS - <sup>13</sup> C <sub>8</sub>		-98.5	-112.4		
6:2 FTS - <sup>13</sup> C <sub>2</sub>		-109.2	-120.1		
<b>Perfluorocarboxylic Acids (PFCA)</b>					
PFPeA	4	-96.1	229.1	6:2 FTS	PFOA
PFHxA	5	-92.7	209.6	6:2 FTS	PFOA
PFHpA	6	-93.2	146.2	6:2 FTS	PFOA
PFOA	7	-93.3	98.7	PFOA	PFOA
PFNA	8	-93.2	55.9	PFOA	PFOA
PFDA	9	-89.7	79.3	PFOS	PFOA
PFUnA	10	-89.8	14.9	PFOS	PFOA
PFDoDA	11	-87.2	-27.7	PFOS	PFOA
PFTriDA	12	-86.2	-39.2	PFOS	PFOA
PFTDA	13	-90.6	-1.4	PFOS	PFOA
PFHxDA	15	-85.5	-15.6	PFOA	PFOA
P37DMOA	9	-85.0	-52.6	PFOS	PFOA
7H-PFHpA	6	-85.4	51.4	6:2 FTS	PFOA
<b>Perfluoroalkyl Sulfonates (PFAS)</b>					
PFBS	4	-85.6	-52.4	6:2 FTS	PFOS
PFPeS	5	-90.1	-60.1	6:2 FTS	PFOS
PFHxS	6	-96.9	-65.3	6:2 FTS	PFOS
PFHpS	7	-84.3	-62.4	6:2 FTS	PFOS
PFOS	8	-171.9	-128.7	PFOS	PFOS
PFNS	9	-87.2	-60.0	PFOA	PFOS
PFDoDS	12	-88.5	-79.3	PFOS	PFOS
PFECHS	8	-84.2	-63.2	6:2 FTS	PFOS
<b>Fluorotelomer sulfates (FTS)</b>					
4:2 FTS	4	-83.6	-55.8	6:2 FTS	6:2 FTS
6:2 FTS	6	-95.2	-48.0	6:2 FTS	6:2 FTS
8:2 FTS	8	-85.7	16.4	PFOA	6:2 FTS
10:2 FTS	10	-82.5	-44.8	PFOS	6:2 FTS
<b>Perfluorooctanesulfonamidoacetic Acids (FOSAA)</b>					
FOSAA	8	-84.2	-44.5	PFOS	PFOA
MeFOSAA	8	-84.3	-65.2	PFOS	PFOA
<b>Perfluorooctanesulfonamides (FOSA)</b>					
PFOSA	8	-88.9	-89.0	PFOS	PFOA
<b>SaMPAP</b>					
diSAMPAP	16	-88.0	-48.1	PFOS	PFOS

## Appendix G      Reference soil

The certificate of analysis for the Standard Reference Material<sup>®</sup> 2781 "Domestic Sludge", used as reference for the PFAS soil analysis, is attached below. The material was provided by the National Institute of Standards & Technology (NIST), USA. The certificate provides certified values for elements, synthetic polycyclic musks, and perfluorinated compounds (PFCs) as perfluorinated Alkyl Acids (PFAAs) and Hexabromocyclododecanes (HBCDs), detected in the domestic sludge. The certified concentration of PFOS was used for verification of the analytical method for PFOS in soil.



# Certificate of Analysis

## Standard Reference Material<sup>®</sup> 2781

### Domestic Sludge

This Standard Reference Material (SRM) is intended primarily for use in the evaluation of methods used for the analysis of sludges and other materials of a similar matrix. Certified values are provided for elements. Reference values are provided for elements, synthetic polycyclic musks, and perfluorinated compounds (PFCs) as Perfluorinated Alkyl Acids (PFAAs) and Hexabromocyclododecanes (HBCDs). Information values are provided for PFAAs. SRM 2781 is a dried, pulverized domestic sludge. A unit of SRM 2781 consists of a bottle containing 40 g of dried, pulverized domestic sludge.

**Certified Mass Fraction Values:** The certified mass fraction values for elements are listed in Table 1; analytical methods are provided in Table 7. A NIST certified value is a value for which NIST has the highest confidence in its accuracy in that all known or suspected sources of bias have been investigated or taken into account [1]. The measurands are the certified mass fractions listed in Table 1 and are metrologically traceable to the SI unit for mass expressed as percentages or as milligrams per kilogram, as indicated in the table.

**Reference Mass Fraction Values:** Reference mass fraction values for elemental and organic constituents are provided in Tables 2 through Table 5; analytical methods are provided in at the end in Table 7. Reference values are noncertified values that are the best estimate of the true values based on available data. The values do not meet NIST criteria for certification and are provided with associated uncertainties that may reflect only measurement reproducibility, may not include all sources of uncertainty, or may reflect a lack of sufficient statistical agreement among multiple analytical methods [1]. The measurands are the mass fractions listed in Tables 2 through 5 as determined by the methods indicated and are metrologically traceable to the SI unit for mass fraction expressed as percentages or as micrograms per kilogram, as indicated in the tables.

**Information Mass Fraction Values:** Information mass fraction values for organic constituents are provided in Table 6. An information value is considered to be a value that will be of interest to the SRM user, but insufficient information is available to assess the uncertainty associated with the value or only a limited number of analyses were performed [1]. Information values may not be used to assess metrological traceability.

**Expiration of Certification:** The certification of **SRM 2781** is valid, within the measurement uncertainty specified, until **31 August 2025**, provided the SRM is handled and stored in accordance with the instructions given in this certificate (see "Instructions for Storage and Use"). The certification is nullified if the SRM is damaged, contaminated, or otherwise modified.

**Maintenance of SRM Certification:** NIST will monitor this SRM over the period of its certification. If substantive technical changes occur that affect the certification before the expiration of this certificate, NIST will notify the purchaser. Registration (see attached sheet or register online) will facilitate notification.

Overall direction and coordination of technical measurements for the original characterization of this SRM was performed by J.D. Fassett of the NIST Chemical Sciences Division. Coordination and certification of additional elements and organic constituents were performed by J.L. Reiner of the NIST Chemical Sciences Division and D.J. O'Kelly formerly of NIST.

Statistical consultation was provided by L.M. Gill and N.A. Heckert of the NIST Statistical Engineering Division.

Carlos A. Gonzalez, Chief  
Chemical Sciences Division

Robert L. Watters, Jr, Director  
Office of Reference Materials

Gaithersburg, MD 20899  
Certificate Issue Date: 15 September 2015  
*Certificate Revision History on Page 6*

Analytical measurements were performed at NIST by M.H. Ahsan, E.S. Beary, C.M. Beck II, D.A. Becker, M.S. Epstein, K. Garrity, R.R. Greenberg, R.M. Lindstrom, E.A. Mackey, J.L. Molloy, J.R. Moody, M.S. Nocun, B.R. Norman, D.J. O'Kelly, P.J. Paulsen, A. Peck, S.A. Rabb, M.S. Rearick, J.L. Reiner, T.A. Rush, R. Saraswati, J.M. Smeller, R.L. Watters, Jr., and L.J. Wood.

Support aspects involved in the issuance of this SRM were coordinated through the NIST Office of Reference Materials.

## INSTRUCTIONS FOR STORAGE AND USE

**Storage:** SRM 2781 must be stored in its original bottle at temperatures less than 30 °C.

**Use:** A minimum sample mass of 100 mg (dry mass; see "Instructions for Drying") should be used and sample preparation procedures should be designed to effect complete dissolution for analytical determinations to be related to the certified values provided.

**Instructions for Drying:** When nonvolatile elements are to be determined, samples should be vacuum dried at room temperature for 24 h or oven dried for 2 h at 110 °C. Volatile elements (e.g., arsenic, mercury, and selenium) and organic constituents should be determined on samples as received; separate samples should be dried according to these instructions to obtain a correction factor for moisture. Moisture corrections are then made to measurement values before comparing them to the certified values. [Note that the mass loss on drying at the time of certification was found to be in the range of 4.7 % to 6.6 % when using the recommended drying procedures.]

## PREPARATION AND ANALYSIS<sup>(1)</sup>

**Source and Preparation of Material:** The U.S. Geological Survey (USGS), under contract to NIST, obtained partially dehydrated sewage cake material from the Metropolitan Denver Sewage Disposal District No. 1. The material (approximately 182 kg) was placed in plastic-lined drums and transported to the USGS facilities (Lakewood, CO) for processing. It was dried at ambient temperature in a forced air chamber, ground to pass a 74 µm (200 mesh) sieve, blended for 24 h to assure homogeneity of the pulverized material. Test samples were taken from the blender for preliminary homogeneity analyses. The material was then radiation sterilized. The sterilized material was shipped in bulk to NIST, where the material was bottled in 40 g units after reblending for 4 h.

**Analysis:** The homogeneity was assessed at USGS on 10 replicate samples of bulk material for over 40 elements using x-ray fluorescence (XRF) and/or inductively coupled plasma atomic emission spectrometry (ICP-AES). Homogeneity was further assessed during certification analysis. At sample sizes of 100 mg or greater, no sample-to-sample variations in excess of those expected from the analytical measurements performed at USGS were detected.

**Value Assignment:** Analyses for value assignment were performed by NIST and collaborating laboratories where appropriate. Values were reported on a dry-mass basis in mass fraction units and are based on measurements using a sample mass of at least 100 mg. Analytical methods are provided in Table 7.

---

<sup>(1)</sup> Certain commercial equipment, instruments, or materials are identified in this report to adequately specify the experimental procedure. Such identification does not imply recommendation or endorsement by the National Institute of Standards and Technology, nor does it imply that the materials or equipment identified are necessarily the best available for the purpose.

Table 1. Certified Mass Fractions for Elements

Element	Mass Fraction (mg/kg)	Element	Mass Fraction (%)
Arsenic (As)	7.81 ± 0.67 <sup>(a)</sup>	Nitrogen (N)	4.78 ± 0.16 <sup>(b)</sup>
Cadmium (Cd)	12.78 ± 0.63 <sup>(a)</sup>		
Chromium (Cr)	202 ± 14 <sup>(a)</sup>		
Copper (Cu)	627.8 ± 18.4 <sup>(b)</sup>		
Lead (Pb)	200.8 ± 4.2 <sup>(b)</sup>		
Mercury (Hg)	3.68 ± 0.14 <sup>(b)</sup>		
Molybdenum (Mo)	46.6 ± 5.4 <sup>(a)</sup>		
Nickel (Ni)	80.2 ± 1.8 <sup>(b)</sup>		
Selenium (Se)	16.0 ± 1.5 <sup>(a)</sup>		
Silver (Ag)	97.6 ± 6.5 <sup>(b)</sup>		
Zinc (Zn)	1273 ± 68 <sup>(a)</sup>		

<sup>(a)</sup> The certified mass fraction value is a weighted mean of the mass fractions determined by the methods indicated for each analyte [1]. The uncertainty listed with each value is an expanded uncertainty about the mean [1,2], with coverage factor,  $k$ , based on the  $t$ -interval where the degrees of freedom is the number of methods minus one and calculated by combining a pooled within-method variance with a between-method variance [3] following the ISO/JCGM Guide [4,5]. The certified values are reported on a dry-mass basis. For certified values to be valid, the material must be dried according to the instructions provided above.

<sup>(b)</sup> The certified mass fraction value is a weighted mean of the mass fractions determined by the methods indicated for each analyte [1]. The expanded uncertainty is the half-width of a symmetric 95 % parametric bootstrap confidence interval [6], which is consistent with the ISO/JCGM Guide [4,5]. The effective coverage factor,  $k$ , is 2. The certified values are reported on a dry-mass basis. For certified values to be valid, the material must be dried according to the instructions provided above.

**Reference Mass Fraction Values:** Each reference mass fraction value, expressed as a mass fraction on a dry-mass basis, is an equally weighted mean of results provided by NIST and/or collaborating laboratories.

Table 2. Reference Mass Fractions for Elements

Element	Mass Fraction ( $\mu\text{g}/\text{kg}$ )	Element	Mass Fraction (%)
Beryllium (Be)	613.3 ± 24.7 <sup>(a)</sup>	Aluminum (Al)	1.6 ± 0.1 <sup>(b)</sup>
		Calcium (Ca)	3.9 ± 0.1 <sup>(c)</sup>
		Iron (Fe)	2.8 ± 0.1 <sup>(c)</sup>
		Magnesium (Mg)	0.59 ± 0.02 <sup>(b)</sup>
		Phosphorus (P)	2.43 ± 0.04 <sup>(b)</sup>
		Potassium (K)	0.49 ± 0.03 <sup>(b)</sup>
		Silicon (Si)	5.1 ± 0.2 <sup>(a)</sup>
		Sodium (Na)	0.21 ± 0.01 <sup>(b)</sup>
		Titanium (Ti)	0.31 ± 0.01 <sup>(b)</sup>

<sup>(a)</sup> The reference mass fraction value was calculated from a single measurement method. The expanded uncertainty is the half width of a 95 % Students  $t$ -confidence interval for  $\mu$ . The reference values are reported on a dry-mass basis. For reference values to be valid, the material must be dried according to the instructions provided above.

<sup>(b)</sup> The reference mass fraction value is a weighted mean of the mass fractions determined by the methods indicated for each analyte [1]. The reference values are reported on a dry-mass basis. The expanded uncertainty is the half-width of a symmetric 95 % parametric bootstrap confidence interval [6], which is consistent with the ISO/JCGM Guide [4,5]. The effective coverage factor,  $k$ , is 2. For reference values to be valid, the material must be dried according to the instructions provided above.

<sup>(c)</sup> The reference mass fraction value is a weighted mean of the mass fractions determined by the methods indicated for each analyte [1]. The uncertainty listed with each value is an expanded uncertainty about the mean [1,2], with coverage factor,  $k$ , based on the  $t$ -interval where the degrees of freedom is the number of methods minus one and calculated by combining a pooled within-method variance with a between-method variance [3] following the ISO/JCGM Guide [4,5]. For reference values to be valid, the material must be dried according to the instructions provided above.



Table 3. Reference Mass Fractions for Polycyclic Musks

	Mass Fraction ( $\mu\text{g}/\text{kg}$ )
1,3,4,6,7,8-Hexahydro-4,6,6,7,8-hexa-methyl-cyclopenta-( $\gamma$ )-2-benzopyran (HHCB)	9200 $\pm$ 1220 <sup>(a)</sup>
7-Acetyl-1,1,3,4,4,6-hexamethyltetralin (AHTN)	19700 $\pm$ 900 <sup>(a)</sup>
5-Acetyl-1,1,2,6-tetramethyl-3-isopropylindan (ATII)	2260 $\pm$ 90 <sup>(a)</sup>
4-Acetyl-1,1-dimethyl-6-tert-butylindan (ADBI)	1140 $\pm$ 60 <sup>(a)</sup>
6-Acetyl-1,1,2,3,3,5-hexamethylindan (AHMI)	142 $\pm$ 6 <sup>(b)</sup>

<sup>(a)</sup> The reference mass fraction value is a weighted mean of the mass fractions determined by the methods indicated for each analyte [1]. The uncertainty listed with each value is an expanded uncertainty about the mean [1,2], with coverage factor,  $k = 2$ , calculated by combining a pooled within-method variance with a between-method variance [3] following the ISO/JCGM Guide [4,5]. The reference values are reported on a dry-mass basis. For reference values to be valid, the material must be dried according to the instructions provided above.

<sup>(b)</sup> The reference mass fraction value is a weighted mean of the mass fractions determined by the methods indicated for each analyte [1]. The expanded uncertainty is the half-width of a symmetric 95 % parametric bootstrap confidence interval [6], which is consistent with the ISO/JCGM Guide [4,5]. The effective coverage factor,  $k$ , is 2. The reference values are reported on a dry-mass basis. For reference values to be valid, the material must be dried according to the instructions provided above.

Table 4. Reference Mass Fractions for Selected Perfluorinated Alkyl Acids (PFAAs)

	Mass Fraction <sup>(a)</sup> ( $\mu\text{g}/\text{kg}$ )
Perfluorohexanoic Acid (PFHxA)	13.0 $\pm$ 2.0
Perfluoroheptanoic Acid (PFHpA)	7.96 $\pm$ 1.50
Perfluorooctanoic Acid (PFOA)	28.5 $\pm$ 3.3
Perfluorohexanesulfonic Acid (PFHxS)	9.39 $\pm$ 1.76
Perfluorooctanesulfonic Acid (PFOS)	225 $\pm$ 41
Perfluorooctane Sulfonamide (PFOSA)	6.31 $\pm$ 0.97

<sup>(a)</sup> The reference mass fraction value is a weighted mean of the mass fractions determined by the methods indicated for each analyte [1]. The uncertainty listed with each value is an expanded uncertainty about the mean [1,2], with coverage factor,  $k = 2$ , calculated by combining a pooled within-method variance with a between-method variance [3] following the ISO/JCGM Guide [4,5]. The reference values are reported on a dry-mass basis. For reference values to be valid, the material must be dried according to the instructions provided above.

Table 5. Reference Mass Fractions for Hexabromocyclododecanes (HBCD)

	Mass Fraction ( $\mu\text{g}/\text{kg}$ )
$\alpha$ -hexabromocyclododecane ( $\alpha$ -HBCD)	17.8 $\pm$ 1.7 <sup>(a)</sup>
$\beta$ -hexabromocyclododecane ( $\beta$ -HBCD)	1.65 $\pm$ 0.39 <sup>(a)</sup>
$\gamma$ -hexabromocyclododecane ( $\gamma$ -HBCD)	9.73 $\pm$ 0.77 <sup>(b)</sup>

<sup>(a)</sup> The reference mass fraction value is a weighted mean of the mass fractions determined by the methods indicated for each analyte [1]. The uncertainty listed with each value is an expanded uncertainty about the mean [1,2], with coverage factor,  $k = 2$ , calculated by combining a pooled within-method variance with a between-method variance [3] following the ISO/JCGM Guide [4,5]. The reference values are reported on a dry-mass basis. For reference values to be valid, the material must be dried according to the instructions provided above.

<sup>(b)</sup> The reference mass fraction value is a weighted mean of the mass fractions determined by the methods indicated for each analyte [1]. The expanded uncertainty is the half-width of a symmetric 95 % parametric bootstrap confidence interval [6], which is consistent with the ISO/JCGM Guide [4,5]. The effective coverage factor,  $k$ , is 2. The reference values are reported on a dry-mass basis. For reference values to be valid, the material must be dried according to the instructions provided above.

Table 6. Information Mass Fraction Values for Selected Perfluorinated Alkyl Acids (PFAAs)

	Mass Fraction ( $\mu\text{g}/\text{kg}$ )
Perfluorononanoic Acid (PFNA)	5.09
Perfluorodecanoic Acid (PFDA)	4.76

Table 7. Methods used for the Analysis of SRM 2781

Analyte	Method <sup>(a)</sup>	Analyte	Method <sup>(a)</sup>
Aluminum	INAA, ICP-AES, XRF	Musks	GC-MS
Arsenic	<b>RNAA, Hyd. AAS, INAA</b>	Nickel	<b>ICP-AES, ID-ICPMS, INAA, TXRF</b>
Beryllium	ICP-MS	Nitrogen	<b>PGAA</b>
Cadmium	<b>ID-ICPMS, PGAA, RNAA, INAA, TXRF</b>	PFAAs	LC-MS/MS
Calcium	INAA, TXRF, ICP-AES, XRF	Phosphorus	Color, ICP-AES, XRF
Chromium	<b>INAA, ICP-OES</b>	Potassium	INAA, TXRF, ICP-AES
Copper	<b>ID-ICPMS, RNAA, INAA, TXRF</b>	Selenium	<b>Hyd. AAS, RNAA, INAA, TXRF</b>
HBCDs	LC-MS/MS	Silicon	XRF
Iron	INAA, TXRF, ICP-AES, XRF	Silver	<b>INAA, ICP-OES</b>
Lead	<b>ICP-AES, ID-ICPMS, TXRF</b>	Sodium	INAA, ICP-AES, XRF
Magnesium	INAA, ICP-AES, XRF	Titanium	INAA, TXRF, XRF
Mercury	<b>FIA-CV-AAS, RNAA, INAA</b>	Zinc	<b>ICP-AES, ID-ICPMS, INAA, TXRF</b>
Molybdenum	<b>ID-ICPMS, ICP-AES, TXRF, INAA</b>		

<sup>(a)</sup> Methods used for establishment of certified mass fraction values are shown in bold-face type; methods used for reference mass fraction values or to corroborate certified mass fraction values are not in bold.

Methods Key:

INAA: Instrumental Neutron Activation Analysis  
 ICP-AES: Inductively Coupled Plasma-Atomic Emission Spectroscopy  
 XRF: X-Ray Fluorescence  
 RNAA: Radiochemical neutron activation analysis  
 Hyd AAS: Hydride Generation Atomic Absorption Spectroscopy  
 ICP-MS: Inductively Coupled plasma – mass spectrometry  
 ID-ICPMS: Isotope Dilution Inductively Coupled Plasma Mass Spectrometry  
 PGAA: Prompt Gamma Activation Analysis  
 TXRF: Total Reflection X-ray Fluorescence Spectrometry  
 ICP-OES: Inductively Coupled plasma  
 LC-MS/MS: Liquid chromatography – Mass Spectroscopy  
 FIA-CV-AAS: Cold Vapor Atomic Absorption Spectroscopy  
 GC-MS: Gas chromatography – Mass Spectroscopy  
 Color: Colorimetry

**Cooperating Analysts and Laboratories:**

University of Illinois, Nuclear Engineering Department, Champaign, IL, S. Landsberger and D. Wu.

USGS, Lakewood, CO, S.A. Wilson, D. Siems, and P. Briggs.

GKSS Research Center, Institute of Physical and Chemical Analytics, Geesthacht, Germany, A. Prange, U. Reus, and R. Neidergesäss.

3M Company; St. Paul, MN.

Colorado School of Mines.

US Environmental Protection Agency; Athens, GA.

Wageningen IMARES; Ijmuiden, The Netherlands.

## REFERENCES

- [1] Rukhin, A.L.; *Weighted Means Statistics in Interlaboratory Studies*; Metrologia, Vol. 46, pp. 323–331 (2009).
- [2] Dersimonian, R.; Laird, N.; *Meta-Analysis in Clinical Trials*; Control Clin. Trials, Vol. 7, pp. 177–188 (1986).
- [3] Horn, R.A.; Horn, S.A.; Duncan, D.B.; *Estimating Heteroscedastic Variance in Linear Models*; J. Am. Stat. Assoc., Vol. 70, pp. 380–385 (1975).
- [4] JCGM 100:2008; *Evaluation of Measurement Data — Guide to the Expression of Uncertainty in Measurement (GUM 1995 with Minor Corrections)*; Joint Committee for Guides in Metrology (JCGM) (2008); available at [http://www.bipm.org/utis/common/documents/jcgm/JCGM\\_100\\_2008\\_E.pdf](http://www.bipm.org/utis/common/documents/jcgm/JCGM_100_2008_E.pdf) (accessed Sep 2015); see also Taylor, B.N.; Kuyatt, C.E.; *Guidelines for Evaluating and Expressing the Uncertainty of NIST Measurement Results*; NIST Technical Note 1297; U.S. Government Printing Office: Washington, DC (1994); available at <http://www.nist.gov/pml/pubs/index.cfm> (accessed Sep 2015).
- [5] JCGM 101:2008; *Evaluation of Measurement Data – Supplement 1 to the Guide to the Expression of Uncertainty in Measurement – Propagation of Distributions Using a Monte Carlo Method*; JCGM (2008); available at [http://www.bipm.org/utis/common/documents/jcgm/JCGM\\_101\\_2008\\_E.pdf](http://www.bipm.org/utis/common/documents/jcgm/JCGM_101_2008_E.pdf) (accessed Sep 2015).
- [6] Efron, B.; Tibshirani, R.J.; *An Introduction to the Bootstrap*; Chapman & Hall (1993).
- [7] Kane, J.S.; *Leach Data vs Total: Which is Relevant for SRMs*; Fresenius J. Anal. Chem. Vol. 352: pp 209–213, (1995).
- [8] U.S. EPA 1991 Code of Federal Regulations, Title 40, Part 136, Paragraph 33.
- [9] Federal Register SW-846, *Test Methods for Evaluating Solid Waste, Physical/Chemical Methods*; available at [www.epa.gov](http://www.epa.gov) (accessed Sep 2015).
- [10] New Jersey Administrative Code, N.J.A.C., 7:14-4 (1994).

<p><b>Certificate Revision History:</b> 15 September 2015 (Change from reference to certified mass fractions and the addition of reference mass fractions for several inorganic and organic constituents; addendum changed to appendix; change of expiration date; editorial changes); 25 October 1996 (Addition of Addendum); 22 June 1995 (Original certificate date).</p>
--

*Users of this SRM should ensure that the Certificate of Analysis in their possession is current. This can be accomplished by contacting the SRM Program: telephone (301) 975-2200; fax (301) 948-3730; e-mail [srminfo@nist.gov](mailto:srminfo@nist.gov); or via the Internet <http://www.nist.gov/srm>.*

## APPENDIX A

### Leachable Mass Fractions Using U.S. EPA and NJDEP Methods for Flame Atomic Absorption Spectrometry and Inductively Coupled Plasma Atomic Emission Spectrometry

To obtain total mass fractions, either subsamples of the SRM must be completely decomposed, or the sample must be analyzed directly in its solid form. For mixed acid dissolution, hydrofluoric acid must be included in the acid mixture to totally dissolve siliceous material present in sludge.

For a number of environmental monitoring purposes, acid extractable mass fractions of elements are often used rather than total mass fractions. Acid extractable methods do not necessarily result in total decomposition of the sludge. It should be noted that results obtained using acid leach conditions are often depicted in reports as total results. However, reported acid labile or extractable mass fractions of elements are generally lower than total mass fractions. Results are often presented as measured mass fractions in the leachate in comparison to the total or certified mass fractions. The recovery of an element as a percent of total is a function of several factors such as the mode of occurrence in the sample, leach medium, leach time, temperature conditions, and pH of the sample-leach medium mixture [7].

In its monitoring programs, the U.S. Environmental Protection Agency (U.S. EPA) has established a number of leach methods, such as Methods 3015, 3050, and 3051 [8,9] for the determination of acid labile or extractable mass fractions of elements. The New Jersey Department of the Environment (NJDEP) has developed its own leach method, NJDEP 100 for state use [10]. The NJDEP and the U.S. EPA prepared samples of SRM 2781 using the NJDEP 100 method and EPA Methods 3050 and 3051 and analyzed the resulting leachates by FAAS and ICP-AES.

Reference values have been established for the acid-leachable mass fractions of several elements in SRM 2781. These values are the means of all results from the different leach measurement methods and combinations used. The reference values are listed in Table A1, along with their uncertainties which are based on 95 % confidence intervals of the means of results. For some of the elements (copper, iron, silver, vanadium), no statistically significant differences were found among results from the two laboratories using three or four combinations of sample preparation and instrumental measurement techniques (NJDEP 100 - FAAS; NJDEP 100 - ICP-AES; EPA 3050 - ICP-AES; EPA 3051 - ICP-AES). For all other elements, statistically significant between-laboratory differences were identified and are included in the stated uncertainties. These differences are small in comparison to control limits for many environmental monitoring programs. Therefore, the reference values are meaningful, despite the between-laboratory differences found.

**Reference Values:** The reference values given in Table A1 are not NIST certified but are provided as a reference for U.S. EPA 3050 and 3051, and NJDEP 100 methods. The uncertainties are based on a 95 % confidence interval for the mean and include an allowance for differences between the analytical methods used.

$$\text{Leach Recovery (\%)} = 100 \times \frac{\text{Leach Value}}{\text{Certified or Reference Value}}$$

Table A1. Reference Leach Values for SRM 2781

Element	Leachable Mass Fraction (mg/kg)		Leach Recovery (%)
Aluminum (Al)	8040	± 980	50
Barium (Ba)	570	± 65	-- <sup>(a)</sup>
Cadmium (Cd)	11	± 2	86
Calcium (Ca)	36440	± 1830	93
Chromium (Cr)	143	± 14	71
Copper (Cu)	601	± 16	96
Iron (Fe)	24300	± 2100	87
Lead (Pb)	183	± 15	91
Magnesium (Mg)	4850	± 290	82
Manganese (Mn)	745	± 33	--
Nickel (Ni)	72.3	± 6.3	90
Silver (Ag)	86.3	± 1.7	88
Vanadium (V)	81.9	± 3.8	--
Zinc (Zn)	1120	± 34	88

<sup>(a)</sup> -- indicates that a certified or reference total mass fraction value was not available for the element.

#### Cooperating Analysts and Laboratories:

S.J. Nagourney; New Jersey Department of the Environment, Trenton, NJ.  
J. Birri, K. Peist; U.S. Environmental Protection Agency, Edison, NJ.



**Norges miljø- og biovitenskapelige universitet**  
Noregs miljø- og biovitenskapelige universitet  
Norwegian University of Life Sciences

Postboks 5003  
NO-1432 Ås  
Norway